Using Scalls to study the thermal behavior of polymers in solution

by

Divann Robertson

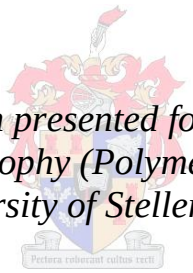

Dissertation presented for the degree
Doctor of Philosophy (Polymer Science) at the
University of Stellenbosch

Supervisor: Prof, Albert J. van Reenen

Faculty of Science
Department of Chemistry and Polymer Science

March 2015

Declaration

By submitting this thesis/dissertation electronically, I declare that the entirety of the work contained therein is my own, original work, that I am the sole author thereof (save to the extent explicitly otherwise stated), that reproduction and publication thereof by Stellenbosch University will not infringe any third party rights and that I have not previously in its entirety or in part submitted it for obtaining any qualification.

March 2015

ABSTRACT

This study involves the analysis of crystallization and melting behavior of polymers in solution, using Solution crystallization by laser light scattering (Scalls) as analytical tool. Various other techniques such as differential scanning calorimetry (DSC), Fourier-transform infrared spectroscopy (FTIR) and dynamic light scattering (DLS) were used for further characterization of the polymer materials. For the first time the solution behavior (crystallization and dissolution kinetics) of two biopolymers namely, poly(lactic acid) (PLA) and poly(butylene succinate) (PBS), was monitored by Scalls.

Non-isothermal solution crystallization and dissolution behavior of both enantiomers (D and L) PLA and their blends were studied. It was found that addition of the D- enantiomer (PDLA) to the L- enantiomer (PLLA) in solution resulted in the formation of stereocomplex crystals (SC) and the nucleation-effect of the crystals were intensified with an increase in PDLA content leading to an earlier onset of crystallization and increased crystallization peak area. DSC analysis confirmed the formation of SC during solution crystallization. Overall, results obtained by Scalls provided promising information regarding PLA crystallization kinetics which significantly influences practical applications of this biopolymer.

Binary blends consisting of PLLA and PBS were prepared in various blend ratios. Scalls was used to investigate the non-isothermal crystallization and melting behavior of these PLLA/PBS blends from dilute solutions. Addition of PBS up to 30 wt% increased crystallization temperatures of PLLA through a nucleation effect in the molten PBS state. Results indicated that the crystallization rate of PLLA can be improved by additions of small amounts of PBS, and this is of significant interest for practical applications due to the low crystallization rate that PLLA is known to exhibit. DSC thermograms showed an increase in PLLA crystallization exotherm at PBS loadings below 50 wt%, providing further evidence of the enhancement in PLLA crystallization kinetics.

A series of linear polyethylene samples with varying molecular weights were studied by Scalls. The effect of molecular weight (M_w) on the solution crystallization temperature (T_c) were monitored and compared to literature where the conventional Crystaf technique was used. Experimental Scalls data correlated well with reported theoretical models. Dissolution studies were also done to study the effect of M_w on the solution melting temperature (T_m) and for the first time, an equation was generated to model solution melting temperatures of linear polyethylenes in Scalls.

The solution behavior of a PE-1-octene linear low-density polyethylene (LLDPE) copolymer in a range of solvents including trichlorobenzene (TCB), ortho-dichlorobenzene (o-DCB), decalin and xylene were successfully studied. Scalls allowed for rapid analysis of crystallization and dissolution during a single experiment and offered clearer insight into crystallization kinetics when using different solvents for fractionation. Peak temperatures for analyses in TCB and o-DCB were almost identical but remarkably different to those observed when decalin and xylene was used. The study revealed that solvent type plays an important role in the solution behavior of polymers as well as ultimately the interpretation of these results.

OPSOMMING

Hierdie studie behels die ontleding van kristallisasie en smelt gedrag van polimere in oplossing, met behulp van Oplossing kristallisasie deur laser lig verstrooiing (Scalls) as analitiese instrument. Verskeie ander tegnieke soos differensiële skandeer kalorimetrie (DSC), fourier-tranform infrarooi spektroskopie (FTIR) en dinamiese lig verstrooiing (DLS) was gebruik word vir verdere Karakterisering van die polimeer materiaal. Vir die eerste keer is die oplossingsgedrag (kristallisasie en smelting kinetika) van twee biopolimere naamlik, poli(melksuur) (PLA) en poli(butileen suksinaat) (PBS), deur Scalls gemonitor.

Nie-isotermiese oplossing kristallisasie en smelt gedrag van beide enantiomere (D en L) van PLA en hul mengsels was ge-analiseer. Daar is gevind dat byvoeging van die D-enantiomeer (PDLA) tot die L-enantiomeer (PLLA) in oplossing gelei het tot die vorming van stereokompleks kristalle (SC) en die nukleasie-effek van die kristalle is versterk met 'n toename in PDLA inhoud wat gelei het tot 'n vroeër aanvang van kristallisasie en toename in kristallisasie piek-area. DSC analise het die vorming van SC gedurende oplossing kristallisasie bevestig. Algeheel, die resultate wat verkry was deur Scalls het belowende inligting oor PLA kristallisasie kinetika verskaf wat aansienlik praktiese toepassing van hierdie biopolimeer beïnvloed.

Binêre mengsels bestaande uit PLLA en PBS was voorberei in verskillende mengsel verhoudings. Scalls was gebruik om die nie-isotermiese kristallisasie en smelt gedrag van hierdie PLLA/PBS mengsels, vir die eerste keer, in verdunde oplossings te ondersoek. Byvoeging van PBS tot 30 wt% het ‘n toename in kristallisasie temperature van PLLA veroorsaak deur 'n nukleasie-effek in die gesmelte PBS toestand. Resultate dui aan dat die tempo van PLLA kristallisasie versnel kan word deur byvoegings van PBS in klein hoeveelhede, en dit is van beduidende belang vir praktiese toepassings weens die lae kristallisasie-tempo waarvoor PLLA bekend is. DSC termogramme het 'n toename in PLLA kristallisasie eksoterm aangedui by PBS inhoud onder 50 wt%, wat 'n verdere bewys is van die verbetering in PLLA kristallisasie kinetika.

'n Reeks lineêre poliëtileen monsters met wisselende molekulêre massas was met Scalls ge-analiseer. Die effek van molekulêre massa (M_w) op die oplossing kristallisasie temperatuur (T_c) was gemonitor en vergelyk met literatuur waar die konvensionele Crystaf tegniek gebruik is. Eksperimentele Scalls data het goed gekorreleer met gerapporteerde teoretiese modelle. Smelting studies is ook gedoen om die effek van M_w op die oplossing smelt temperatuur (T_m) te bestudeer en vir die eerste keer, is 'n vergelyking ge-genereer vir die modellering van oplossing smelt temperature van lineêre poliëtileen met behulp van Scalls.

Die oplossing-gedrag van ‘n PE-1-okteen lineêre lae-digtheid poliëtileen (LLDPE) kopolimeer was suksesvol bestudeer in 'n verskeidenheid oplosmiddels, insluitend trichlorobenseen (TCB), orto-dichlorobenseen (o-DCB) , decalin en xileen. Scalls het toegelaat vir vinnige analise van die kristallisasie en smelting in 'n enkele eksperiment en het dieper insig gegee oor die kristallisasie kinetika tydens fraksionering met die gebruik van verksillend oplosmiddels. Piek temperature vir analises in TCB en o-DCB was byna identies, maar merkwaardig verskillend van dié wat waargeneem was in die geval waar decalin en xileen gebruik was. Hierdie studie het getoon dat die tipe oplosmiddel 'n belangrike rol speel in die oplossing-gedrag van polimere en uiteindelik asook die interpretasie van hierdie resultate.

Verder blyk Scalls na ‘n nuttige metode vir die ontleding van polimere in oplossing te wees.

Dedicated to:

My father, Johan

and

My mother, Sylvia

For their love, support and motivation throughout my studies.

Acknowledgements

I would like to thank the following people for their support and contributions during the course of this study:

- Prof. Albert J. van Reenen – I would like to express my gratitude to him for his advice, aspiring guidance and motivation during the time of research and writing of this thesis.
- The Olefins research group – for their support and stimulating discussions.
- Administrative and technical staff at Polymer Science Institute.
- The Laser Research Institute at University of Stellenbosch – for technical assistance with the Scalls instrumentation during the study.
    - Prof. E. Rohwer, Dr. P. Neethling, J. Germishuizen, G. Louwrens
- NRF – for funding.
- Corbion Purac® (Netherlands) – for providing us with the free poly(lactic acid) samples used for analyses during the thesis.
- To all my friends - for their support, inputs, good times and navigation throughout this academic journey.
- Last but definitely not the least, I would like to thank my Mom (Sylvia), Dad (Johan), brother (Heinrich) and the Rinkwest family for their endless support and encouragement.

Contents

List of contents

Chapter 1: Introduction and overview

Chapter 2: Historical background and literature review

List of figures

List of tables

List of schemes

List of equations

List of abbreviations

CC	comonomer content
CCD	chemical composition distribution
CEF	crystallization elution fractionation
m-CEF	multiple crystallization elution fractionation
Crystaf	crystallization analysis fractionation
DLS	dynamic light scattering
DP	degree of polymerization
DSC	differential scanning calorimetry
FTIR	fourier transform infrared spectroscopy
iPP	isotactic polypropylene
LLDPE	linear low-density polyethylene
M_n	number-average molecular weight
M_w	weighted-average molecular weight
nm	nanometer
o-DCB	ortho-dichlorobenzene
PBS	poly(butylene succinate)
PDI	polydispersity index
PLA	poly(lactic acid)
PLLA	poly(L-lactic acid)
PDLA	poly(D-lactic acid)
PDLLA	poly(DL-lactic acid)

PE	polyethylene
POM	polarized optical microscopy
ROP	ring-opening polymerization
SC	stereocomplex crystals
Scalls	solution crystallization analysis by laser light scattering
SCB	short chain branching
SEM	scanning electron microscopy
T_c	crystallization peak temperature
T_m	melting peak temperature
TCB	1,2,4 - trichlorobenzene
TMDSC	temperature modulated differential scanning calorimetry
Tref	temperature rising elution fractionation
a-Tref	analytical temperature rising elution fractionation
p-Tref	preparative temperature rising elution fractionation
wt%	weight percentage
ZnSe	zinc selenide

Chapter 1

Introduction and Overview

This chapter offers a brief overview on the different chapters of the manuscript and indicates briefly what will be discussed in the various sections.

1.1) Introduction

Various well-established solution fractionation methods are currently used for analysis of semi-crystalline polymers, especially polyolefins. During this manuscript we discuss the results obtained for solution analysis of not only polyolefins but also for the first time, the solution behavior of biopolymer systems using an in-house developed technique which we call "solution crystallization by laser light scattering" (Scalls).

1.2) Aims and objectives

The main objective of this research study was to evaluate the solution behavior (including crystallization and dissolution) of various polymer systems using Scalls as the main analytical tool. Under this objective, the aims are:

- Evaluation of poly(lactic acid) (PLA) solution crystallization behavior
- Evaluation of poly(lactic acid) dissolution behavior
- Study possible methods of increasing PLA crystallization kinetics
- Study the molecular weight dependency of solution crystallization temperature (T_c) and solution melting temperature (T_m) in linear polethylenes
- Study the effect of various solvents on the solution behavior of linear low density polyethylene (LLDPE)

1.3) Outline of this manuscript

1.3.1) Chapter 2

Some background information and previous work done on the topics that will be discussed in this thesis is given in this section.

1.3.2) Chapter 3

An overview of the materials used during this study as well as the experimental techniques used for the various analyses is given in this chapter.

1.3.3) Chapter 4

This chapter focuses on the results obtained for PLLA/PDLA binary blends and evaluating the effect of PDLA addition on PLLA solution behavior.

1.3.4) Chapter 5

This chapter focuses on the results obtained for PLLA/PBS binary blends and evaluating the effect of PBS addition on PLLA solution behavior.

1.3.5) Chapter 6

This chapter focuses on the molecular weight dependency of T_c and T_m of linear PE samples in Scalls and the construction of a prediction model.

1.3.6) Chapter 7

This chapter focuses on the analysis of LLDPE in various solvents and effect of solvent on solution crystallization and dissolution.

1.3.7) Chapter 8

This chapter concludes the main findings of the thesis.

Chapter 2

Historical background and literature review

This chapter provides background information and previous work done on topics and techniques that will be discussed in this thesis.

2.1) Introduction

Solution crystallization techniques can provide promising results to assist understanding of microstructural behavior in polymers and to construct much needed structure-property relationships in polymer systems. The most common, conventional techniques used for these studies thus far, are crystallization analysis fractionation (Crystaf) and temperature rising elution fractionation (Tref). Both these techniques require complex instrumentation and long analysis times. More recently crystallization elution fractionation (CEF) has been developed for analysis of semi-crystalline polymers (mainly petrochemical-based polyolefins). Biopoloymers are becoming appropriate alternatives to these petroleum-based semi-crystalline polymers. In order to understand where biodegradable and biocompatible polymers can be applied/used, it is critical to first evaluate the properties these systems exhibit.

2.2) Solution fractionation techniques

2.2.1) Temperature Rising Elution Fractionation (Tref)

Tref is a solution fractionation method used to separate semi-crystalline polymer chains according to crystallizability. This is dependent on the chemical composition and molecular structure. Since the development of Tref, this technique has become a powerful tool for determining crystallinity distributions of polyalkenes.[1-3] According to Soares *et. al* [3], two important aspects must be kept in mind when considering Tref: First, Tref only fractionates semi-crystalline polymers, is not applicable to amorphous samples and is predominantly sensitive to differences in crystallinity and solubility. Second, the technique fractionates according to molecular structure that directly influences crystallinity/solubility of chains. Over the years Tref has been used to extensively study polyolefins. Certain features of polyolefin crystallization makes Tref a suitable technique. Crystallizable poyolefins only dissolve in high-boiling point solvents at elevated temperatures, which make the control of temperature ramps simple. The heterogeneous structures found in commercial polyolefins, as well as broad distribution in tacticty, molecular weight and molecular composition result in fractions eluting over a wide temperature range.[4]

The Tref procedure consist of two sequential experimental steps; the first being a crystallization step and the second an elution step.

2.2.1.1) Crystallization: Step one

Polymer sample is transferred to a glass reaction vessel containing a suitable solvent (mostly xylene or trichlorobenzene, TCB, in the case of polyolefins). The solution is heated under reflux at roughly 130 °C and under continuous stirring until complete dissolution of polymer. It is also common to add ± 0.2 wt% stabilizer to the mixture to minimize thermal degradation during dissolution at elevated temperature. After complete dissolution, inert supports (which may include silica or sand particles 60/80 mesh size, glass beads or steel granules) are added until it completely covers the polymer solution. Multiple reaction vessels (containing polymer and support) are then placed in a pre-heated oil bath or oven (130 °C) to allow for polymer crystallization under controlled cooling. Typical cooling rates applied during Tref are below 5 °C/h (130 °C to room temperature). This is a very time-consuming process and may take up to a week for complete crystallization. Crystallization occurs on the basis of chain crystallizability which in turn is affected by molecular structure and sample composition. The result is often depicted as an onion-like structure with the support particle found on the inner-most region and polymer chains arranged with decreasing crystallizability towards the outer layers. Figure 2.1 provides such a representation of the polymer layers, crystallized onto the support.

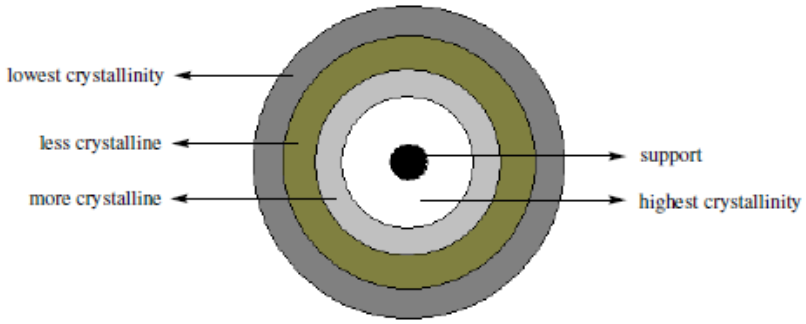

Figure 2.1: Formation of onion-like polymer layered structure according to crystallizability onto a support during Tref cooling cycle (step one).[5]

2.2.1.2) Elution: Step two

Following step one, the crystallized material are transferred to a column and placed into a programmable oven (shown in Figure 2.2) where both oven and column temperature can be monitored. Polymer elution occurs by pumping solvent through the column while a temperature ramp is being applied. In contrast to the crystallization event, the least crystalline species situated

on the outer layer will elute first followed by the higher crystallinity species eluting at elevated temperatures. A simplistic illustration of the elution process is given in Figure 2.3. Two main elution processes are used, depending on the specific laboratory facilities namely, Analytical Tref (continuous elution) and Preparative Tref (step-wise elution). Differences between these two modes are stipulated in the following section.

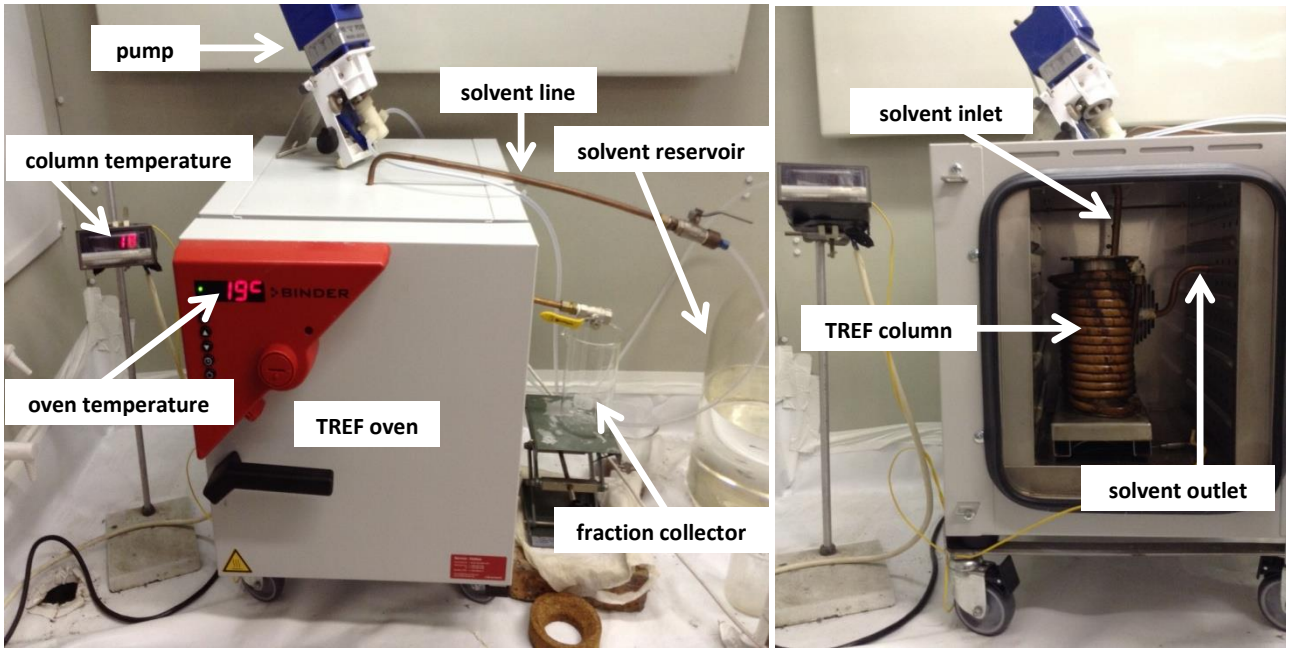

Figure 2.2: An example of the Tref instrumentation used for fractionation at our laboratory facilities.

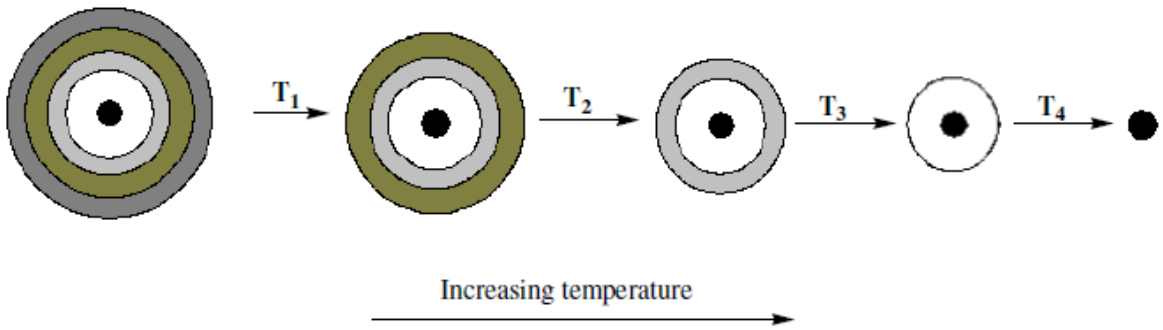

Figure 2.3: Simplistic representation of dissolution process during Tref elution cycle (step two).[5]

2.2.1.3) Preparative Tref (p-Tref)

p-Tref is a step-wise elution procedure where polymer fractions are collected at set temperature intervals. This mode allows for the analysis of fractions by additional characterization techniques to gain information on molecular structure. Large sample sizes are required with the major drawback being the time-consuming and tedious elution process. Nonetheless, detailed information regarding polymer microstructure can be acquired with p-Tref.[6]

2.2.1.4) Analytical Tref (a-Tref)

Unlike p-Tref, a-Tref is a continuous procedure whereby solvent is continuously pumped through the column with a steady increase in elution temperature. Controllable parameters during this mode are the heating rate as well as solvent flow rate. Through the use of a calibration curve, macromolecular information of the polymer fractions can be obtained in an on-line manner. a-Tref is a much faster elution method, making it less time-consuming mode but is inferior to p-Tref when considering microstructural information obtained for polymer samples.

2.2.2) Crystallization Analysis Fractionation (Crystaf)

2.2.2.1) Overview

In addition to the tedious Tref procedure, Crystallization Analysis Fractionation (Crystaf) was developed, initially to gain more in-depth information on short chain branching (SCB) of linear low-density polyethylene (LLDPE) as well as tacticity distributions in polypropylene (PP).[7] This is a single-step crystallization technique based on the continuous crystallization of semi-crystalline polymers from dilute solution. After the development of Crystaf, extensive research has been done by several groups using this technique, especially for the solution crystallization analysis of polyolefins.[8-13] Crystaf is often used as a complimentary technique to Tref and similar results are obtained with the main difference being the shifts in peak temperatures due to the variation in operating procedures between the two systems. Some of the main advantages of Crystaf over Tref include, much shorter analysis times, smaller sample sizes required and with the benefit of having five reactor vessels, more than one polymer sample can be analyzed during a single Crystaf cooling cycle. Furthermore, less solvent are used during the experimental Crystaf procedure in comparison to Tref.

2.2.2.2) Operating procedure

The polymer sample is transferred to a crystallization vessel inside the Crystaf oven. Up to five different samples can be prepared and analyzed during one run. A suitable high temperature solvent (TCB; o-dichlorobenzene, o-DCB) are used to dissolve the polymer at 130 °C. After complete dissolution, the dilute solution is stabilized slightly above the starting temperature. Parameters like stabilization temperature, dissolution temperature, crystallization temperature range and cooling rate can be varied using the Crystaf software and is also dependent on the specific polymer to be analyzed. Similar to Tref, during Crystaf cooling, polymer chains will crystallize from solution according to their crystallizability with the more crystalline chains crystallizing out of solution first. Typical cooling rates used are between 0.l – 0.2 °C/min. Stirring is crucial during the crystallization process in order to keep the concentration uniform throughout the run. At predetermined temperatures during crystallization, small samples of the polymer solution are taken by means of an automated process and sent through the detector. This results in the construction of a cumulative curve, plotting polymer concentration versus crystallization temperature. In order to analyze crystallization peak temperatures, peak widths and amount of material crystallizing, the first derivative of the cumulative curve is taken which lead to construction of the Crystaf profiles. Figures 2.4 and 2.5 display a screenshot of the operating procedure and typical profiles obtained from Crystaf respectively.

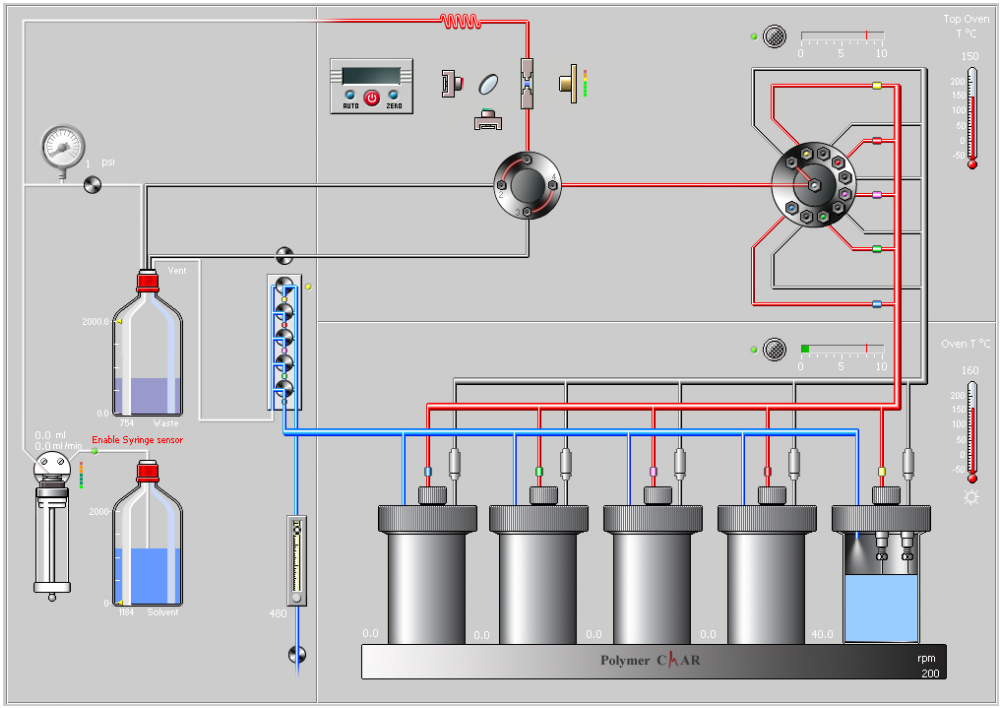

Figure 2.4: Screenshot of solution crystallization procedure during Crystaf analysis.

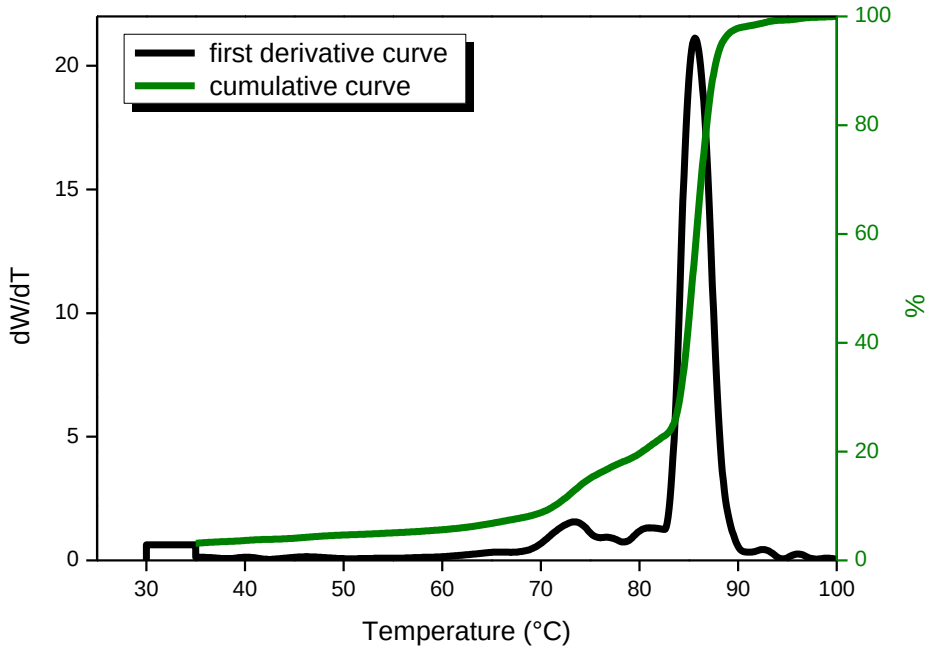

Figure 2.5: Typical Crystaf crystallization profiles: cumulative curve (green) and first derivative curve (black).

2.2.3) Crystallization Elution Fractionation (CEF)

2.2.3.1) Overview

The chemical composition distribution (CCD) of semi-crystalline polymers is one of the most discriminating structural parameters. Usually solution fractionation techniques like aforementioned Tref and Crystaf are used for analysis of these composition distributions. Recently a new technique namely Crystallization Elution Fractionation (CEF) has been developed, combining the separation mechanisms of Tref and Crystaf and also separates according to crystallizability.[14] The CEF procedure can be split into three steps: Step 1 involves the dissolution of polymer sample in a suitable solvent (usually o-DCB) for injection onto the column. Step 2 consists of a dynamic crystallization (similar to Crystaf) event whereby polymer crystallization occurs in the presence of a small flow of solvent to assist the separation process and thus result in superior separation resolution. Step 3 involves the elution of polymer fraction (similar to Tref) with the help of a temperature ramp and solvent flow through the column. Figure 2.6 illustrates the different steps. CEF analysis times are much shorter than the conventional techniques used and one sample can be analyzed within 30 minutes.

Various parameters can influence the separation when using this method of fraction. Some of the parameters are listed below:

- solvent flow rate during crystallization
- solvent flow rate during elution
- heating rate

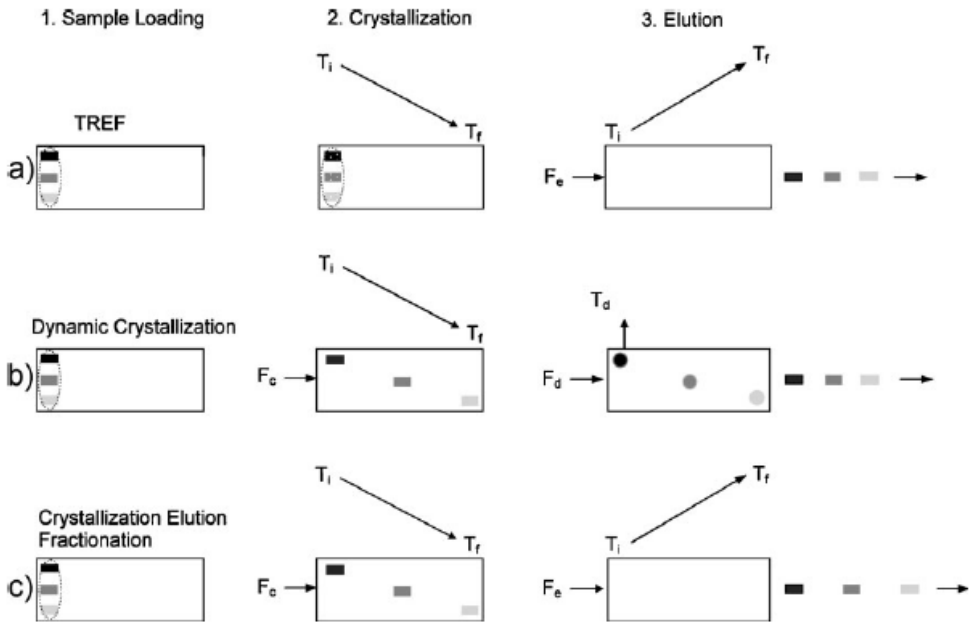

Figure 2.6: Illustration of the various steps involved during a CEF experiment.[14]

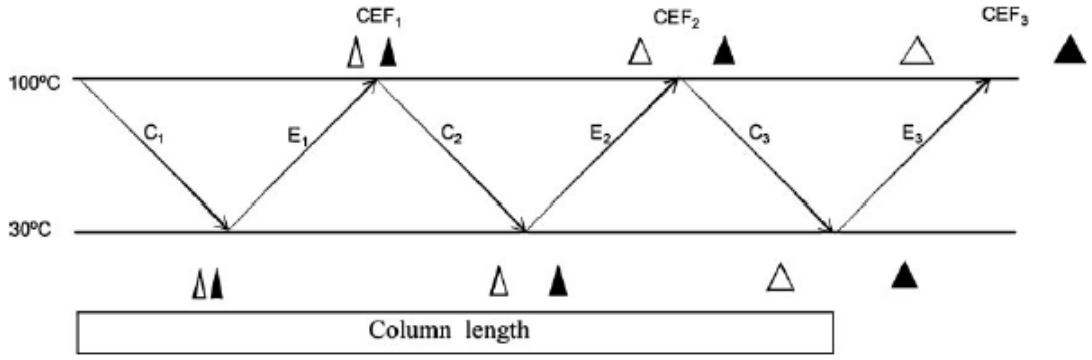

Figure 2.7: Multiple CEF (m-CEF) setup developed by Monrabal et al. to optimization fractionation during the crystallization cycle. [15]

Further optimization was done to the CEF method to minimize co-crystallization events. Monrabal *et al.*[15] realized that optimization was necessary during the dynamic crystallization cycle in the column. They came up with a multiple CEF (m-CEF) setup which consists of several cooling and heating cycles (shown in Figure 2.7). It was shown that with each cycle, extended separation was obtained and co-crystallization could be minimized for closer investigation into the composition distributions. A comparison between CEF and Crystaf was done by Suriya et al. while studying co-crystallization effect in ethylene/1-octene copolymer blends.[16] It was found that CEF provided much better CCD estimations in shorter analysis times as compared to Crystaf, making CEF a very suitable analytical tool for semi-crystalline polymers. Additional emphasis on the advantages of CEF, over Crystaf and Tref, were made during the study of metallocene-catalyzed LLDPE samples.[17] Herein, the effect of comonomer content, co-crystallization of blends, cooling/heating rates and molecular weights were extensively analyzed and found that CEF provided results with superior resolution.

2.2.4) Solution crystallization analysis by laser light scattering (Scalls)

2.2.4.1) Overview of turbidity analysis

The measurement of solution turbidity is not a totally new method for studying crystallization behavior in polymer systems. Reported literature exists from as early as the 1950's where light scattering techniques were applied to gain information on polymer crystallization.[18-21] Molecular characterization of polyethylene solutions was also reported in the 1980's with the use of laser light scattering methods.[22,23] Unfortunately only qualitative information regarding crystallization and polymer microstructure could be obtained at that stage. As a result of more innovative research over the years, more advanced turbidimetric tools were developed. Heck *et al.*[24] made use of time dependent light attenuated measurements to study early stage spherulitic growth based on the Rayleigh-Debye-Gans theory. The motivation of this development was said to be due to the fact that most methods used for studying polymer crystallization kinetics (x-ray scattering, differential calorimetry, dilatometry), has similar sensitivity and initial stages of crystal growth is not taken into account, giving data of crystallinity close to the final values. Several groups have implemented this time dependent light scattering tool.[25,26]

SCB distributions in LLDPE polymers play a major role in the physical and mechanical properties of materials which in turn affects the final application of the polymers. A simplistic turbidity analyzer was developed by Shan *et al.*[27] specifically to study the SCB in polyethylenes. This resulted in comparable data to the conventional Crystaf and Tref techniques with the main advantages being the inexpensive/simple experimental setup, wide variety of solvents that can be used and the ability to track crystallization as well as solution melting events. Following this report, a Scalls instrument was developed in-house by our group and a schematic diagram can be found in Figure 2.8.

2.2.4.2) Scalls experimental procedure

Scalls is a solution fractionation technique based on the intensity measurement of an incident laser beam. The increase and decrease in laser intensity caused by formation and dissolution of polymer crystal allows for the analysis of solution behavior form dilute solutions. Various studies have already been done using this unique analytical method.[28-30] Detailed information concerning the Scalls instrumentation have been discussed in previous literature and can also be found in the experimental section of this manuscript. Only a brief overview on the experimental procedure will be discussed in the sections below.

2.2.4.3) Scalls cooling

Polymer solutions are prepared, transferred to a quartz tube and placed into the sample holder. Thereafter the solution is kept at an elevated temperature to allow for complete dissolution of polymer. At this stage, the intensity of incident laser beam is very high due to the clear solution. Temperature is decreased in a controlled manner to 100 °C and stabilized again. The crystallization cycle follows by controlled cooling to 30 °C. Formation of polymer crystals during cooling results in a scattering of incident beam and thus a decrease in beam intensity (examples of Scalls curves shown in Figure 2.9). The rate at which the intensity decreases allows for analysis of crystallization kinetics. It is known that the ability of a particle to scatter a laser beam is dependent on the wavelength of the beams. Therefore the simultaneous use of lasers with varying wavelengths (blue = 405 nm, green = 432 nm, red = 635 nm) can give useful insight into the rate of crystal growth in solution.

2.2.4.4) Scalls heating

One of the advantages of the Scalls method is the ability to study the solution melting/dissolution behavior of the crystallized material during a single experiment directly after the cooling cycle. A controlled temperature ramp is applied to allow for dissolution of the crystallized polymer (from solution crystallization step). During this step the increase in laser intensity are detected as a result of the dissolution of crystals. Similar to crystallization, the "real time" cumulative raw voltage data curve can be converted into a first derivative curve to analyze peak area, peak width and peak temperatures. Some of the main advantages of Scalls are listed below:

- inexpensive/cost-effective instrumentation setup
- small amounts of solvent used
- short analysis times
- crystallization and dissolution measurements during a single experiment

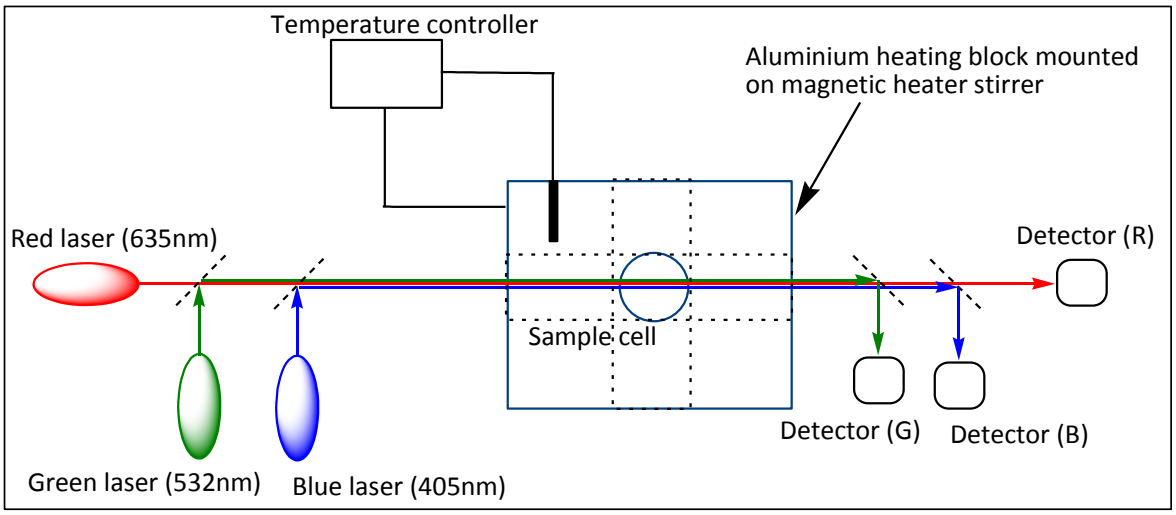

Figure 2.8: Schematic representation of Scalls instrumentation.

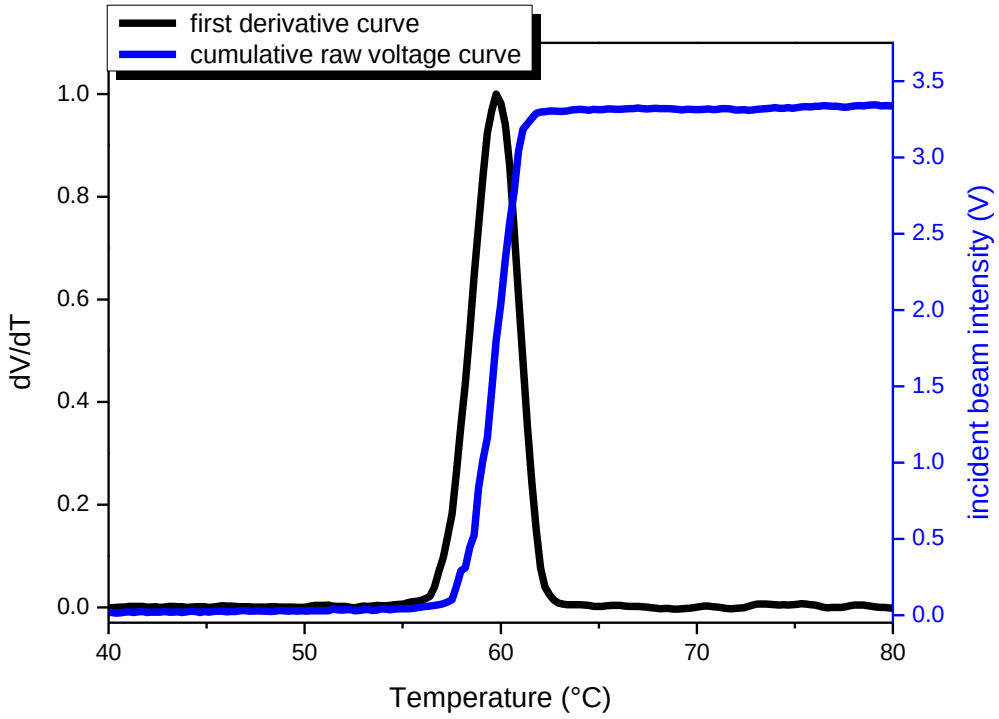

Figure 2.9: Typical Scalls crystallization profiles: raw voltage data (blue) and first derivative curve (black).

2.3) Biopolymers

2.3.1) Introduction

Similar to synthetic polymer systems, biopolymers are made up of several monomeric units to form long polymer chains. Biopolymers are polymers produced from sustainable resources and thus making them biodegradable (degraded by microorganisms and enzymes) and advantageous to use over their more conventional petroleum-based counterparts.[31] Cellulose obtained from plants and isolated by chemical extraction, is the most abundant biopolymer and falls under the polysaccharide biopolymer family which consists of polymeric carbohydrate structures.[32] Two other classes exist namely polypeptides and polynucleotides, which are made up of short amino acids and nucleotide monomers respectively. Currently the major concern to the plastic industry is the lack of ability to properly recycle plastic items after reaching the end of its lifespan and thus opening the door for bio-based materials.[33] The increase in non-biodegradable waste is mainly due to the fact that synthetic polymers have displaced ceramics, wood and metals in a vast number of applications.[34] This is especially true for the packaging industry, making use of mainly polyethylene, poly(propylene), poly(styrene) and poly(vinyl chloride). During recent years, biodegradable and

biocompatible polymers have received great attention both in academics and industry due to their ability to substitute commercially used petroleum-based polymers for several applications. Table 2.1 presents the classification of some biopolymers.

2.3.2) Poly(lactic acid) (PLA)

Among the biopolymers, PLA has been used most extensively, not only for the reasons that it is biocompatible and biodegradable but also because it can be obtained from renewable resources. PLA is a linear aliphatic thermoplastic polyester, generally produced by the ring-opening polymerization of the lactide monomer. Lactide is a cyclic dimer prepared by the controlled polymerization of lactic acid, which in turn is obtained by the fermentation of corn, sugar cane, sugar beet, etc.[35] It has three isomeric forms namely poly(L-lactic acid) (PLLA), poly(D-lactic acid) (PDLA) and poly(DL-lactic acid) (PDLLA) which is a racemic mixture of L-and D-lactic acid. PLA can exhibit a variety of different properties depending on the isomeric forms present. The ease of processing, its stiffness and good strength makes this polymer a promising material and suitable to replace non-degradable commodity plastics. This polymer is a well-defined thermoplastic and will hydrolyze into natural, harmless products and the shelf-life is reasonably good for single-use packaging applications.[36]

PLA is synthesized through ring-opening polymerization (ROP) of lactic acid. Due to different enantiomers, three different lactides can be formed resulting in the different stereo-regular PLA polymers after polymerization. The range of different lactides, obtained from fermentation of the various lactic acids as well as the lifecycle of PLA, is shown in Schemes 2.1 and 2.2 respectively.

Table 2.1: Classification of some commercial biodegradable polymers.[34]

Material class	Manufacturer	Product name
Cellulose acetate	Mazzucchelli	BIOCETA®
	Planet Polymer	EnviroPlastic®-Z
Copolyester	BASF	Ecoflex
	Eastman	Easter Bio™
Polycaprolactone (PCL)	Birmingham Polymers	Poly(ε-caprolactone)
	Planet Polymer	Enviroplastic®-C
	Solvay	CAPA®
	Union Carbide	TONE®
Poly(ester amide)	Bayer	BAK 1095
		BAK 2195
Poly(ethylene terepthalate) (PET)-modified	DuPont	Biomax®
Polyglycolide (PGA)	Alkermes	Medisorb®
	Birmingham Polymers	Poly(glycolide)
	Boehringer Ingelheim	Resomer®
	PURAC	PURASORB® PG
Polyhydroxyalkanoates (PHA)	Metabolix	PHA
	Biomer	Biomer™
	Monsanto	Biopol®
Poly(lactic acid) (PLA)	Alkemers	Medisorb®
	Birmingham Polymers	Poly(L-lactide) & Poly(DL-lactide)
	Boehringer Ingelheim	Resomer®
	Cargill Dow Polymers	EcoPLA®
	Chronopol	Heplon™
	Hygail	PLA
	Neste	Poly(L-lactide)
	PURAC	PURASORB® PL/PD/PDL
Poly(vinyl alcohol) (PVOH)	Idroplast	Hydrolene®
	Novon	Aqua-NOVON®
	Planet Polymer	Aquadro™
	Texas Polymer	Vinex™
Starch & starch blends	AVEBE	Paragon™
	BioPlastic (Michigan)	Envar™
	BIOTEC	Bioplast®, Bioflex®, Biopur®
	Buna Sow Leuna	Sconacell®
	Earth Shell	Starch-based composite
	Midwest Grain	Polytriticum™ 2000
	Novamont	Mater-Bi™
	Novon	Poly-NOVON®
	Starch Tech	ST1, ST2, ST3
Other blends	Alkermers	Medisorb®
	Bio Plastic (Colorado)	Biocomposite material
	Birmingham Polymers	Poly(DL-lactide-co-caprolactone) & Poly(DL-lactide-co-glycolide)
	Boehringer	Resomer®
	Planet Polymer	EnviroPlastic®-U
	PURAC	PURASORB® PLG, PURASORB® PDLG

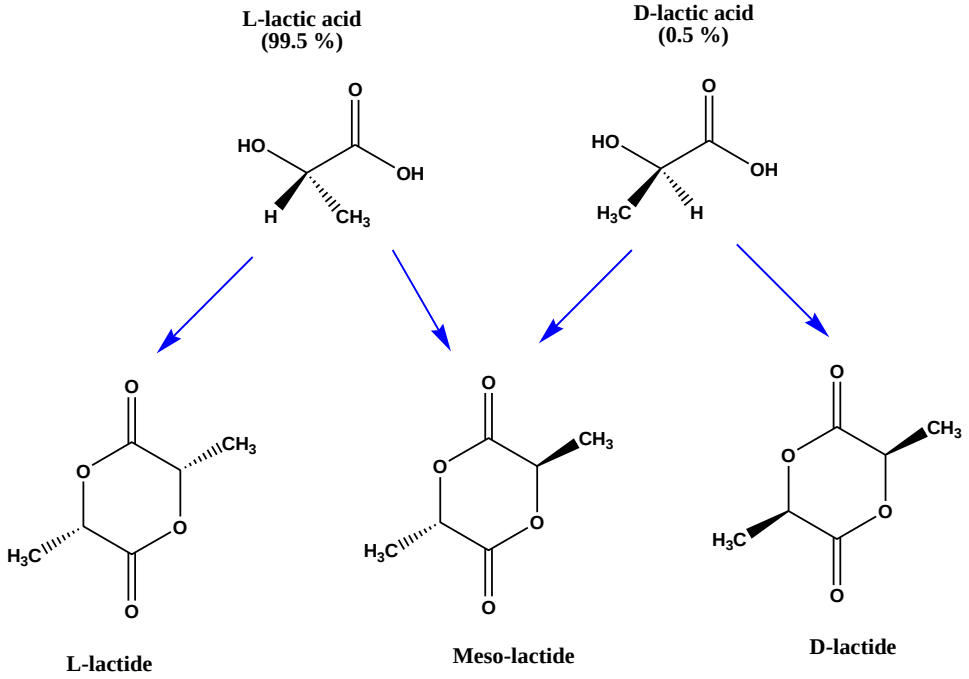

Scheme 2.1: Different lactides formed after fermentation of various lactic acids.

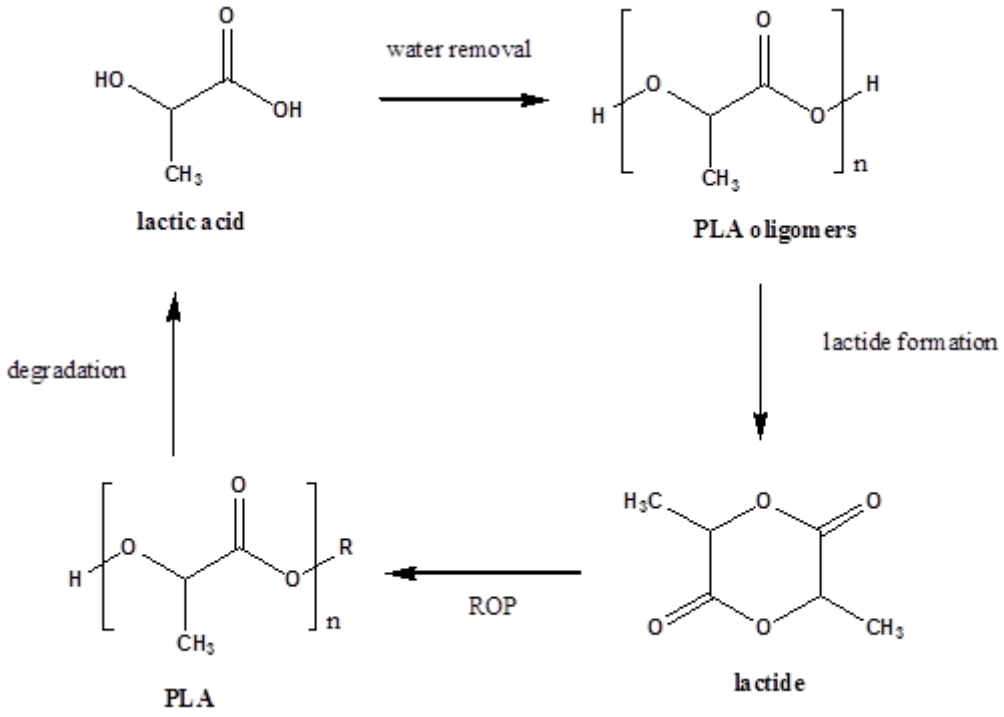

Scheme 2.2: Simplistic schematic of poly(lactic acid) lifecycle.

2.3.2.1) Crystallization kinetics of poly(L-lactic acid) (PLLA)

The major drawback, when it comes to PLA, is the polymer's low rate of crystallization and low crystallinity compared to other commonly used thermoplastics.[37] Ikada et al.[38] was the first to report formation of a stereocomplex when blending PLLA and PDLA in a 1:1 ratio. The stereocomplex displayed a different crystal structure to those of the homopolymers. Since Ikada's findings, extensive work has been done to increase the crystallization rate and to enhance the crystallization of especially PLLA and study the crystal structure of these systems. These include the investigation of asymmetric blends of PLLA and PDLA[37], the effect of blend ratios,[39,40] the nucleation effect of stereocomplex crystals,[41,42] cold-crystallization studies and blending of PLLA with inorganic nucleating agents.[35,43,44] These studies were all done by calorimetric measurements from the melt using DSC. To the best of our knowledge, the crystallization and melting of PLLA and PDLA homopolymers and PLLA/PDLA blends from dilute solutions have not been reported. No research has been carried out on solution crystallization and solution melting behavior of PLA, not even with conventional solution crystallization techniques.

Another approach for increasing the crystallization kinetics as well as lowering costs, when considering certain applications of this polymer, is the blending of PLA with other polymers.[43,45-47] Poly(butylene succinate) (PBS), like PLA, is a aliphatic polyester having excellent biocompatibility and biodegradability. Double melting behavior in addition to recrystallization events for PBS has been reported in literature using differential scanning calorimetry (DSC) and temperature modulated DSC (TMDSC) after non-isothermal crystallization from the melt.[48] Shibata et al.[49] reported that a 99/1 wt% PLLA/PBS blend resulted in higher tensile strength and modulus than neat PLLA, indicating the enhanced effect of PBS on the mechanical properties of PLLA. The effect of blending PBS on PLA crystallization rates was investigated by Yokohara et al.[50] and it was mentioned that these polymers are immiscible in the molten state and displays phase-separated arrangements. Additionally, it was found that addition of PBS accelerates PLA crystallization from the melt whereby molten PBS droplets act as nucleating sites for PLA. This phenomenon was also reported by Zhou et al.[51] when studying the biodegradability and mechanical behavior of PBS/PLLA blends.

2.4) Effect of molecular weight on crystallization

Crystallization of long-chain molecules form the melt gives rise to polycrystalline material with rather complex structures. When considering polymer molecules it is therefore important to understand the effect of chain length on crystallization and melting.[52] Fatou et al. studied the crystallization kinetics of low molecular weight polyethylene fractions and concluded that different three distinct crystal regimes existed within the fractions.[53] This behavior was confirmed by Chiu et al.[54] when looking at the molecular weight (M_w) dependence on melt crystallization of linear polyethylenes. They reported that lower M_w fractions showed higher crystallization rates at similar undercooling but lower rates at the same crystallization temperature. It was also mentioned that the dominant crystal structure was an orthorhombic structure irrespective of M_w or crystal growth regime. Nieto and co-workers made use of Flory's distribution to model the molecular weight dependency of solution crystallization temperature (T_c) in Crystaf.[10] Here it was reported that crystallization peaks broadened with a decrease in molecular weight and the low crystallinity tailing was due to molecules with increased amounts of terminal methyl groups. A sharp increase in T_c was observed but reached a plateau and became independent of molecular weight at M_n = 18 000 g/mol. The estimation equation for modeling this behavior and chain length dependence is given below in Equation 2.1 and Figure 2.10 respectively. Similar work has been done on branched polyethylenes. This includes the study of crystal growth regimes present in various molecular weights, nucleation rates as well as the competing influence of comonomer content (CC) and molecular weight in the case of ethylene/α-olefins (LLDPE samples).[55-57] Comonomer content and molecular weight are both important structural parameters that affect the crystallization behavior of LLDPE and therefore Anantawaraskul et al. analyzed these systems using stochastic simulations. The outcome was that solution crystallization peak temperature was more affected by a variation in (CC) throughout the molecular weight range used thus making CC the more determining factor for T_c in Crystaf.[57]

Various investigations have also been conducted on the effect of molecular weight on crystallization events in isotactic polypropylene (iPP) including the influence on crystal growth regimes.[58-60] For this polymer, the tacticity (isotaticity distributions) and molecular weight are both structural factors contributing towards the positioning of crystallization peaks.[61]

$$T_c = \frac{89(r - 13.3)}{r} - 4.4$$

Tc = crystallization peak temperature

r = polymer chain length (degree of polymerization)

Equation 2.1: Theoretical equation for prediction of crystallization temperature for ethylene homopolymers in Crystaf.[10]

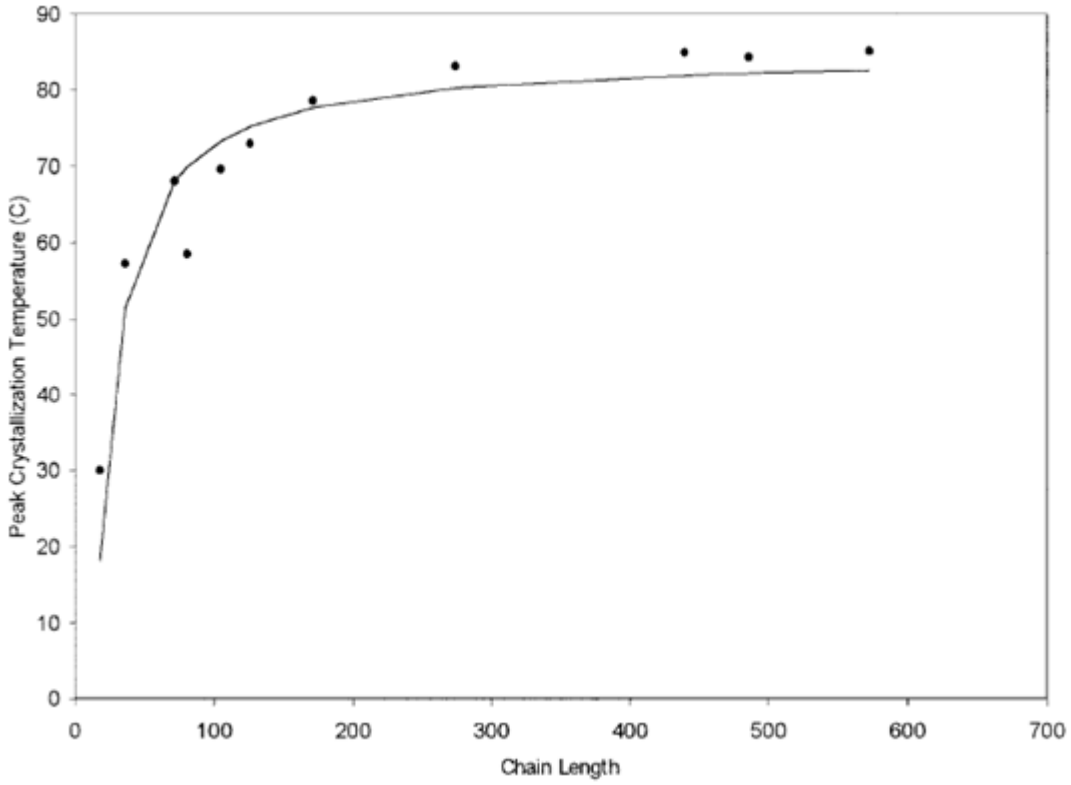

Figure 2.10: Relationship between polymer chain length and Crystaf crystallization peak position for ethylene homopolymers. Theoretical model fit (solid line) and experimental data points.[10]

2.5) Concluding remarks

As discussed in this chapter, various fractionation techniques exist to study crystallization behavior of semi-crystalline polymers; however research of biopolymers in solution is in its infancy. Because biopolymers are becoming suitable alternatives to commodity polyolefin materials due to their biodegradability and biocompatibility, this was the main motivation for the current study. It was therefore decided to investigate these complex biopolymer systems in solution using the Scalls technique as main analytical tool. It was also necessary to compare Scalls data to well-established theoretical models during polyolefin analyses.

2.6) References:

(1) Wild, L. & Glöckner, G. **1991**, "Temperature rising elution fractionation" in *Separation Techniques Thermodynamics Liquid Crystal Polymers*, Springer, , pp. 1-47.

(2) Gloeckner, G. **1990,** "Temperature rising elution fractionation: A review", *Journal of Applied Polymer Science*, vol. 45, no. 0, pp. 1-24.

(3) Soares, J. & Hamielec, A. **1995,** "Temperature rising elution fractionation of linear polyolefins", *Polymer*, vol. 36, no. 8, pp. 1639-1654.

(4) Xu, J. & Feng, L. **2000,** "Application of temperature rising elution fractionation in polyolefins", *European polymer journal*, vol. 36, no. 5, pp. 867-878.

(5) Robertson, D. **2012,** *Studying crystallization kinetics using solution crystallization analysis by laser light scattering (Scalls)*, .

(6) Anantawaraskul, S., Soares, J.B.P. & Wood-Adams, P.M. **2005,** *Fractionation of semicrystalline polymers by crystallization analysis fractionation and temperature rising elution fractionation*.

(7) Monrabal, B. 1996, "Crystaf: Crystallization analysis fractionation. A new approach to the composition analysis of semicrystalline polymers", *Macromolecular Symposia*, Online Library, , pp. 81.

(8) Britto, L.J.D., Soares, J.B.P., Penlidis, A. & Monrabal, B. **1999,** "Polyolefin Analysis by Single-Step Crystallization Fractionation", *Journal of Polymer Science, Part B: Polymer Physics*, vol. 37, no. 6, pp. 539-552.

(9) Pasch, H., Brüll, R., Wahner, U. & Monrabal, B. **2000,** "Analysis of polyolefin blends by crystallization analysis fractionation", *Macromolecular Materials and Engineering*, vol. 279, pp. 46-51.

(10) Nieto, J., Oswald, T., Blanco, F., Soares, J.B. & Monrabal, B. **2001,** "Crystallizability of ethylene homopolymers by crystallization analysis fractionation", *Journal of Polymer Science Part B: Polymer Physics*, vol. 39, no. 14, pp. 1616-1628.

(11) Monrabal, B. **2006,** *Microstructure characterization of polyolefins. TREF and CRYSTAF*.

(12) Fischlschweiger, M., Aust, N., Oberaigner, E.R. & Kock, C. **2010,** "Mathematical modeling and optimization of run parameters of crystallization analysis fractionation (CRYSTAF)", *Macromolecular Chemistry and Physics*, vol. 211, no. 4, pp. 383-392.

(13) Anantawaraskul, S., Soares, J.B.P. & Wood-Adams, P.M. **2004,** "An experimental and numerical study on crystallization analysis fractionation (Crystaf)", *Macromolecular Symposia*, vol. 206, no. 1, pp. 57-68.

(14) Monrabal, B., Sancho-Tello, J., Mayo, N. & Romero, L. **2007,** "Crystallization Elution Fractionation. A New Separation Process for Polyolefin Resins", *Macromolecular Symposia*, vol. 257, no. 1, pp. 71-79.

(15) Monrabal, B., Romero, L., Mayo, N. & Sancho-Tello, J. **2009,** "Advances in Crystallization Elution Fractionation", *Macromolecular Symposia*, vol. 282, no. 1, pp. 14-24.

(16) Suriya, K., Anantawaraskul, S. & Soares, J.B. **2011,** "Cocrystallization of ethylene/1-octene copolymer blends during crystallization analysis fractionation and crystallization elution fractionation", *Journal of Polymer Science Part B: Polymer Physics*, vol. 49, no. 9, pp. 678-684.

(17) Alghyamah, A.A. & Soares, J.B. 2012, "Crystallization Elution Fractionation of LLDPEs Made with Metallocene Catalysts", *Macromolecular Symposia*Wiley Online Library, , pp. 43.

(18) Hawkins, S.W. & Richards, R.B. **1949,** "Light transmission and the formation and decay of spherulites in polythene", *Journal of Polymer Science*, vol. 4, no. 4, pp. 515-522.

(19) Keane, J.J. & Stein, R.S. **1956,** "The scattering of light from thin polymer films. II. Scattering from polyethylene", *Journal of Polymer Science*, vol. 20, no. 95, pp. 327-350.

(20) Levy, B. **1961,** "The development of crystallinity and transparency in irradiated polyethylene", *Journal of Applied Polymer Science*, vol. 5, no. 16, pp. 408-423.

(21) Mayhan, K.G., James, W.J. & Bosch, W. **1965,** "Poly(ethylene terephthalate). I. Study of crystallization kinetics", *Journal of Applied Polymer Science*, vol. 9, no. 11, pp. 3605-3616.

(22) Chu, B., Onclin, M. & Ford, J.R. **1984,** "Laser light scattering characterization of polyethylene in 1, 2, 4-trichlorobenzene", *The Journal of physical chemistry*, vol. 88, no. 26, pp. 6566-6575.

(23) STEJSKAL, J., HORSKA, J. & KRATOCHVIL, P. **1982,** "LIGHT SCATTERING FROM POLYETHYLENE SOLUTIONS.", *J APPL POLYM SCI*, vol. V 27, no. N 10, pp. 3929-3944.

(24) Heck, B., Kawai, T. & Strobl, G. **2006,** "Time dependent light attenuation measurements used in studies of the kinetics of polymer crystallization", *Polymer*, vol. 47, no. 15, pp. 5538-5543.

(25) Hoffmann, A. & Strobl, G. **2003,** "Investigating polymer crystallization by time-dependent light scattering: a direct approach in the data analysis applied for s-polypropylene", *Polymer*, vol. 44, no. 19, pp. 5803-5809.

(26) Somwangthanaroj, A., Lee, E.C. & Solomon, M.J. **2003,** "Early stage quiescent and flow-induced crystallization of intercalated polypropylene nanocomposites by time-resolved light scattering", *Macromolecules*, vol. 36, no. 7, pp. 2333-2342.

(27) Shan, C.L.P., Degroot, W.A., Hazlitt, L.G. & Gillespie, D. **2005,** "A new turbidimetric approach to measuring polyethylene short chain branching distributions", *Polymer*, vol. 46, no. 25, pp. 11755-11767.

(28) Van Reenen, A.J., Rohwer, E.G., Walters, P., Lutz, M. & Brand, M. **2008,** "Development and use of a turbidity analyzer for studying the solution crystallization of polyolefins", *Journal of Applied Polymer Science*, vol. 109, no. 5, pp. 3238-3243.

(29) Van Reenen, A., Brand, M., Rohwer, E. & Walters, P. **2009,** "Solution crystallization analysis by laser light scattering (SCALLS)", *Macromolecular Symposia*, vol. 282, no. 1, pp. 25-32.

(30) Cheruthazhekatt, S., Robertson, D.D., Brand, M., van Reenen, A. & Pasch, H. **2013,** "Solution Crystallization and Dissolution of Polyolefins as Monitored by a Unique Analytical Tool: Solution Crystallization Analysis by Laser Light Scattering", *Analytical Chemistry*, vol. 85, no. 15, pp. 7019-7023.

(31) Barbara, H.S. **2002,** "Polymer analysis", .

(32) Chandra, R. & Rustgi, R. **1998,** "Biodegradable polymers", *Progress in Polymer Science*, vol. 23, no. 7, pp. 1273-1335.

(33) Udipi, K. & Zolotor, A. 1993, "POLYMERS AND THE ENVIRONMENT—THE NEXT DECADE", *Polymers to the year 2000 and beyond: a memorial symposium for Herman F. Mark*John Wiley & Sons, , pp. 109.

(34) Mohanty, A., Misra, M. & Hinrichsen, G. **2000,** "Biofibres, biodegradable polymers and biocomposites: an overview", *Macromolecular Materials and Engineering*, vol. 276, no. 1, pp. 1-24.

(35) Ray, S.S. & Okamoto, M. **2003,** "Biodegradable polylactide and its nanocomposites: opening a new dimension for plastics and composites", *Macromolecular Rapid Communications*, vol. 24, no. 14, pp. 815-840.

(36) Garlotta, D. **2001,** "A literature review of poly (lactic acid)", *Journal of Polymers and the Environment*, vol. 9, no. 2, pp. 63-84.

(37) Sun, J., Yu, H., Zhuang, X., Chen, X. & Jing, X. **2011,** "Crystallization Behavior of Asymmetric PLLA/PDLA Blends", *The Journal of Physical Chemistry B*, vol. 115, no. 12, pp. 2864-2869.

(38) Ikada, Y., Jamshidi, K., Tsuji, H. & Hyon, S.H. **1987,** "Stereocomplex formation between enantiomeric poly (lactides)", *Macromolecules*, vol. 20, no. 4, pp. 904-906.

(39) Woo, E.M. & Chang, L. **2011,** "Crystallization and morphology of stereocomplexes in nonequimolar mixtures of poly(l-lactic acid) with excess poly(d-lactic acid)", *Polymer*, vol. 52, no. 26, pp. 6080-6089.

(40) Yamane, H. & Sasai, K. **2003,** "Effect of the addition of poly(d-lactic acid) on the thermal property of poly(l-lactic acid)", *Polymer*, vol. 44, no. 8, pp. 2569-2575.

(41) Narita, J., Katagiri, M. & Tsuji, H. **2011,** "Highly enhanced nucleating effect of melt-recrystallized stereocomplex crystallites on poly(L-lactic acid) crystallization", *Macromolecular Materials and Engineering*, vol. 296, no. 10, pp. 887-893.

(42) Xu, H., Tang, S. & Chen, J. **2013,** "Unique Crystallization Behavior of Poly(L-lactic acid) Nucleated by Stereocomplex with Different Fine Structure", *Polymer - Plastics Technology and Engineering*, vol. 52, no. 7, pp. 690-698.

(43) Ashabi, L., Jafari, S.H., Khonakdar, H.A., Häussler, L., Wagenknecht, U. & Heinrich, G. **2013,** "Non-isothermal crystallization behavior of PLA/LLDPE/nanoclay hybrid: Synergistic role of LLDPE and clay", *Thermochimica Acta*, .

(44) As' habi, L., Jafari, S.H., Khonakdar, H.A., Kretzschmar, B., Wagenknecht, U. & Heinrich, G. **2013,** "Effect of clay type and polymer matrix on microstructure and tensile properties of PLA/LLDPE/clay nanocomposites", *Journal of Applied Polymer Science*, .

(45) Chen, H., Pyda, M. & Cebe, P. **2009,** "Non-isothermal crystallization of PET/PLA blends", *Thermochimica Acta*, vol. 492, no. 1, pp. 61-66.

(46) Battegazzore, D., Bocchini, S. & Frache, A. **2011,** "Crystallization kinetics of poly(lactic acid)-talc composites", *Express Polymer Letters*, vol. 5, no. 10, pp. 849-858.

(47) Akos, N.I., Wahit, M.U., Mohamed, R. & Yussuf, A.A. **2013,** "Preparation, characterization, and mechanical properties of poly(e-caprolactone)/polylactic acid blend composites", *Polymer Composites*, vol. 34, no. 5, pp. 763-768.

(48) Qiu, Z., Komura, M., Ikehara, T. & Nishi, T. **2003,** "DSC and TMDSC study of melting behaviour of poly (butylene succinate) and poly (ethylene succinate)", *Polymer*, vol. 44, no. 26, pp. 7781-7785.

(49) Shibata, M., Inoue, Y. & Miyoshi, M. **2006,** "Mechanical properties, morphology, and crystallization behavior of blends of poly (l-lactide) with poly (butylene succinate-co-l-lactate) and poly (butylene succinate)", *Polymer*, vol. 47, no. 10, pp. 3557-3564.

(50) Yokohara, T. & Yamaguchi, M. **2008,** "Structure and properties for biomass-based polyester blends of PLA and PBS", *European Polymer Journal*, vol. 44, no. 3, pp. 677-685.

(51) Zhou, J., Wang, X., Hua, K., Duan, C., Zhang, W., Ji, J. & Yang, X. **2013,** "Enhanced mechanical properties and degradability of poly(butylene succinate) and poly(lactic acid) blends", *Iranian Polymer Journal (English Edition)*, vol. 22, no. 4, pp. 267-275.

(52) Fatou, J. & Mandelkern, L. **1965,** "The Effect of Molecular Weight on the Melting Temperature and Fusion of Polyethylene1", *The Journal of physical chemistry*, vol. 69, no. 2, pp. 417-428.

(53) Fatou, J.G., Marco, C. & Mandelkern, L. **1990,** "The crystallization kinetics of low-molecular-weight polyethylene fractions", *Polymer*, vol. 31, no. 5, pp. 890-898.

(54) Chiu, F.-., Fu, Q. & Hsieh, E.T. **1999,** "Molecular weight dependence of melt crystallization behavior and crystal morphology of low molecular weight linear polyethylene fractions", *Journal of Polymer Research*, vol. 6, no. 4, pp. 219-229.

(55) Lambert, W.S. & Phillips, P.J. **1996,** "Crystallization kinetics of fractions of branched polyethylenes: 2. Effect of molecular weight", *Polymer*, vol. 37, no. 16, pp. 3585-3591.

(56) Shen, H., Xie, B., Yang, W. & Yang, M. **2013,** "Non-isothermal crystallization of polyethylene blends with bimodal molecular weight distribution", *Polymer Testing*, vol. 32, no. 8, pp. 1385-1391.

(57) Anantawaraskul, S., Soares, J.B., Wood-Adams, P.M. & Monrabal, B. **2003,** "Effect of molecular weight and average comonomer content on the crystallization analysis fractionation (Crystaf) of ethylene α-olefin copolymers", *Polymer*, vol. 44, no. 8, pp. 2393-2401.

(58) Cheng, S.Z., Janimak, J.J., Zhang, A. & Cheng, H. **1990,** "Regime transitions in fractions of isotactic polypropylene", *Macromolecules*, vol. 23, no. 1, pp. 298-303.

(59) Arranz-Andrés, J., Peña, B., Benavente, R., Pérez, E. & Cerrada, M. **2007,** "Influence of isotacticity and molecular weight on the properties of metallocenic isotactic polypropylene", *European polymer journal*, vol. 43, no. 6, pp. 2357-2370.

(60) Arranz-Andrés, J., Suárez, I., Peña, B., Benavente, R., Pérez, E. & Cerrada, M.L. **2007,** "Metallocenic isotactic poly(propylene) and its copolymers with 1-hexene and ethylene", *Macromolecular Chemistry and Physics*, vol. 208, no. 14, pp. 1510-1521.

(61) Lu, H., Qiao, J., Xu, Y. & Yang, Y. **2002,** "Effect of isotacticity distribution on the crystallization and melting behavior of polypropylene", *Journal of Applied Polymer Science*, vol. 85, no. 2, pp. 333-341.

Chapter 3

Experimental

This chapter focuses on the materials studied and experimental techniques used for analysis during this study.

3.1) Materials

Poly(L-lactic acid) (PLLA, Purasorb® PL) and poly(D-lactic acid) (PDLA, Purasorb® PD) were supplied by Purac Co. (Netherlands). Poly(1,4-butylene succinate) (PBS) extended with 1,6-diisocyanatohexane was purchased from Sigma-Aldrich. The polymers were used as obtained from suppliers. 1,2,4-Trichlorobenzene (TCB, spectrophotometric grade, (Sigma-Aldrich, > 99 % purity) were used as purchased.

A commercially available metallocene-catalyzed ethylene-1-octene copolymer from the Engage™ range was obtained from Dow Chemical Co. The weight-average molar mass (M_w) and PDI was 224 kg/mol and 2.9 respectively, and polymer samples were used as obtained from the supplier. All solvents were used as purchased: TCB and o-DCB (spectrophotometric grade, >99% purity, Sigma-Aldrich); decalin (synthesis grade, Merck) and reagent grade xylene.

A series of linear polyethylene (PE) standards were purchased from PSS (Polymer Standard Service, Germany). Weight - average molecular weight (M_w) ranged from 1 200 – 181 000 g/mole and polydispersity index (PDI) varied between 1.1 and 1.6.

3.2) Sample preparation

3.2.1) PLLA/PDLA

Sample concentrations were kept constant at 1 mg/ml. The solutions were made up by dissolving 20 mg of polymer in 20 ml TCB. For PDLA/PLLA specimens, homopolymers were transferred to the quartz sample holder containing the TCB. Samples were thus solution mixed within the tube during the dissolution process before crystallization studies started. The labeling was as follows: DL10/90 refers to a blend containing 10 wt% PDLA and 90 wt% PLLA.

3.2.2) PLLA/SC

Following the DL50/50 analyses, stereocomplex crystals were isolated from this blend. Blends of PLLA/SC were prepared in various blend ratios through the addition of small amounts of SC (up to 10wt%) to PLLA. Sample concentrations were 1 mg/ml in TCB.

3.2.3) PLLA/PBS

Blends of PLLA and PBS were obtained by mixing the neat polymers in various ratios. Mixing compositions for PLLA/PBS blends were: 100/0, 90/10, 70/30, 50/50, 30/70, 10/90 and 0/100 wt%. Sample concentration and stirring speed were fixed at 1 mg/ml and 500 rpm respectively.

3.3) Experimental techniques

3.3.1) Solution crystallization analysis by laser light scattering (Scalls)

A general schematic representation of the Scalls setup was shown in the preceding chapter. Figures 3.1 and 3.2 provide some graphical images of the instrumentation. The development along with detailed information regarding the layout has been discussed in literature.[1-3] The technique is based on the measurement of laser light intensity. A quartz tube containing the polymer solution is placed in a special opening within an aluminum block, mounted on a magnetic heater stirrer. Upon cooling, polymer crystals are formed which scatters the laser beam and results in a decrease in laser intensity. Likewise, during heating, the increase in laser intensity is measured due to dissolution of polymer. Openings in the block allow the laser beam to pass through the solution and the changes in laser beam intensity are picked up by photodiode detectors. The first derivative of the raw voltage data allow for the analysis of peaks associated with crystallization and dissolution events. Three lasers with wavelengths of 405 nm (denoted blue), 532 nm (green) and 635 nm (red) were used. Crystallization studies were done by controlled cooling of polymer solutions from 100 °C to 30 °C at various rates between 0.2 °C/min and 3 °C/min. Heating rates were kept constant at 1 °C/min and solutions were heated from 30 °C to 130 °C during dissolution analyses. Stirring speed was set to 500 rpm. Reproducibility runs were also done during the study for confirmation of results obtained.

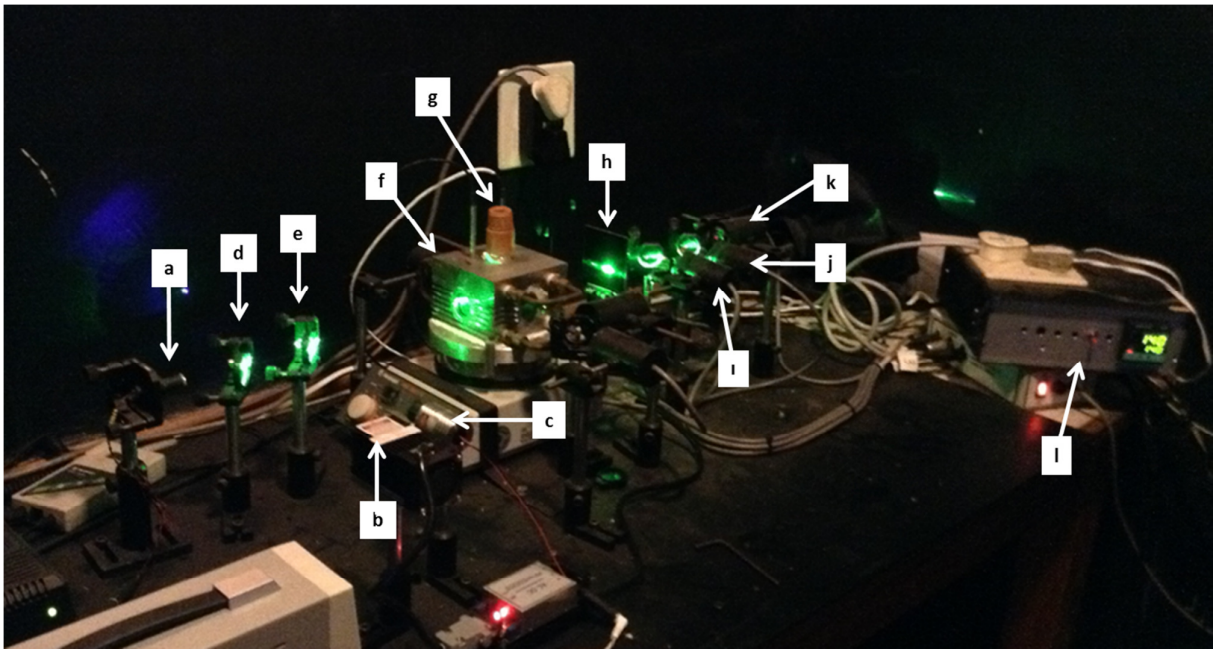

Figure 3.1: Visual image of Scalls experimental setup.

Figure 3.1 annotations:

a) red laser (635nm)
b) green laser (532nm)
c) blue laser (405nm)
d) dichromic mirror
e) dichromic mirror
f) aluminum block
g) sample holder
h) neutral-density filter
i) detector
j) detector
k) detector
l) temperature controller

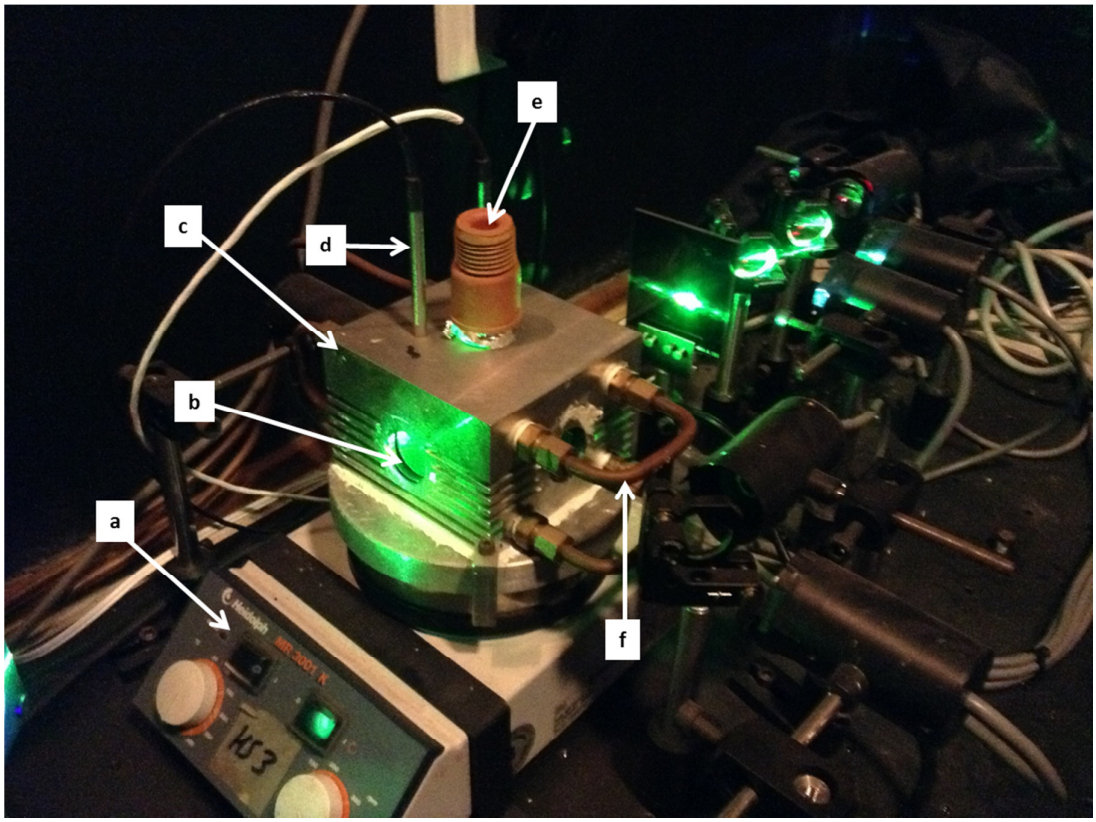

Figure 3.2: Scalls aluminum block with quartz sample holder.

Figure 3.2 annotations:

a) magnetic heater/stirrer
b) opening for incident laser beams
c) aluminum block
d) temperature probe
e) quartz sample holder
f) water channel

3.3.2) Differential scanning calorimetry (DSC)

Thermal analysis studies were done by DSC under N_2 atmosphere. The instrument used was a TA Instruments Q100 calorimeter calibrated with an indium metal standard according to standard procedures. Specific cooling and heating rates are given within the respective results sections of this dissertation.

3.3.3) Attenuated Total Reflectance – Fourier Transform Infrared Spectroscopy (ATR-FTIR)

Infrared analyses of the crystallized material were done using a Nicolet iS10 Spectrometer (Thermo Scientific) equipped with a zinc selenide (ZnSe) crystal. Spectral resolution was 4 cm^{-1} and 32 scans were recorded per sample. Data collection and processing were done with Thermo Scientific OMNIC software.

3.3.4) Dynamic Light Scattering (DLS)

Polymer solutions from Scalls analyses were diluted with TCB to 0.5 mg/ml, to avoid saturation of detector, and transferred to a glass cuvette. DLS measurements were conducted with a Malvern Zetasizer Nano S instrument, operating at 30 °C. The wavelength of operation was 633 nm.

3.3.5) Scanning Electron Microscopy (SEM)

SEM was used to study the surface morphology of polymer films formed through solution casting after Scalls analyses. A Leo® 1430VP scanning electron microscope was used and the samples were gold-coated before the imaging procedure.

3.4) References:

(1) Van Reenen, A.J., Rohwer, E.G., Walters, P., Lutz, M. & Brand, M. **2008,** "Development and use of a turbidity analyzer for studying the solution crystallization of polyolefins", *Journal of Applied Polymer Science,* vol. 109, no. 5, pp. 3238-3243.

(2) Van Reenen, A., Brand, M., Rohwer, E. & Walters, P. **2009,** "Solution crystallization analysis by laser light scattering (SCALLS)", *Macromolecular Symposia,* vol. 282, no. 1, pp. 25-32.

(3) Cheruthazhekatt, S., Robertson, D.D., Brand, M., van Reenen, A. & Pasch, H. **2013,** "Solution Crystallization and Dissolution of Polyolefins as Monitored by a Unique Analytical Tool: Solution Crystallization Analysis by Laser Light Scattering", *Analytical Chemistry,* vol. 85, no. 15, pp. 7019-7023.

Chapter 4

Results and Discussion:

PLLA/PDLA blends

This chapter focuses on the results obtained for PLLA/PDLA binary blends; studying the effect of PDLA addition on the solution behavior of PLLA.

The bulk of this chapter has been published in the journal Polymer Testing:

D.D. Robertson, R. Neppalli, A.J. van Reenen, Solution crystallization analysis of poly(lactic acid) by Scalls: A facile approach for thermal analysis of polymers in solution, Polymer Testing (2014), doi: 10.1016/j.polymertesting.2014.08.015.
Accepted 13 August 2014; Available online 4 September 2014.

The influence of poly(D-lactic acid) (PDLA) on the solution behavior of poly(L-lactic acid) (PLLA) is discussed in this chapter. Effects on solution crystallization kinetics, dissolution kinetics, particle size of crystallites and surface morphology are discussed and some conclusions drawn.

4.1) PLLA and PDLA homopolymers

The crystallization profiles, as obtained from Scalls for PLLA and PDLA polymers are shown in Figure 4.1 where Figure 4.1a) and 1b) represents the raw voltage data for the blue laser signal response during cooling at different controlled rates (0.2 to 3.0 °C/min). The decrease in voltage correlates to a decrease in laser intensity, so as soon as crystals are formed in solution, the laser beam is scattered and a decrease in laser intensity is detected. From the first derivative plots (Figure 4.1c) and 4.1d), it is clear that both PLLA and PDLA crystallization phenomena can be tracked in solution due to the presence of well-defined and distinct peaks. This is advantageous due to the fact that biocompatible and biodegradable polymers such as PLA will, in the near future, become suitable alternatives to traditional petroleum-based polymers. Blends of PLA with petroleum-based polymers might soon become appropriate options and therefore it is necessary to first understand the behavior of neat PLA in solution, hence the motivation for this study.

For both enantiomeric forms, solution peak temperatures (T_c) shifted towards lower values with an increase in cooling rate. Figure 4.2 illustrates the decrease in peak temperatures. A broadening in peak width was also directly related to an increase in the cooling rate. Information on crystallization kinetics such as crystallization time can be acquired when looking at peak widths and slopes of the laser response. A steeper slope for the laser response correlates to a narrower peak which indicates that crystallization occurred over a wide temperature range when moving to higher rates. Because Scalls is a direct intensity measuring method, it provides real-time information on solution phenomena, unlike Crystaf where solution concentration changes are measured in a “delayed” fashion.

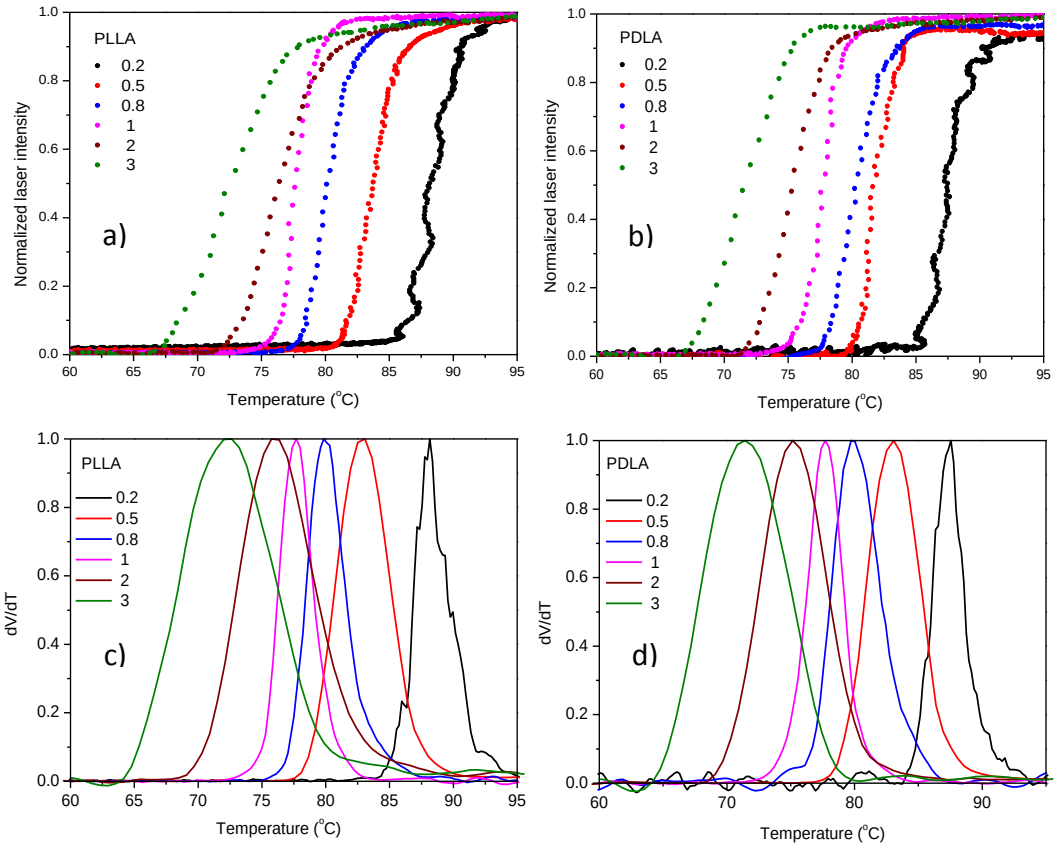

Figure 4.1: Overlays of normalized Scalls cooling profiles for PLLA and PDLA pristine polymers (different cooling rates). (a) and (b) represents the raw data laser response for PLLA and PDLA respectively. (c) PLLA and (d) PDLA are the resultant first derivative curves.

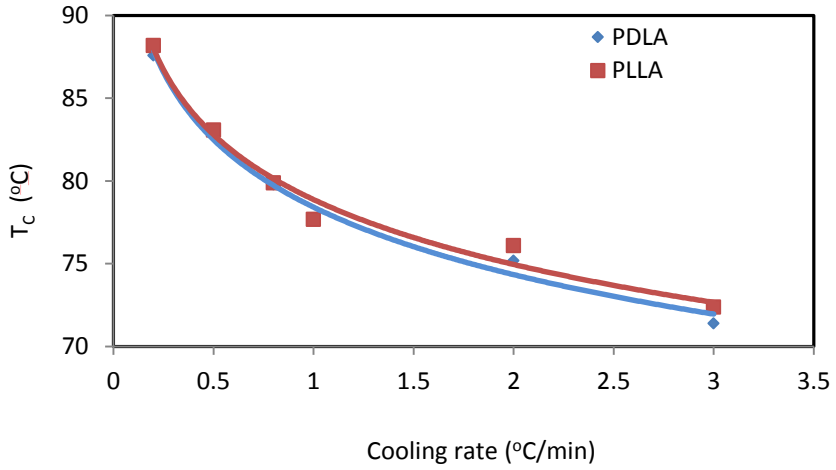

Figure 4.2: Plots of cooling rate *versus* crystallization peak temperature (T_c) for PDLA and PLLA.

Figure 4.3 compares the crystallization profiles of PLLA and PDLA at different cooling rates. With the lowest cooling rate, i.e. 0.2 °C/min, some shoulders on the main peak were observed, which can be attributed to the structural changes at molecular level in solution during the crystallization process. All other conditions resulted in smooth uni-modal profiles, indicating slightly more uniform crystallization at these rates. As expected, no major difference in T_c were observed throughout the cooling rate range for the two enantiomers. The main difference was the earlier onset of crystallization for PLLA at higher cooling rates, indicating definite differences in crystallization behavior and kinetics for the two optical isomers under these conditions, when subjected to higher cooling rates.

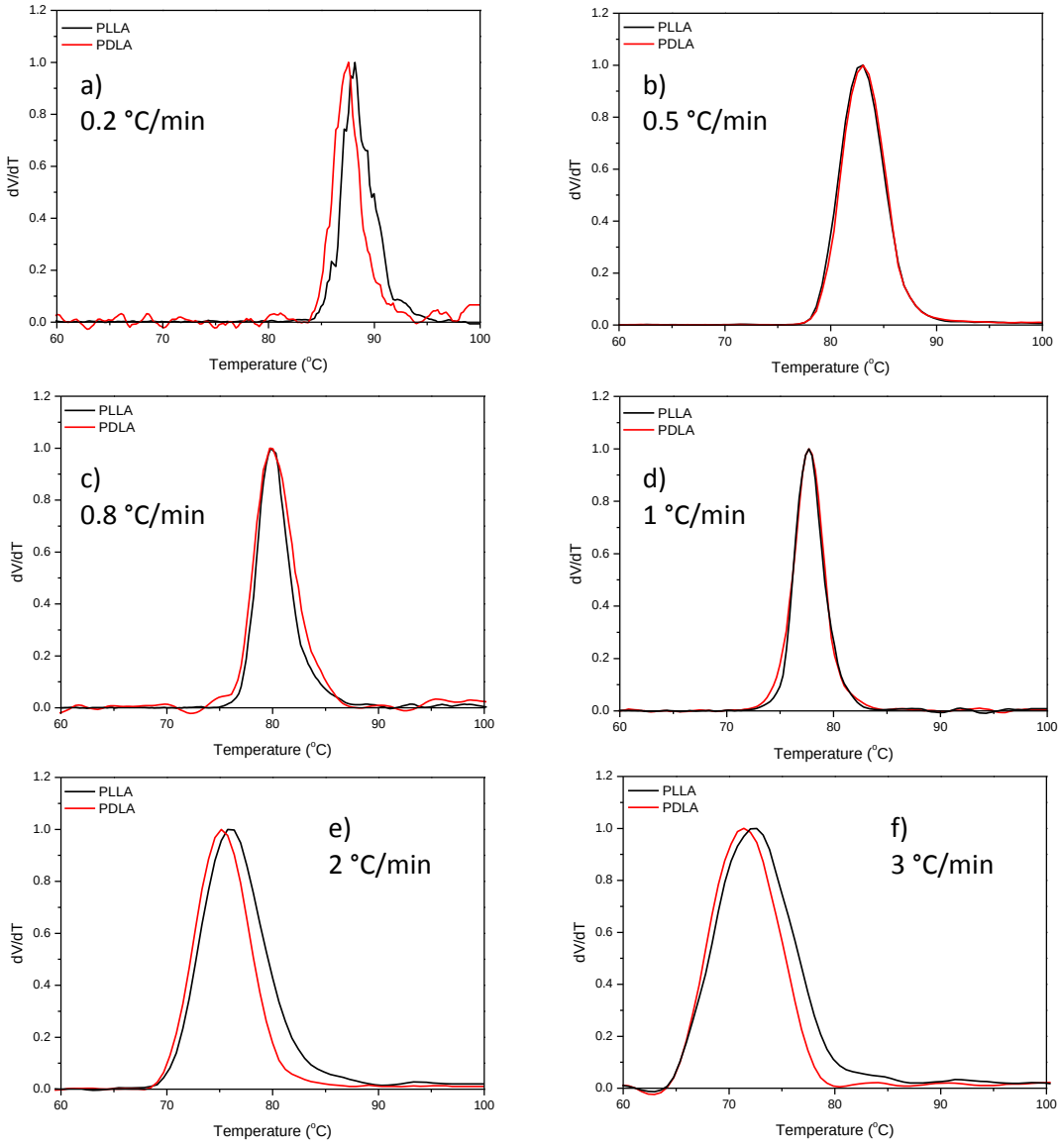

Figure 4.3: Overlay of PDLA and PLLA at different cooling rates. (a) 0.2 °C/min, (b) 0.5 °C/min, (c) 0.8 °C/min, (d) 1 °C/min, (e) 2 °C/min, (f) 3 °C/min.

4.2) PLLA/PDLA blends

The effect of the addition of PDLA on the thermal behavior of PLLA from the melt has extensively been studied by several groups.[1-5] Tsuji et al.[6] studied the effect of stereocomplex crystals (SC) as nucleating agent during melt crystallization and reported that the crystallization peak temperature shifts towards slightly higher temperatures as PDLA content was increased. The molecular weight of the PDLA used also significantly affects the behavior and formation of stereocomplex crystals.[5] In Figure 4.4, a comparison of crystallization peaks during first non-isothermal cooling of pristine polymers and their blends are shown. The first noticeable difference was the shift in T_c towards the lower temperature region when PDLA-content was increased from 10 wt% to 50 wt%. This phenomenon is entirely contradictory to the melt crystallization.[6] The main reason would probably be the difference in polymer chain mobility in the melt and solution. Stereocomplex nucleation sites could have disturbed the PLLA chain mobility because stereocomplex crystals will preferentially form. There will also be homocrystallites forming during cooling as there are only a limited number of PDLA crystallites that will be able to associate with PLLA to form SC. In this manner an increase in SC could hinder homocrystallite association, resulting in a lower T_c for the blends with higher PDLA concentrations as compared to the neat polymers. It might therefore be assumed that solvent effects play an important role during poly(lactic acid) solution crystallization especially for PLLA/PDLA blends.

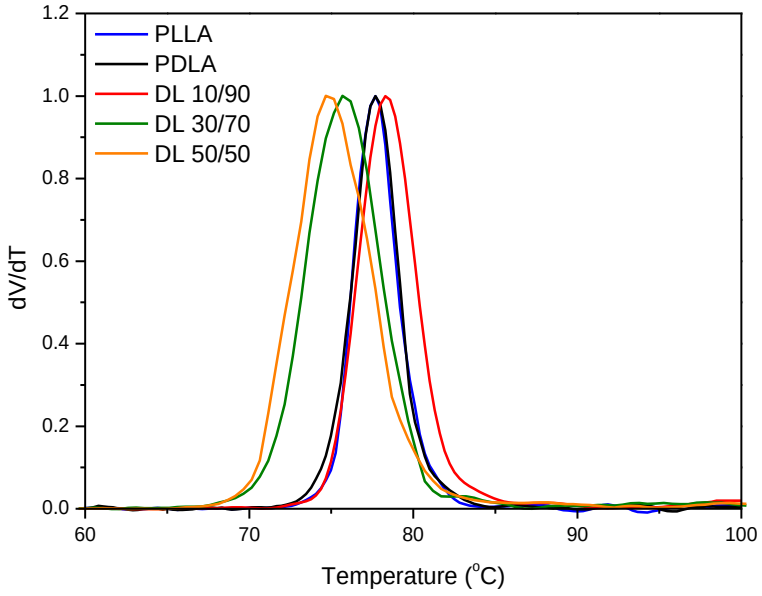

Figure 4.4: Comparison of Scalls first cooling profiles for PLA homopolymers and blends with various D/L blend ratios with cooling of 1 °C/min.

4.2.1) Stereocomplex formation

As mentioned earlier, blending of enantiomeric poly(lactides) results in the formation of stereocomplex crystals upon crystallization from the melt.[1-5] To study the possible formation of SC during solution crystallization, it was decided to heat up the turbid mixtures obtained from the first cooling cycle to 130 °C to allow for the dissolution of homopolymer crystallites. During this period, the laser intensities increased sharply as the solution became less turbid due to dissolution of polymer crystals. If any SC were formed during the first cooling it would stay unmelted at this point. The polymer solutions were then subjected to a second cooling cycle to study if any noticeable variations could be identified between the two cooling profiles. Figure 4.5a) and 4.5b) illustrate the peak overlays for PLLA and PDLA respectively. It is clear to see that near perfect fits were obtained and data was very identical for two sequential crystallization events when looked at features such as peak shapes, crystallization onset and crystallization peak temperatures. Solutions of PLLA/PDLA blends with varying PDLA-content were also subjected to similar sequential cooling cycles as the pristine polymers. Remarkably, the profiles for the blends differed when comparing the first and second cooling results. Noticeable changes were seen in the T_c values as well as the onset of crystallization. T_c values shifted marginally towards higher temperature during second cooling, though the changes were not significant. The major difference was certainly the onset of crystallization, which increased and shifted towards the higher temperature range. This behaviour was observed for all blend compositions and is shown in Figure 4.6. As this behavior was not observed for pristine polymers, but in the blends, it can be attributed to the nucleating effect of PDLA on PLLA crystallization due to the unmelted SC present at the start of the second cooling. The unmelted SC resulted in an earlier onset of crystallization, by creating nucleation sites for the formation of homocrystallites, when compared to the first cooling. But as the PDLA content (and amount of stereocomplex crystallites) increased, it became more difficult for homocrystals to associate and hence the lowering of T_c during both coolings when compared to pristine polymers. Increasing PDLA content to 30 wt% and higher, had a confining effect on PLLA crystallization As there is no literature to fall back on, this appeared to be the first evidence of possible SC formation during solution crystallization of blends of enantiomeric poly(lactide).

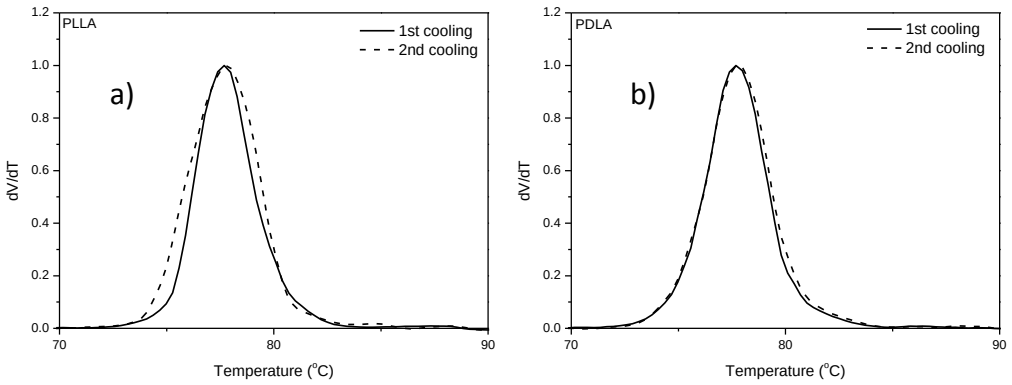

Figure 4.5: Overlays of first and second cooling of PLA enantiomers: (a) PLLA, (b) PDLA.

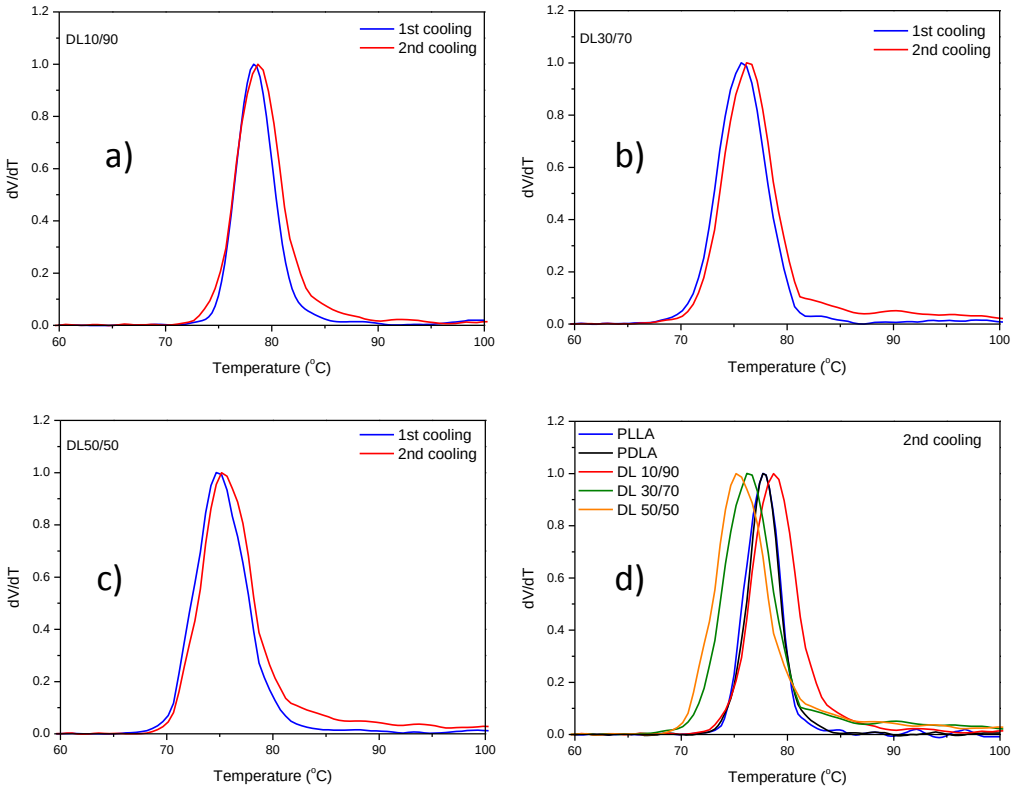

Figure 4.6: First and second cooling overlays are illustrated for the respective blends in (a) DL10/90, (b) DL30/70 and (c) DL50/50. (d) Represents the second cooling for the neat polymers and blends. (cooling rate of 1 °C/min)

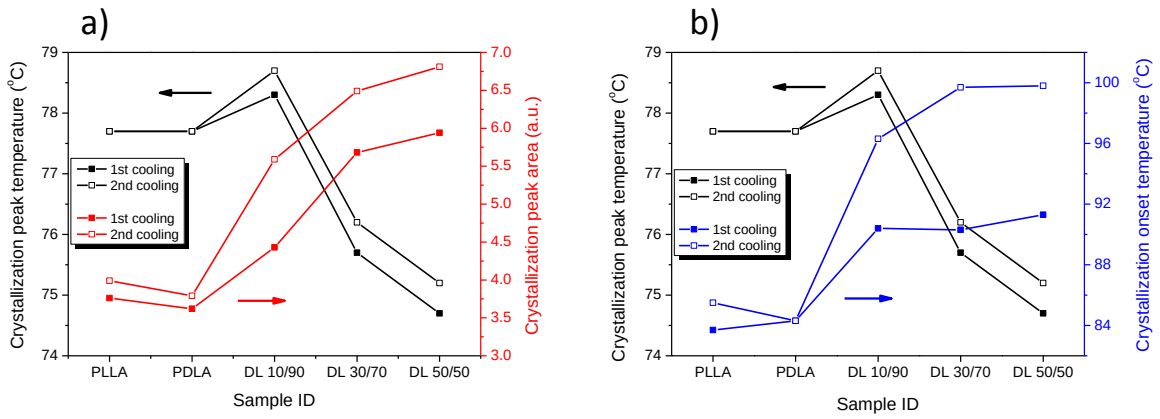

Figure 4.7: Scalls data for 1st and 2nd cooling of homopolymers and blends, a) crystallization peak temperature and crystallization area, b) crystallization peak temperature and crystallization onset temperature.

Crystallization peak areas, which are directly related to the amount of crystallized material as well as the crystallinity of samples, were calculated and represented in Figure 4.7a). The results from the crystallization onset (Figure 4.7b) and peak areas complement each other very well, both increasing with an increase in PDLA content. Table 1 illustrates the increase in crystallization peak areas and hence an increase in the amount of crystallized material for the binary blends as compared to neat PLLA. An evident increase was noticed suggesting that PLLA crystallization kinetics were increased in the presence of PDLA in dilute solution.

Table 4.1: Amount of material crystallized in D/L blends relative to neat PLLA

Sample	Percentage increase in amount of material crystallized w.r.t. neat PLLA (%)	
	1st cooling	2nd cooling
DL10/90	17.8	40.1
DL30/70	51.1	62.7
DL50/50	58.0	70.7

Although the multiple dissolution peaks (shown later in Figure 4.15a) for PLA homocrystallites (around 105 °C and 120 °C) and onset of SC dissolution transitions (around 155 °C) could be observed with Scalls, it was not possible to obtain fully resolved dissolution peaks for SC in the higher temperature range as the setup at time of this study did not allow for dissolution analyses much higher than 160 °C. It is well-known that poly(lactide) stereocomplex crystals formed during melt crystallization of PLLA/PDLA blends, melts at temperatures above 200 °C, much higher than the homocrystallites.[3,7,8] To acquire further evidence of SC formation, the crystallized material from Scalls were analyzed by DSC. Melting endotherms of SC crystallites were visible at roughly 225 °C for the binary blends (peaks absent for homopolymers) and can be observed in Figure 4.8. The melting enthalpies for these peaks increased with an increase in PDLA content and are represented in Table 4.2. Besides the SC endotherms, three other events namely melting (T_{m1}), re-crystallization and re-melting (T_{m2}) due to PLA homocrystallites were visible at around 157 °C, 160 °C and 178 °C respectively. Peak temperatures of these transitions were unaffected by PDLA addition. However, enthalpies of these homocrystallite endotherms decreased (see Table 4.3) with increasing concentration of PDLA confirming that less homocrystallites and more SC crystallites formed in the presence of PDLA during non-isothermal solution crystallization of the PLLA/PDLA blends.

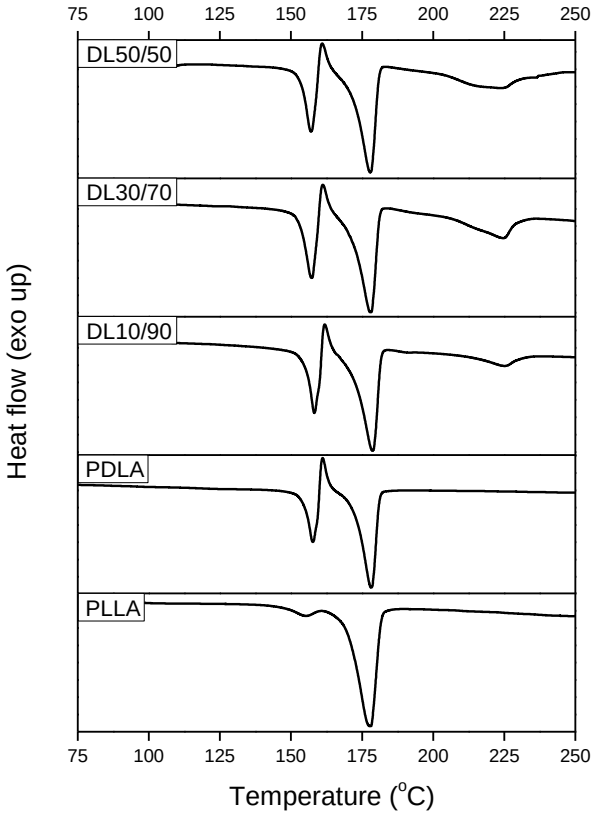

Figure 4.8: DSC heating thermographs (first heating) for PLA samples after Scalls analyses.

Table 4.2: DSC data of stereocomplex endotherm for PLLA/PDLA blends after Scalls

Sample	SC T_m (°C)	SC ΔH_f (J/g)
DL10/90	225.2	7.2
DL30/70	224.7	13.1
DL50/50	224.0	18.2

Table 4.3: DSC data of homocrystallite endotherms after Scalls

Sample	T_{m1} (°C)	ΔH_{m1} (J/g)	T_{m2} (°C)	ΔH_{m2} (J/g)
PLLA	155.0	2.6	177.9	49.8
PDLA	157.7	17.5	178.1	53.2
DL10/90	158.3	17.4	178.8	42.8
DL30/70	157.4	15.2	178.2	37.2
DL50/50	157.1	13.8	177.9	36.2

However, some valuable information could be obtained from the Scalls solution melting results for the homocrystallites. Figure 4.9 shows an overlay of heating profiles for homopolymers and blends after cooling at 1 °C/min and represents the laser intensity response as a function of temperature. An increase or decrease in laser intensity refers to dissolution or crystallization events respectively. Four distinct events were detected and marked as regions (a) to (d). Regions (a), (c) and (d) represent the multiple melting behavior of PLA similar to the DSC endotherms shown previously and can be seen by the strong increase in laser intensity due to the dissolution of homocrystallites back into solution. A slight decrease in laser intensity was seen in region (b) relating to recrystallization events. These recrystallization events emphasize the low crystallization kinetics of

PLA upon cooling. Interestingly, the decrease in laser intensity observed in this region were much more subtle for the blends than for the pristine polymers and suggest that the addition of PDLA lead to an increase in solution crystallization kinetics, resulting in less re-organization of polymer chains during dissolution. This provides critical information with regards to applications of PLA, as thermal properties are directly related to certain applications of these biopolymer materials.[9]

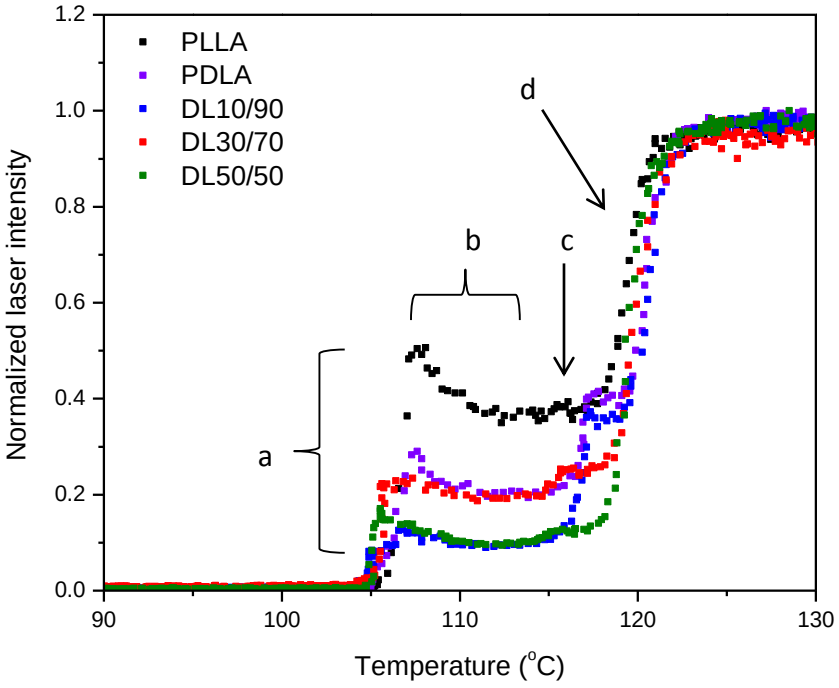

Figure 4.9: Detector responses for solution melting of PLLA, PDLA and their blends heated at 1 °C/min. (After cooling at 1 °C/min)

4.2.2) Effect on particle size

This section deals with the effect of PDLA addition on the crystallite particle size distribution of PLLA/PDLA binary blends after solution crystallization by Scalls. As mentioned before, it is known that PDLA leads to a nucleating effect via the formation of SC in these blends. To gain further insight into the crystal growth rates, the laser light scattering data of two lasers with different wavelengths (blue = 405 nm; red = 635 nm) were compared. Here, we focused on the relative shifts in peak position as detected by the different laser beams. Smaller particles will scatter the blue laser (lower wavelength) first followed by the higher wavelength beam at larger crystallite sizes. Figure 4.10 illustrates an overlay of Scalls crystallization profiles obtained by the different laser beams for two consecutive cooling experiments. After the first cooling (Figures 4.10a – 4.10c) no noticeable difference was observed when comparing the various blends in terms of peak positioning relative to each other. It can therefore be assumed that the crystal growth rate were almost identical during this cooling step regardless of PDLA concentration. Slightly different findings were made after the second cooling (Figures 4.10d – 4.10f) with the most obvious being the earlier onset of crystallization due to unmelted SC present in solution at the start of crystallization and thus nucleating PLLA crystallization. A higher PDLA content resulted in more SC formation and hence the more enhanced nucleation with increase in PDLA content. Apart from the onset of crystallization being different, the spacing between blue and red laser profiles were similar for DL30/70 and DL50/50 blends. This indicates that although crystallization occurred at an earlier stage with 50 wt% PDLA, the growth rate were almost identical to the blend containing 20 wt% less PDLA (DL30/70). Interestingly, for the DL10/90 sample, a much higher degree of peak overlapping was observed, suggesting that the crystal growth rate were somewhat different at lower PDLA concentrations. Furthermore the overlapping of peaks indicate that polymer crystallites grew at a faster rate in DL10/90, reaching a bigger size sooner than in the other two blend compositions and finally resulted in virtually simultaneous scattering of the different wavelength laser beams.

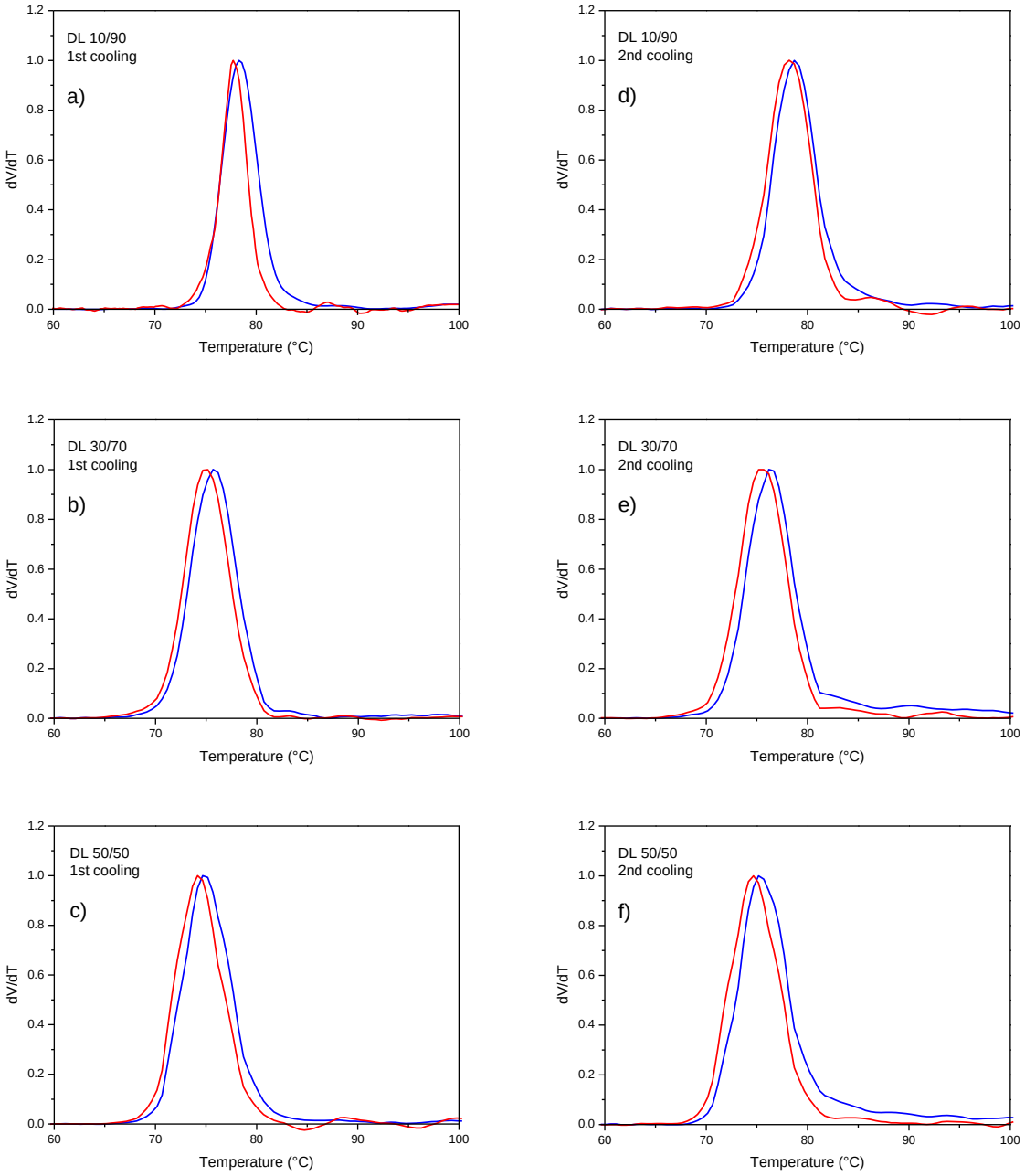

Figure 4.10: Comparison of Scalls crystallization profiles for various PLLA/PDLA blends as detected by blue (405nm) and red (635nm) laser beams. (a-c) first cooling and (d-f) second cooling at 1 °C/min.

Directly after solution crystallization, DLS measurements were performed at a solution temperature of 30 °C to study the effect of blend ratio on particle sizes of the crystallized material. Figure 4.11 shows the various distributions namely intensity, volume and number distributions, obtained after first cooling by Scalls. Looking at the homopolymers it is noticeable that the average size of neat PDLA particles formed during solution crystallization was smaller when compared to neat PLLA.

This is remarkable because the crystallization profiles of these two enantiomeric forms are almost indistinguishable up to 1 °C/min cooling. The DLS data indicates that despite the crystallization kinetics being similar, the resultant particle size distributions for the homopolymers were different during non-isothermal crystallization for dilute solution. A decrease in particle size was also observed for the blends with increased PDLA concentrations possibly due to the nucleating effect of the SC, crystallizing earlier than PLLA homocrystallites. This trend was also reported for melt-crystallization behavior whereby spherulite sizes, analysed by polarized optical microscopy (POM), decreased with increasing PDLA concentration.[1,6,10] It was concluded that the nucleation efficiency was higher for the blends compared to PLLA homopolymer and thus leading to smaller spherulites. Moreover, DLS trends were somewhat different after the second crystallization cycle with average sizes increasing slightly as PDLA content increased and might be due to a certain extent of aggregation within the solution. These results are illustrated in Figure 4.12 and overall particle sizes were smaller after second cooling event, throughout the blend composition range. The smaller sizes can be attributed to the presence of unmelted SC in solution, promoting heterogeneous nucleation of PLLA and giving rise to higher nucleation efficiency, as mentioned earlier, caused by enhanced nucleation sites available for PLLA crystallites. Interestingly, no distributions were seen for DL10/90 within the range shown in Figure 4.12. On further investigation it was found that DL10/90 resulted in the formation of much larger particles compared to the other blends. Results for DL10/90 after second cooling can be seen in Figure 4.13 and not only were the particles much larger but the average size distributions were also much broader than the other blend compositions. It was assumed that the rate of crystallization for this specific blend was one of the main reasons for the increased particle size, mainly due to the fact that laser beam profiles were shifted much closer together for the DL10/90 blend as observed in Figure 4.10d).

With very few literature references to fall back onto, it is very difficult to precisely conclude the exact reason for the behavior at this specific blend ratio. Wei *et al.*[10] reported that the influence of SC on PLLA melt-crystallization rate is twofold: firstly, SC enhances nucleation rates through heterogeneous nucleation and secondly it has a confining effect on crystallization by decreasing the mobility of PLLA homopolymer chains. In this current study, it might be that 10 wt% of PDLA provided a good balance between nucleation efficiency and sufficient mobility for diffusion for PLLA chains whereas higher PDLA loadings had more of a restraining effect due to more SC present. Crystallization peak shifts towards lower temperatures (seen in Figure 4.10) confirms this restraining effect.

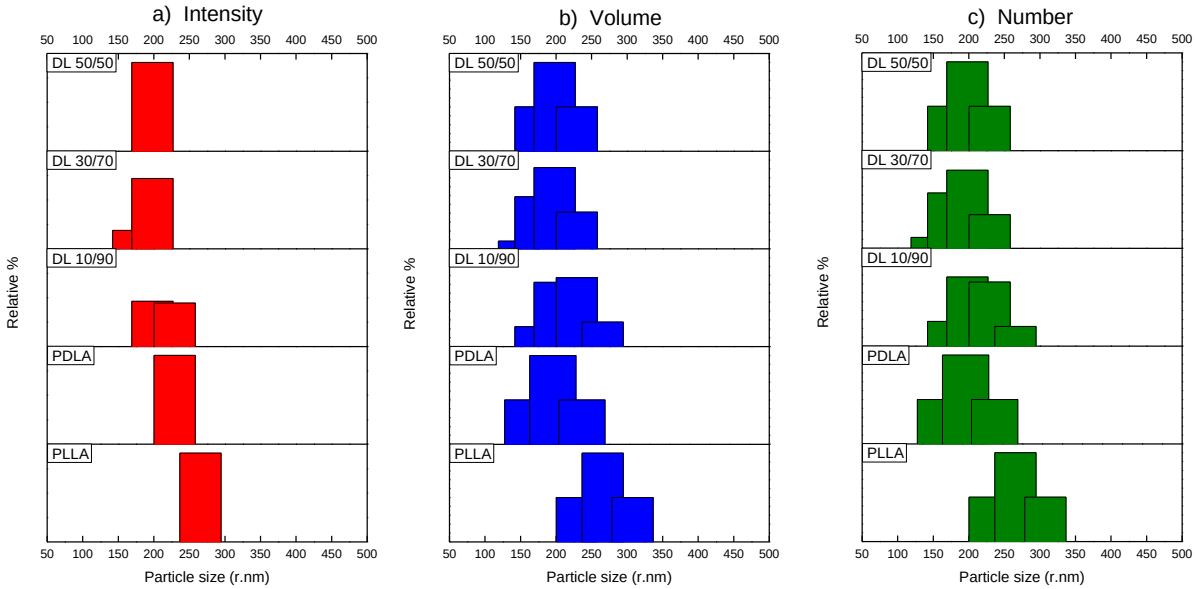

Figure 4.11: DLS distributions of PLLA/PDLA blends after first cooling in Scalls. a) intensity, b) volume, c) number.

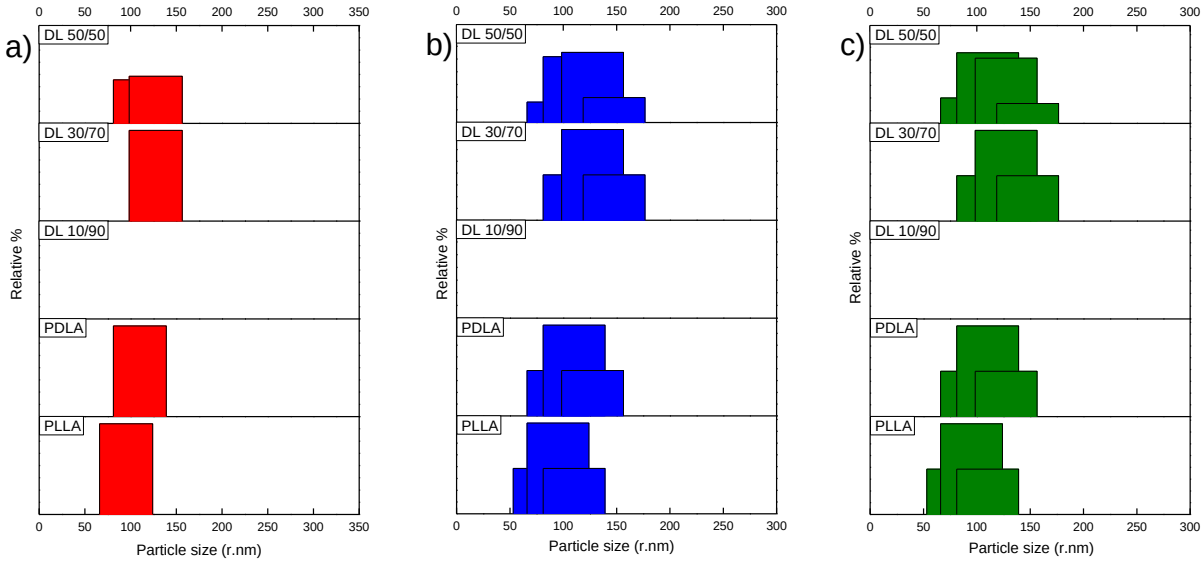

Figure 4.12: DLS distributions of PLLA/PDLA blends after second cooling in Scalls. a) intensity, b) volume, c) number.

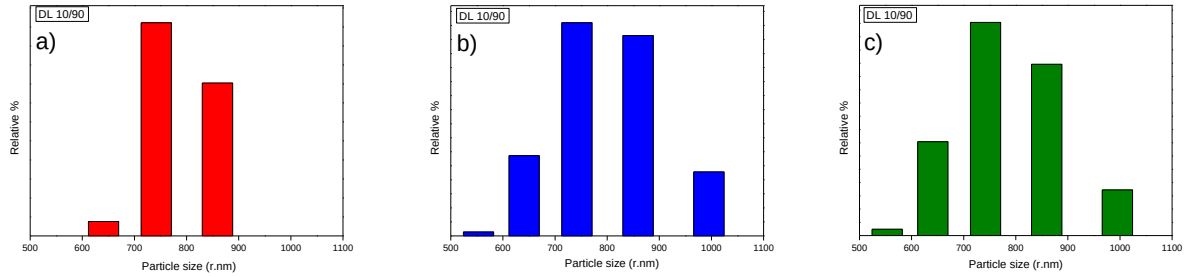

Figure 4.13: DLS distributions of DL10/90 after second cooling in Scalls. a) intensity, b) volume, c) number.

In addition, the polymer solutions were left in the laboratory at room for one week followed by another set of DLS measurements for the DL10/90 blend to study any changes in particle size distributions. Figure 4.14 compares results for the DL10/90 composition obtained at different stages during the study. A bimodal distribution was noticed after allowing the sample to stand for one week. The number distribution (Figure 4.14c) clearly illustrates the large number of smaller particle (increased relative intensity) as well as the presence of some particles with much larger sizes. In contrast, when looking at the volume distribution in Figure 4.14b), the relative intensity of the larger distribution were much higher and can be attributed to the enhanced ability of larger particles to scatter the DLS beam due to the larger volume of these particles as opposed to smaller particles in solution. The presence of a second, much larger particle size distribution signifies that further crystal growth occurred at room temperature during the one week "isothermal" storage period. It can therefore be said that a small fraction of polymer remained in solution and did not crystallize during non-isothermal solution crystallization by Scalls. This once again highlights the low crystallization rate of poly(lactic acid), which is a major drawback when considering actual industrial applications.

Figure 4.15a) provides the dissolution data obtained from Scalls. Three evident events could be detected when looking at the neat PLLA namely, first melting (106 °C), re-crystallization (111 °C) and second melting (small shoulder at 114 °C and larger peak at 120 °C), indicating that the polymer exhibited multiple solution melting behavior. Similar to solution crystallization data, the dissolution profiles for DL10/90 were quite different from the rest of the samples when looking at the ratios of the two melting peaks at higher temperature. This might imply that the crystallization kinetics was indeed different at this blend ratio and resulting in the distinctive DLS distributions. It

was remarkable to notice the dramatic decrease in re-crystallization event for the blends (designated by the arrows). This suggest that addition of PDLA to PLLA resulted in more "sufficient" crystallization during cooling, leaving a reduced amount of unordered polymer chains that will re-organize during solution melting and hence a decrease in re-crystallization peak. It is well-known from previous literature reports that differential scanning calorimetry (DSC) provides an easy pathway to validate the presence of poly(lactic acid) stereocomplex crystals as they melt at much higher temperatures (above 200 °C) compared to the homocrystallites (multiple melting peaks in the vicinity of 170 °C).[6,7,10-12] DSC thermograms of the Scalls crystallized material are illustrated in Figure 4.15b). Melting endotherms seen for the blends at roughly 225 °C confirmed the formation of SC during solution crystallization and certainly contributed to the differences in crystallization and dissolution profiles, meaning that SC had an effect on the thermal behavior of PLLA in solution. Only homopolymer melting events were observed for neat PLLA with the absence of the higher temperature SC endotherm.

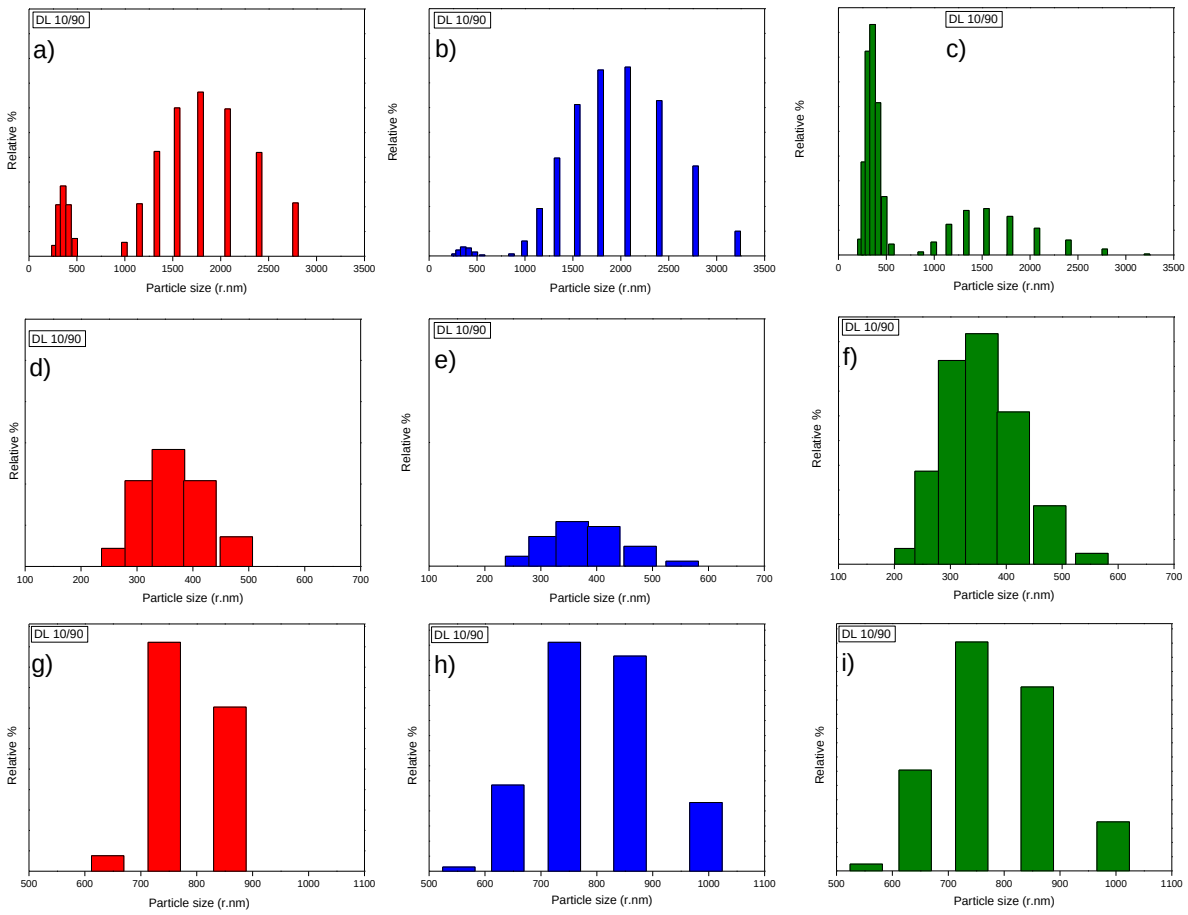

Figure 4.14: DLS results of DL10/90 at various stages during the study: a) – c) total distributions after 1 week, d) – f) lower size distribution section after one week, g) – i) total distributions after second cooling.

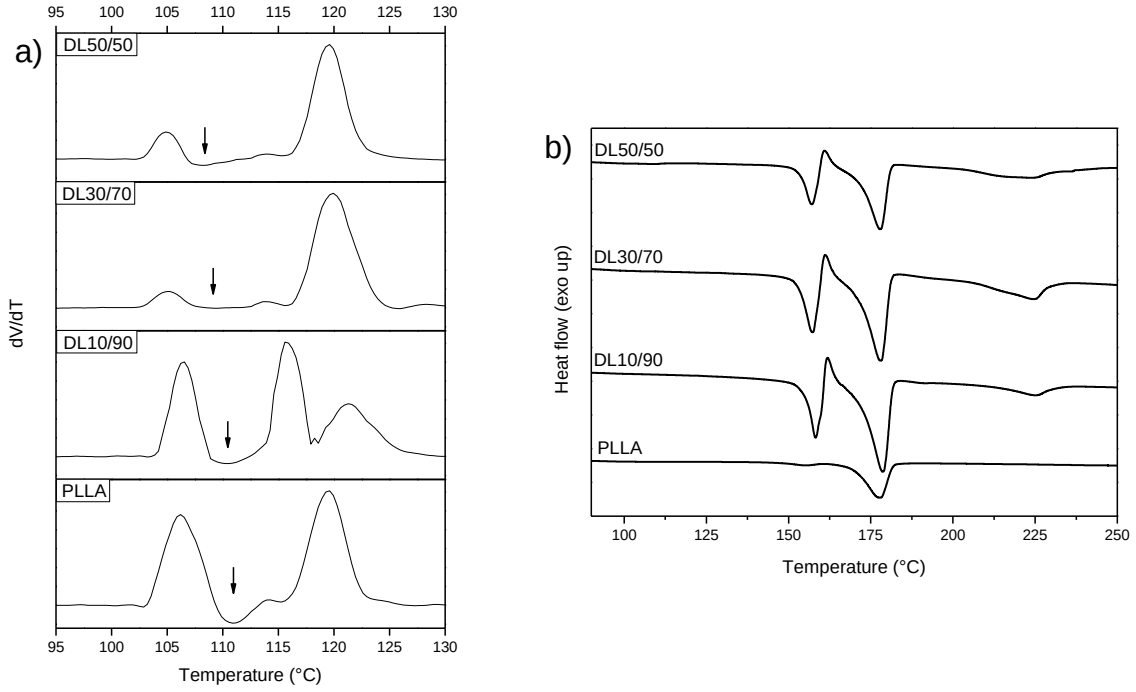

Figure 4.15: a) Scalls dissolution profiles, heated at 1 °C/min after crystallization at 1 °C/min. b) DSC first heating thermograms of solution crystallized material (heating rate = 10°C/min)

4.2.3) Surface morphology analysis

After subjecting the polymer solutions to a 0.5 °C/min cooling cycle in Scalls, part of the crystallized turbid solution were transferred to a petri dish to allow for solvent evaporation. Morphologies of the resultant polymer films were then analyzed by scanning electron microscopy (SEM). Homopolymer results are shown in Figure 4.16. Although no distinct differences could be observed in the solution crystallization kinetics (discussed earlier) of PLLA and PDLA homopolymers, remarkable observations were made from SEM results. It was found that PDLA films were much smoother than that of PLLA and could clearly be seen in the magnified images (Figure 4.16b and 4.16d). Additionally, binary PLLA/PDLA blends gave rise to even smoother film morphologies as illustrated by Figure 4.17 with the addition of only 10 wt% PDLA. This phenomenon could have been due to the influence of the stereocomplex network as solvent evaporation occurred and implies that addition of PDLA can improve the crystallization kinetics of PLLA as well as affecting the morphology in binary PLA blend films.

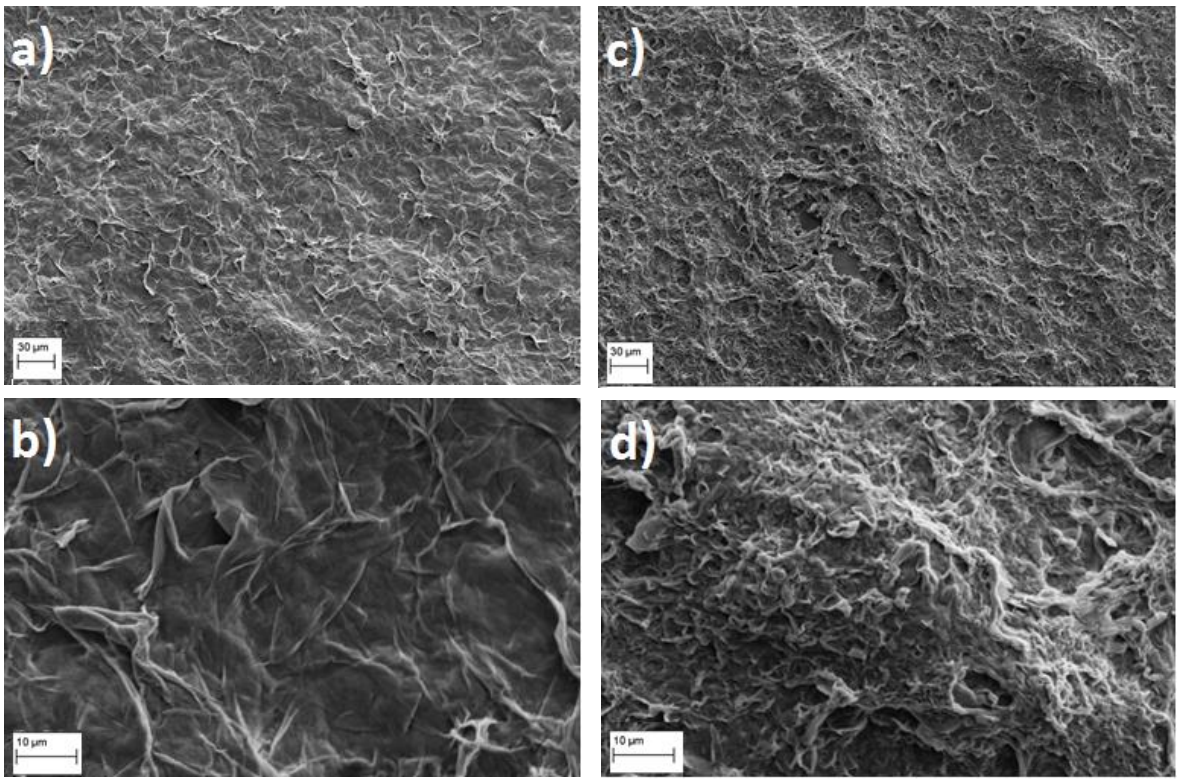

Figure 4.16: SEM images of solution casted films for PLA homopolymers after Scalls: a – b) PDLA and c – d) PLLA.

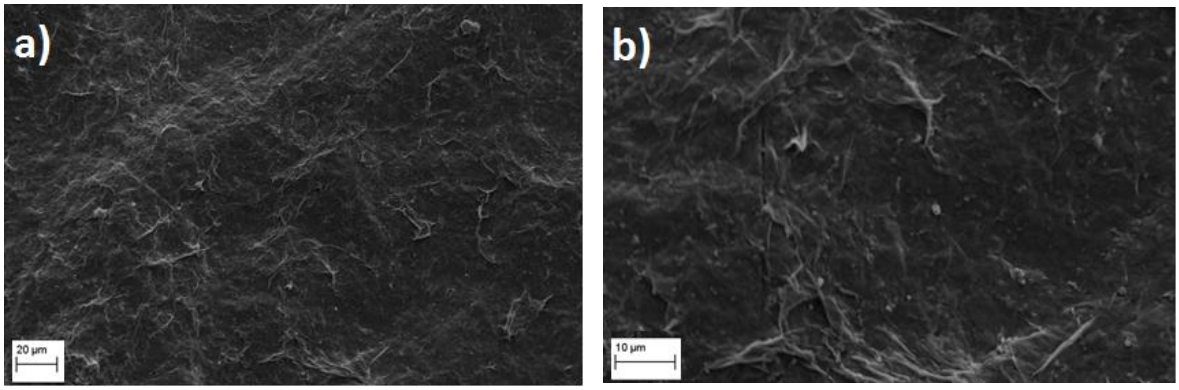

Figure 4.17: SEM images of solution casted films for DL 10/90 blend after Scalls: a) low magnification, b) higher magnification.

4.3) Addition of stereocomplex crystals (SC) to PLLA

After solution crystallization of the 50/50 PLLA/PDLA blend, small amounts (up to 10 wt%) of SC crystals (procedure discussed in experimental section) formed in this blend composition was added to PLLA to study the effect on the crystallization kinetics of PLLA in solution. Figure 4.18 represents an overlay of the various PLLA/SC blends during Scalls solution crystallization at 1 °C/min. Addition of 2 wt% of SC resulted in a slight broadening of crystallization profile with very similar crystallization onset and crystallization end point temperatures. A noticeable increase in crystallization onset temperature was seen at higher SC content with 10 wt% SC having the highest onset temperature. These results allow us to make the assumption that the unmelted stereocomplex crystals had an enhanced nucleation effect on PLLA homopolymer crystallites. An increase in SC content resulted in more enhanced nucleation effect and thus an earlier onset of crystallization.

Furthermore the addition of SC had an effect on the total crystallization temperature range. Crystallization events occurred down to lower temperatures with an increase in SC content and were visible from the shift in crystallization profiles towards lower temperatures. Relative areas under profiles shown in Figure 4.18 were calculated to get an idea of the amount of crystallized material and can be found in Table 4. An increase in SC wt% lead to an increase in peak area suggesting that more material crystallized when blending with SC, compared to homopolymer PLLA crystallization. With as little as 2 wt% SC present, 14% more material crystallized when compared to homopolymer crystallization in the absence of SC. These results accentuate the nucleation efficiency of SC on PLLA by providing nucleation sites for homocrystallites during crystallization events and improving the low crystallization kinetics that PLLA is known to exhibit. Crystallization peak temperature (T_c) was unaffected by addition of stereocomplex crystals.

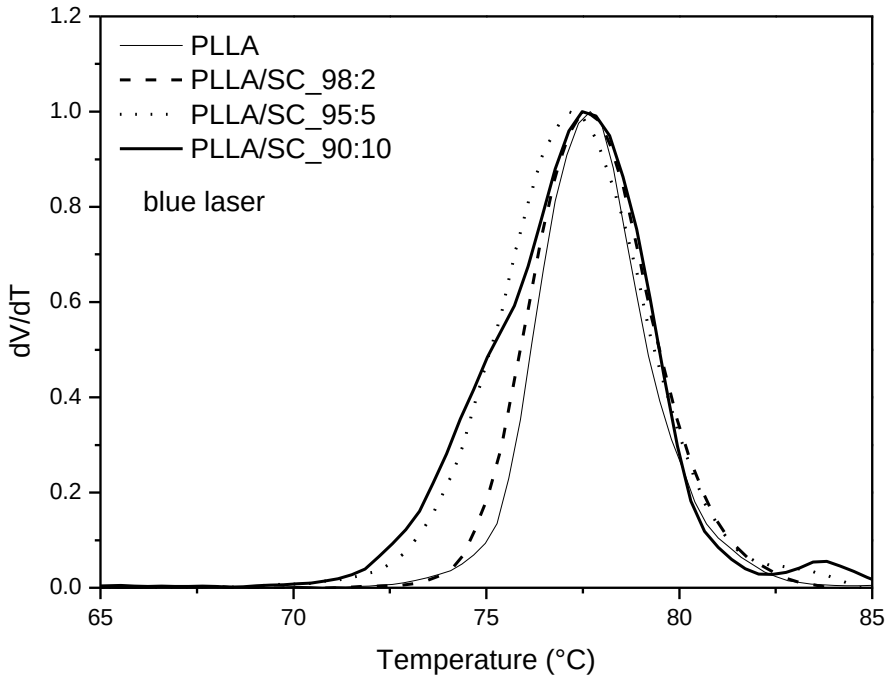

Figure 4.18: Crystallization profiles of PLLA homopolymer and PLLA/SC blends cooled at 1 °C/min.

Table 4.4: Solution crystallization temperature (T_c), peak area and crystallinity data for PLLA/SC blends

Sample ID	T_c (°C)	Peak area (a.u.)	Increase in degree of crystallinity w.r.t neat PLLA (%)
PLLA	77.7	3.41	
PLLA/SC 98:2	77.5	3.89	14.1
PLLA/SC 95:5	77.1	4.69	37.5
PLLA/SC 90:10	77.5	4.75	39.3

A graphical illustration of crystallization peak area and T_c as a function of SC content is given in Figure 4.19. A steep increase in peak area was noticed up to 5 wt% SC and levels off at higher loadings. The plateau region might be due to hindrance of PLLA crystallization caused by the increased amount of unmelted SC present in solution. At 10 wt% SC the mobility of PLLA homocrystallites could have been decreased to a larger extent and hence the crystallization event occurring over a broader temperature range. A near straight line represents the T_c values for homopolymer and blends, and illustrates the independence of T_p on blend composition.

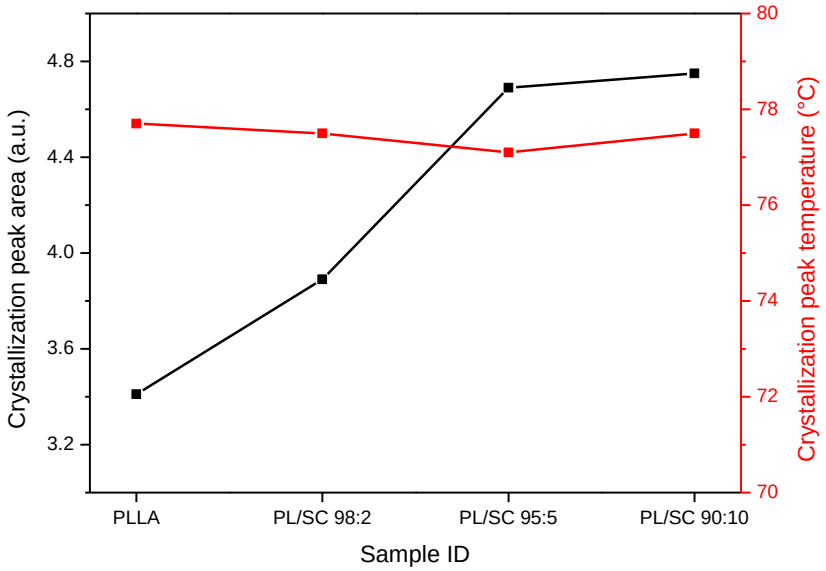

Figure 4.19: Scalls crystallization peak area and T_c as a function of SC content.

In order to further study the crystallization kinetics of these blends, we analyzed the results obtained during simultaneous measurements by three lasers with different wavelengths (blue = 405nm, green = 532nm, red = 635nm). Using lasers with differing wavelengths allow for the tracking of crystal growth with the blue laser beam (lowest wavelength; smaller particles) scattering first followed by the green laser and finally the red laser beam (highest wavelength, larger particles) scattering last. Figure 4.20 shows an overlay of the Scalls crystallization profiles obtained by the different laser beams. The spacing between the different laser profiles is an indication of the crystal growth rate. In Figures 4.20a) and 4.20b), the different laser profiles could clearly be distinguished with T_p also being shifted towards lower temperatures with increasing laser wavelength. It can be said that more

uniform crystal growth occurred in the blend with 2 wt% SC present, leading to systemic scattering of the wavelength laser beams. The close resemblance of these profiles signifies that the crystal growth rate was not greatly influenced by addition of 2 wt% of SC. At higher SC loadings, shown in Figures 4.20c) and 4.20d), the different profiles were shifted very close to each other suggesting that the crystal growth rate were quite fast as all laser beams were almost scattered simultaneously. These results allow us to conclude that although the nucleation effect was larger with increased SC content, the crystal growth rate during solution crystallization, at higher SC loadings, was also greatly affected when compared to neat PLLA behavior.

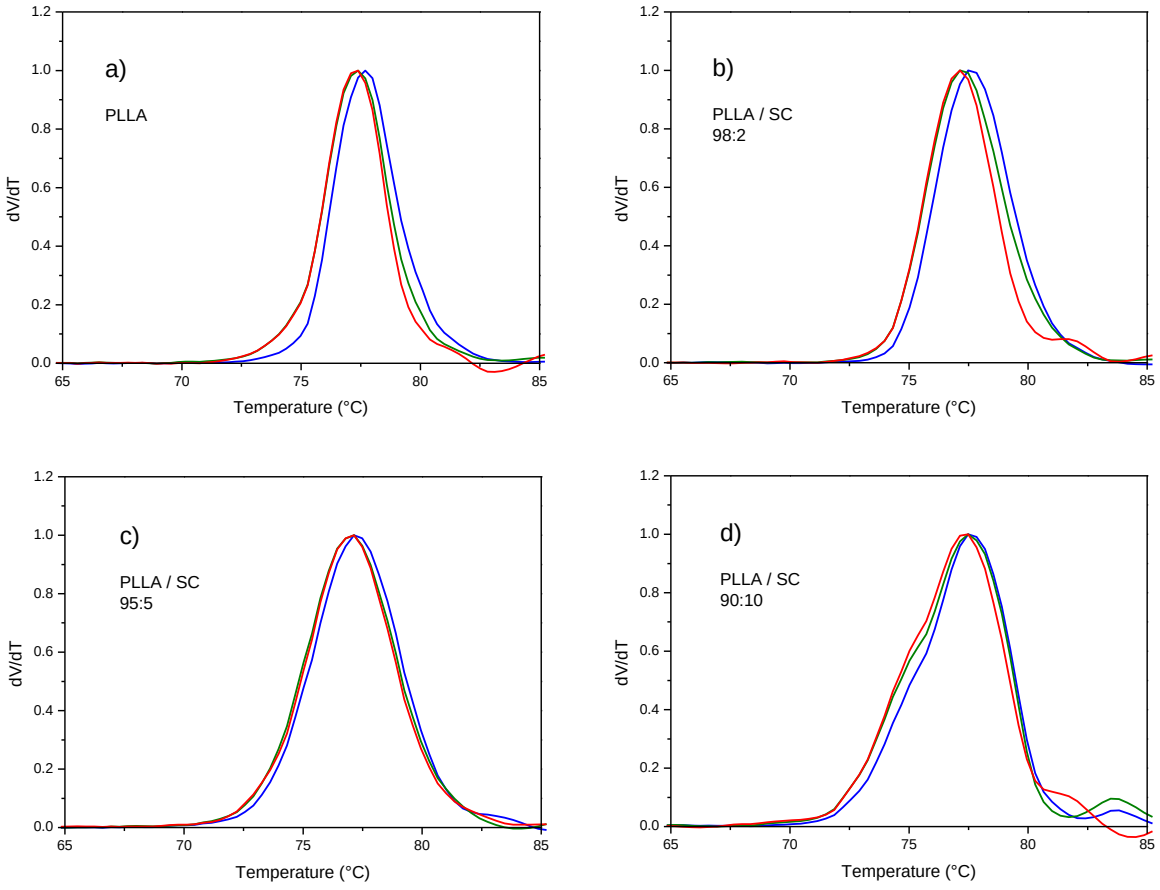

Figure 4.20: Overlay of different laser beams for PLLA/SC crystallization at 1 °C/min.

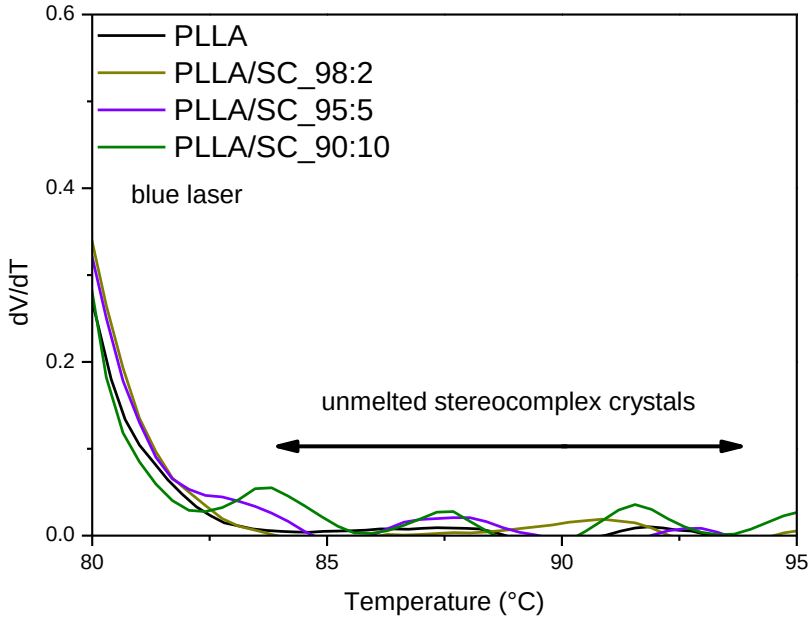

Figure 4.21: Temperature region during cooling cycle before crystallization onset indicating the scattering caused by unmelted stereocomplex crystals in solution.

To conclude, Figure 4.21 illustrates the Scalls profiles in the region before crystallization onset. Compared to the blends, the profile for neat PLLA was very flat and smooth in the temperature region before onset of crystallization at roughly 83 °C. This implies that no material was present at this initial stage to cause scattering of the laser beams. In contrast to this, slightly irregular profiles were observed for the blends and was assumed to be due to unmelted SC present is solution and resulted in some scattering of the incident beams even before the start of crystallization events. With an increase in SC concentration, the scattering increased. This is further evidence of SC being present before PLLA crystallization and providing heterogeneous nucleation sites to enhance the crystallization behavior.

4.4) Summary

PLA homopolymers and binary blends with various blends compositions were successfully analyzed in solution. Blends of PLLA and PDLA resulted in the formation of stereocomplex crystals (SC) upon crystallization. These SC had a nucleating effect on PLLA homocrystallites resulting in an earlier onset of crystallization and increased crystallization peak area. Addition of PDLA resulted in decreased crystallite particle sizes due to higher nucleation efficiency in the blends. SEM images indicated that the surface morphology was influenced when the two PLA enantiomers were blended.

4.5) References:

(1) Yamane, H. & Sasai, K. **2003,** "Effect of the addition of poly(d-lactic acid) on the thermal property of poly(l-lactic acid)", *Polymer*, vol. 44, no. 8, pp. 2569-2575.

(2) Brizzolara, D., Cantow, H., Diederichs, K., Keller, E. & Domb, A.J. **1996,** "Mechanism of the stereocomplex formation between enantiomeric poly (lactide) s", *Macromolecules*, vol. 29, no. 1, pp. 191-197.

(3) Li, Y. & Han, C. **2012,** "Isothermal and Nonisothermal Cold Crystallization Behaviors of Asymmetric Poly(L-lactide)/Poly(D-lactide) Blends", *Industrial & Engineering Chemistry Research*, vol. 51, no. 49, pp. 15927-15935.

(4) Narita, J., Katagiri, M. & Tsuji, H. **2013,** "Highly Enhanced Accelerating Effect of Melt-Recrystallized Stereocomplex Crystallites on Poly(L-lactic acid) Crystallization, 2?Effects of Poly(D-lactic acid) Concentration", *Macromolecular Materials and Engineering*, vol. 298, no. 3, pp. 270-282.

(5) Narita, J., Katagiri, M. & Tsuji, H. **2013,** "Highly enhanced accelerating effect of melt-recrystallized stereocomplex crystallites on poly(L-lactic acid) crystallization: effects of molecular weight of poly(D-lactic acid)", *Polymer International*, vol. 62, no. 6, pp. 936-948.

(6) Tsuji, H., Takai, H. & Saha, S.K. **2006,** "Isothermal and non-isothermal crystallization behavior of poly(l-lactic acid): Effects of stereocomplex as nucleating agent", *Polymer*, vol. 47, no. 11, pp. 3826-3837.

(7) Sun, J., Yu, H., Zhuang, X., Chen, X. & Jing, X. **2011,** "Crystallization Behavior of Asymmetric PLLA/PDLA Blends", *The Journal of Physical Chemistry B*, vol. 115, no. 12, pp. 2864-2869.

(8) Narita, J., Katagiri, M. & Tsuji, H. **2011,** "Highly enhanced nucleating effect of melt-recrystallized stereocomplex crystallites on poly(L-lactic acid) crystallization", *Macromolecular Materials and Engineering*, vol. 296, no. 10, pp. 887-893.

(9) Engelberg, I. & Kohn, J. **1991,** "Physico-mechanical properties of degradable polymers used in medical applications: a comparative study", *Biomaterials*, vol. 12, no. 3, pp. 292-304.

(10) Wei, X., Bao, R., Cao, Z., Yang, W., Xie, B. & Yang, M. **2014,** "Stereocomplex Crystallite Network in Asymmetric PLLA/PDLA Blends: Formation, Structure, and Confining Effect on the Crystallization Rate of Homocrystallites", *Macromolecules*, vol. 47, no. 4, pp. 1439-1448.

(11) Woo, E.M. & Chang, L. **2011,** "Crystallization and morphology of stereocomplexes in nonequimolar mixtures of poly(l-lactic acid) with excess poly(d-lactic acid)", *Polymer*, vol. 52, no. 26, pp. 6080-6089.

(12) Xu, H., Tang, S. & Chen, J. **2013,** "Unique Crystallization Behavior of Poly(L-lactic acid) Nucleated by Stereocomplex with Different Fine Structure", *Polymer - Plastics Technology and Engineering*, vol. 52, no. 7, pp. 690-698.

Chapter 5

Results and Discussion:

PLLA/PBS blends

This chapter focuses on the results obtained for PLLA/PBS binary blends; studying the effect of PBS addition on the solution behavior of PLLA

It has to be noted that the Scalls results discussed in this chapter are only those obtained from the normalized signals of the 405 nm (blue) laser. Similar data can be acquired from the green and red laser responses and will be discussed at a later stage in future work. Scalls profiles were normalized for the ease of representation.

5.1) PLLA and PBS homopolymers

5.1.1) Solution Crystallization

The crystallization for the homopolymers resulted in distinct peaks for PLLA and PBS within different temperature ranges. This indicates that the polymers crystallized readily from solution and crystallization behavior of both these polymers can clearly be tracked in solution which is of great importance when studying blends of these materials and investigating features such as miscibility and phase separation. Figure 5.1 illustrates the solution crystallization data at different cooling rates for the individual polymers. For both polymers, a slight broadening in peaks as well as a lowering in crystallization peak temperature (T_c) was observed with an increase in cooling rate. The PLLA crystallized earlier than PBS (see Figure 5.1). Values for T_c of PLLA were roughly 25 °C higher than that of PBS throughout the cooling rate range, confirming the earlier onset of crystallization for PLLA.

5.1.2) Dissolution

Figure 5.2 shows the dissolution profiles for PLLA and PBS at a heating rate of 1 °C/min following the solution crystallization at the cooling rates indicated in Figure 5.1. PBS showed bimodal melting profiles with a lower melting peak around 75 °C and a higher melting peak at 85 °C. This multiple melting behavior is in agreement with literature values reported after the non-isothermal melt crystallization of neat PBS. The bimodality can be attributed to a melting-recrystallization-melting phenomenon.[1-5] As the cooling rate increased, the melting peak observed at the higher temperature became more predominant. It can be said that during solution melting of PBS, crystallites of lower thermal stability melt first (lower melting peak), followed by reorganization of these chains. Upon further heating we observed the melting of crystallites with higher thermal stability formed during the re-crystallization process and hence the double solution melting profile for PBS.

Similar to the crystallization data, the dissolution peaks for PLLA were detected at higher temperatures compared to PBS. During solution melting, PLLA showed two melting peaks and a much larger re-crystallization event than PBS. The re-crystallization event is represented by the negative peak roughly at roughly 112 °C due to scattering of the laser beam as crystals are formed during this process. This indicates one of the advantages of the Scalls technique for easily distinguishing between dissolution and crystallization events that occurs during the same heating cycle. Due to the magnitude of the re-crystallization peak of PLLA, it can be reasoned that the crystallization kinetics of PBS is faster than that of PLLA during cooling from dilute solution. Despite the cooling rates, no major differences in the dissolution peak temperatures (T_m) for both homopolymers were observed.

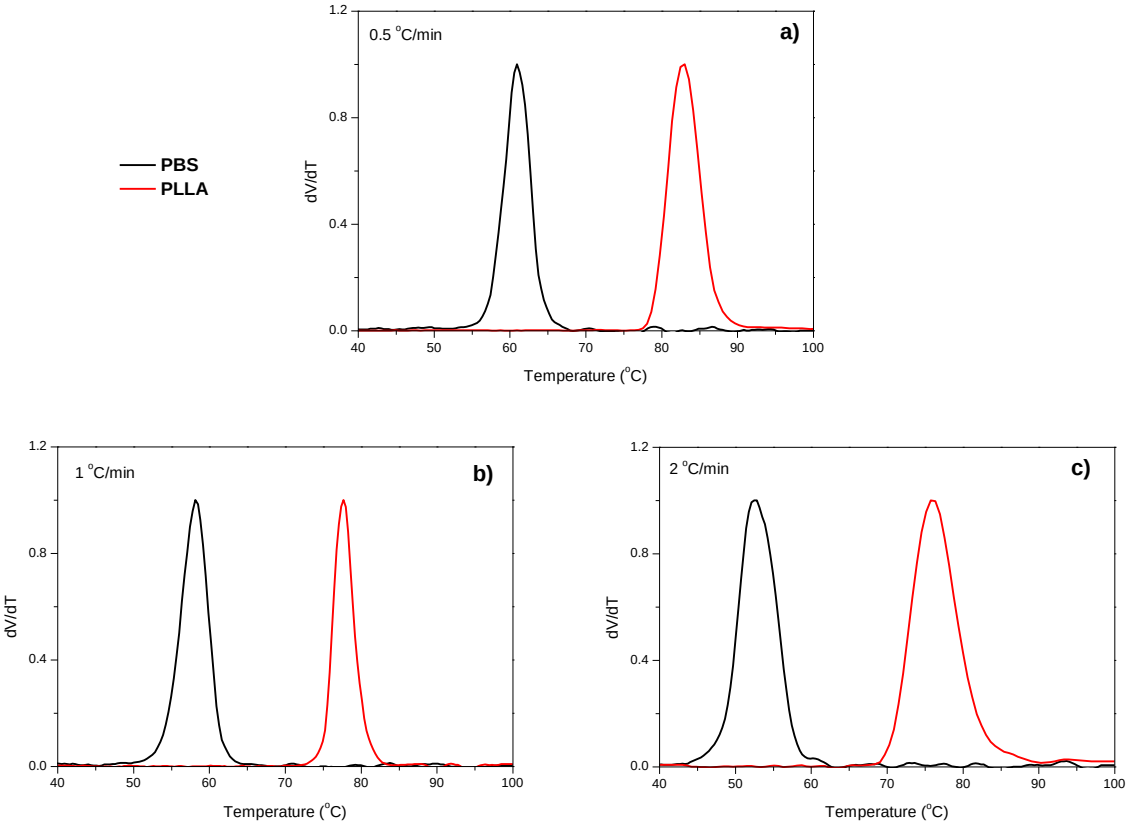

Figure 5.1: Scalls cooling profiles for PLLA (red) and PBS (black) homopolymers at different cooling rates: (a) 0.5 °C/min; (b) 1 °C/min; (c) 2 °C/min.

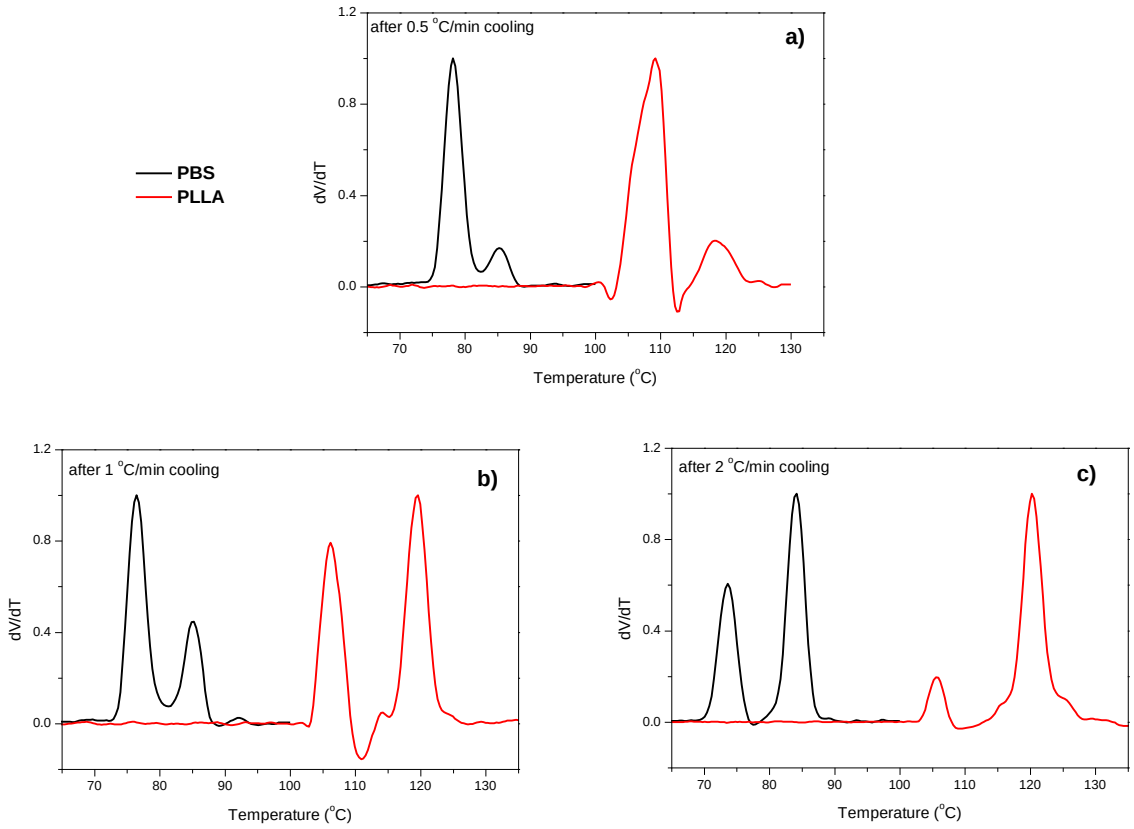

Figure 5.2: Scalls heating profiles for PLLA (red) and PBS (black) homopolymers at a heating rate of 1 °C/min precede by different cooling rates: (a) after 0.5 °C/min; (b) after 1 °C/min; (c) after 2 °C/min.

5.2) PLLA/PBS blends

5.2.1) Solution Crystallization

After investigating the solution characteristics of the homopolymers, various blends of PLLA/PBS were prepared with the intention of studying the effect of PBS on thermal behavior of PLLA in solution. Dilute solutions of the blends were cooled at a constant rate of 1 °C/min. The solutions were subjected to three sequential cooling cycles. Figure 5.3 illustrates the Scalls results for the different cooling cycles. Two distinct crystallization peaks could be seen when PBS content was higher than 50 wt%. This indicates the phase separation of the PLLA/PBS binary system during solution crystallization. In comparison to the homopolymers, T_c for PBS in the blends was very similar to that of the neat polymer. This was observed for all cooling cycles and indicates that the crystallization kinetics of PBS was unchanged in the blends. From Figure 5.3(a) it is clear that the

T_c for PLLA in the blends was shifted towards lower temperatures and a broadening of peaks was observed. At this stage it was concluded that the addition of PBS had a definite influence on the crystallization kinetics of PLLA despite the phase separation, resulting in a delay in crystallization of PLLA as well as the PLLA component crystallizing over a larger temperature range during first cooling from solution. No specific trends that could be correlated to the blend ratios were observed.

The second and third cooling cycles resulted in very similar profiles but intriguingly different to those detected during the first cooling analysis. Peak temperatures for PBS were once again unaffected by the blend ratio. An increase in PBS content above 30 wt%, resulted in a lowering of T_c for PLLA. During the second cooling, a shoulder was observed on the higher temperature side of the PBS peak (not present during first cooling) for the blend consisting of only 10 wt% PLLA. This might be due to a nucleating effect of the PBS on the PLLA during sequential crystallization steps. In Figure 5.3(c) the shoulder clearly increased into a separate peak, indicative of phase separation during solution crystallization. Although no clear peak could be seen for PBS at low loadings, T_c and crystallization onset for PLLA increased by roughly 6 ^oC (PLLA90/PBS10) compared to the neat polymer. Because of the PBS component still being in the molten state at the point whereby PLLA crystallizes, the only explanation for the increase in $T_{c\ (PLLA)}$ might be that molten PBS droplets acts as nucleation sites for PLLA crystallites and thus an increase in PBS content above 30 wt% hinders PLLA crystallization and hence the lowering of $T_{c\ (PLLA)}$ at higher PBS loadings. However, the crystallization onset of PLLA was shown to be improved by blending with as little as 10 wt% PBS. This nucleation phenomenon during melt crystallization was previously reported.[6,7] With the combined results from the three cooling cycles it can be said that the addition of PBS definitely has an effect on PLLA crystallization and that the crystallization kinetics varies during consecutive coolings.

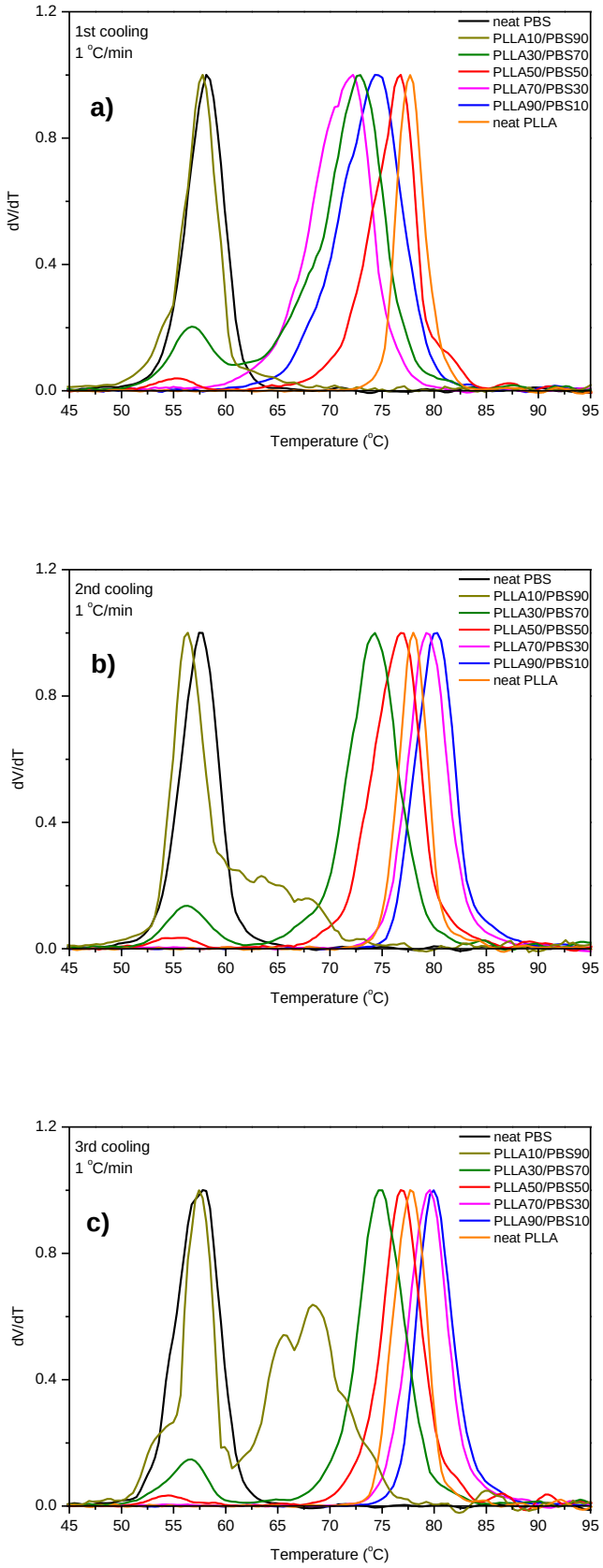

Figure 5.3: Scalls cooling profiles for PLLA/PBS blends during consecutive cooling cycles at 1 °C/min: (a) 1st cooling; (b) 2ndcooling; (c) 3rd cooling.

5.2.2) Dissolution

After crystallization, polymer solutions were heated to 130 °C to study the solution melting/dissolution of the crystallized material. During this step the solution turbidity decreased with an increase in temperature and by measuring the increase in laser intensity allowed for the dissolution analysis of polymer crystals formed during crystallization. An overlay of dissolution profiles for the homopolymers and blends can be found in Figure 5.4. Both, neat PBS and PLLA showed two peaks due to re-crystallization of less organized polymer chains with lower thermal stability (lower temperature peaks). At low PBS loadings (up to 30 wt%) the PLLA melting peak located at lower temperature (107 °C), was much smaller compared to neat PLLA and the peak at 120 °C became more pronounced. These results suggest that well-organized PLLA crystals were formed in these blends compared to the neat PLLA, where two large distinct peaks were observed. The recrystallization occurrence is very clear in the case of PLLA homopolymer by the presence of an exothermic peak at 114 °C and is evident of the slow crystallization kinetics of PLLA upon cooling. Addition of PBS led to a noticeable decrease in magnitude and slight decrease in peak temperature of the exotherm. The decrease in peak magnitude can directly be correlated to the amount of material crystallized during the cooling step, with a smaller recrystallization peak pointing to more efficient crystallization upon cooling. For blends with PBS content below 50 wt%, no distinct melting peaks for the PBS component could be seen which were similar to the crystallization observations shown in Figure 5.3. Park et al.[7] reported that PLLA/PBS blends having less than 40 wt% PBS showed no significant crystallization-induced phase separation during melt crystallization. Following this report, two possibilities exist for the absence of PBS crystallization and dissolution peaks in PLLA70/PBS30 and PLLA90/PBS10 binary blends. First, there might have been some extent of solution miscibility in blends with PBS content less than 50 wt%. Second, as mentioned earlier, PBS crystals were not formed as a result of the low content but still enhanced the crystallization of the blends with possible molten PBS droplets acting as crystallization nuclei for PLLA. Further investigation is needed to address this complex behavior, but from the Scalls results it can be stated with certainty that the crystallization kinetics of PLLA can be improved by addition of small amounts of PBS.

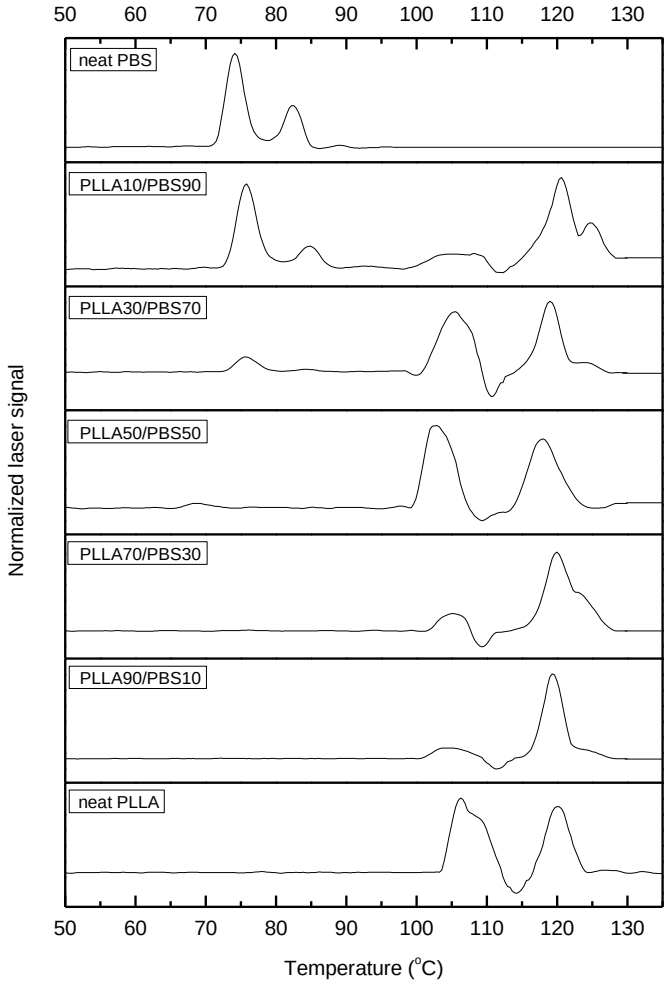

Figure 5.4: Scalls heating profiles for PLLA/PBS blends at a heating rate of 1 °C/min.

5.2.3) Attenuated total reflectance-Fourier transform infrared spectroscopy (ATR-FTIR)

After solution characterization, samples were dried for FTIR analysis of the crystallized material. This was done to confirm that both PLLA and PBS were indeed present during crystallization. The FTIR transmission spectra of the homopolymers and binary blends are illustrated in Figure 5.5. Due to the chemical groups of the two polyesters being very similar, the resultant FTIR spectra were very similar as well. Apart from some small differences in the fingerprint region, the main noticeable difference is the shift in carbonyl peak position which appeared at 1755 cm^{-1} and 1711 cm^{-1} for PLLA and PBS respectively (indicated by arrows on spectra).The presence of these two carbonyl peaks throughout the blend composition confirms that both PLLA and PBS components were present in the crystallized material obtained from solution crystallization of the blends.

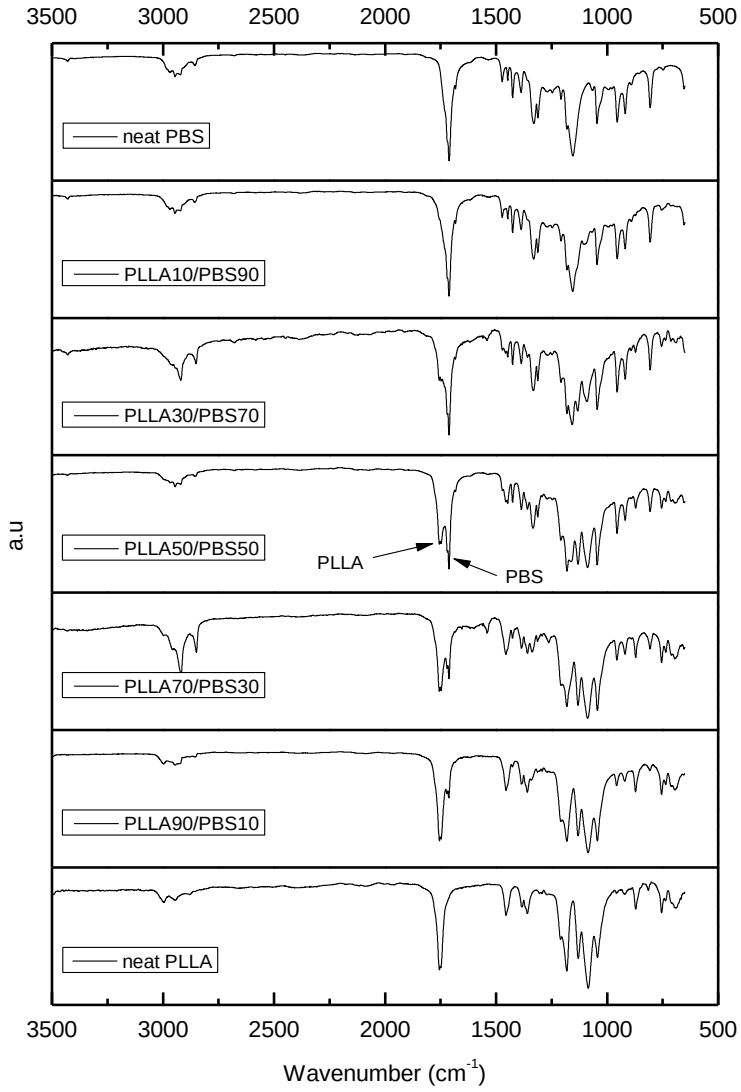

Figure 5.5: ATR-FTIR spectra of PLLA/PBS blends after solution crystallization.

5.2.4) Differential Scanning Calorimetry (DSC)

Further thermal analysis on the solution crystallized material was done by DSC. The thermograms for the melting and crystallization cycles are presented in Figures 5.6 and 5.7 respectively. From the results presented in Figure 5.6, the presence of PLLA and PBS could be seen throughout the blend compositions. Compared to the homopolymers, no major shift in peak temperatures was observed for the blends. Interesting observations were made from the melt-crystallization results shown in Figure 5.7. Crystallization peaks for PBS and PLLA were present at 80 °C and 105 °C respectively. Similar to the melting thermograms, no obvious peak shifts were noticed, emphasizing the

difference in crystallization behavior between solution crystallization (Scalls) and melt crystallization (DSC) of the blends. As expected, crystallization exotherms for PBS decreased with a decrease in PBS content due to less material present. On the contrary, for PLLA, this peak is larger than the homopolymer exotherm at PBS content up to 30 wt%, with PLLA90/PBS10 showing the largest crystallization peak and a 30% increase in peak area compared to PLLA homopolymer. These results suggest that 10 wt% PBS had the greatest enhancing effect on PLLA crystallization by increasing the crystallization rate, despite the fact that PBS is in the molten state at the point of PLLA crystallization. Results obtained from calorimetry studies correlated well with those from Scalls, showing that small amounts of PBS increased the crystallization rate of PLLA. This is advantageous for processing and applications of these biopolymer materials.

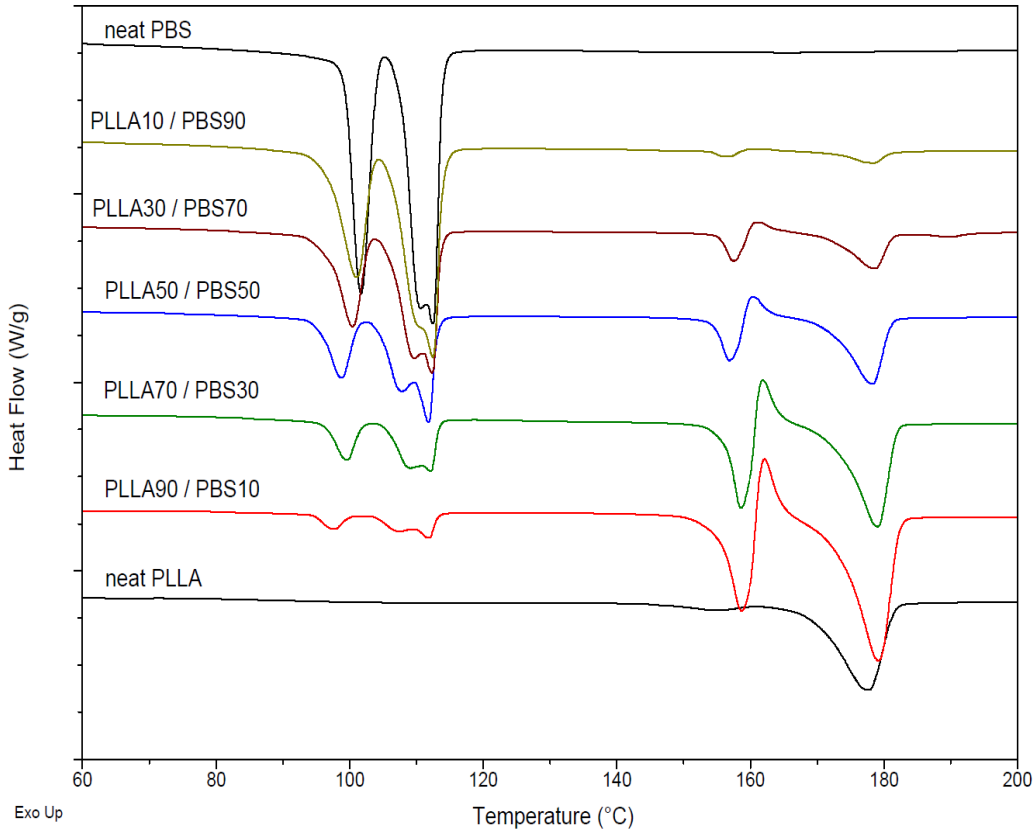

Figure 5.6: DSC heating thermograms of PLLA/PBS blends at a heating rate of 10 °C/min.

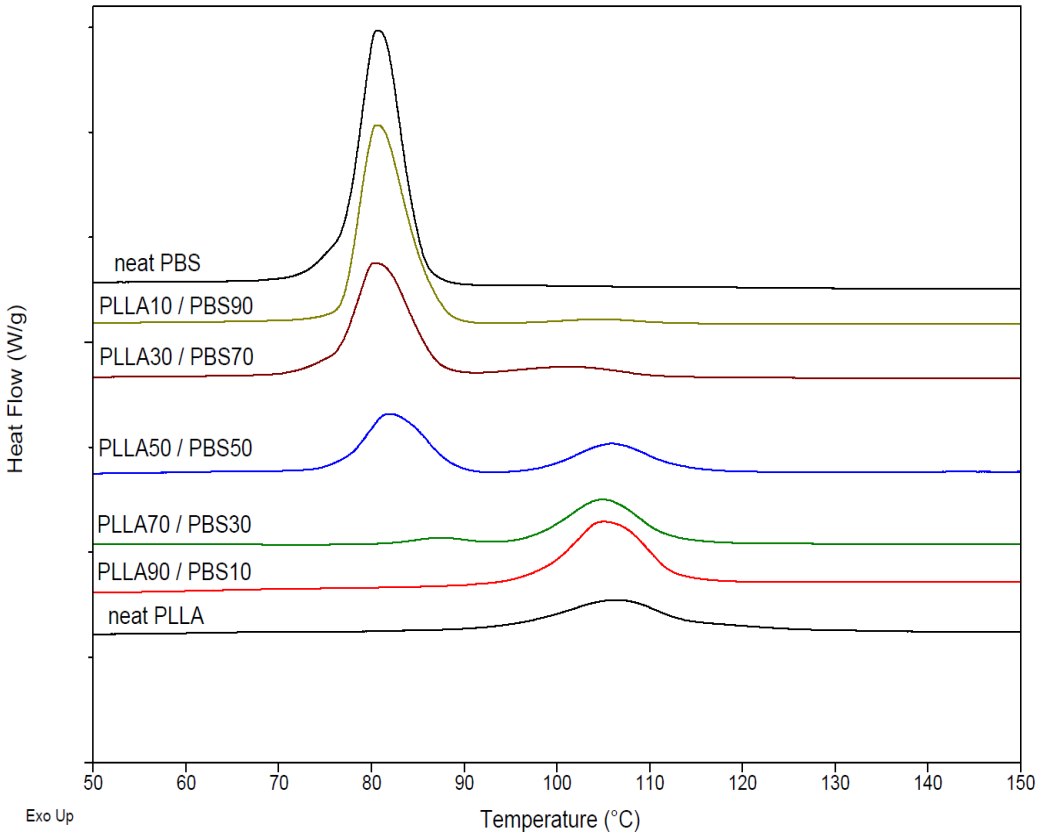

Figure 5.7: DSC cooling thermograms of PLLA/PBS blends at a cooling rate of 5 °C/min.

5.3) Summary

Binary blends of PLLA/PBS were successfully studied. At PBS content up to 30 wt%, T_c for PLLA shifted to higher temperatures compared to neat PLLA. This nucleation phenomenon occurred in the molten PBS state as PLLA crystallized at much higher temperatures than PBS. Above 30 wt% PBS, crystallization of PLLA was hindered and peaks shifted towards lower temperatures. Re-crystallization events in PLLA decreased with addition of PBS, implying that more PLLA crystallized upon cooling of the blends. DSC analyses confirmed the increase in crystallization kinetics upon small additions of PBS to PLLA.

5.4) References:

(1) Wang, Y. & Mano, J.F. **2007,** "Biodegradable poly(L-lactic acid)/poly(butylene succinate-co-adipate) blends: Miscibility, morphology, and thermal behavior", *Journal of Applied Polymer Science*, vol. 105, no. 6, pp. 3204-3210.

(2) Yasuniwa, M. & Satou, T. **2002,** "Multiple melting behavior of poly (butylene succinate). I. Thermal analysis of melt-crystallized samples", *Journal of Polymer Science Part B: Polymer Physics*, vol. 40, no. 21, pp. 2411-2420.

(3) Yasuniwa, M., Tsubakihara, S., Satou, T. & Iura, K. **2005,** "Multiple melting behavior of poly (butylene succinate). II. Thermal analysis of isothermal crystallization and melting process", *Journal of Polymer Science Part B: Polymer Physics*, vol. 43, no. 15, pp. 2039-2047.

(4) Yoo, E.S. & Im, S.S. **1999,** "Melting behavior of poly(butylene succinate) during heating scan by DSC", *Journal of Polymer Science, Part B: Polymer Physics*, vol. 37, no. 13, pp. 1357-1366.

(5) Qiu, Z., Komura, M., Ikehara, T. & Nishi, T. **2003,** "DSC and TMDSC study of melting behaviour of poly (butylene succinate) and poly (ethylene succinate)", *Polymer*, vol. 44, no. 26, pp. 7781-7785.

(6) Yokohara, T. & Yamaguchi, M. **2008,** "Structure and properties for biomass-based polyester blends of PLA and PBS", *European Polymer Journal*, vol. 44, no. 3, pp. 677-685.

(7) Park, J.W. & Im, S.S. **2002,** "Phase behavior and morphology in blends of poly (L-lactic acid) and poly (butylene succinate)", *Journal of Applied Polymer Science*, vol. 86, no. 3, pp. 647-655.

Chapter 6

Results and Discussion:

Effect of molecular weight on solution crystallization and dissolution behavior of linear polyethylenes

This chapter focuses on the results obtained for a range of linear polyethylenes; studying the molecular weight dependency of T_c and T_m

6.1) Introduction

The solution crystallization behavior of semi-crystalline polymers has been studied extensively by several groups in the material science and engineering field. These studies mainly made use of the more conventional fractionation techniques namely crystallization analysis fractionation (Crystaf), temperature rising elution fractionation (Tref) and more recently, crystallization elution fractionation (CEF).[1-6] In this study Scalls was used as analytical method. As mentioned previously, our solution crystallization by laser light scattering (Scalls) setup allows for the measurement of solution crystallization and dissolution of polymers in a single experiment under controlled conditions. Due to Scalls being a fairly recently developed technique (compared to aforementioned, well-established methods), it is important to compare results obtained by the different techniques when doing similar experiments and hence the motivation for this particular section of the study. During this study we analyzed the effect of molecular weight of linear polyethylene (PE) on the solution crystallization as well as solution melting/dissolution. A series of linear PE's with varying molecular weights, ranging from 1 000 – 181 000 g/mole were used as purchased and the characterization details are given in Table 6.1.

Table 6.1: Characterization data of polyethylene samples used during this study.

Sample ID	M_w (g/mole)	M_n (g/mole)	M_p (g/mole)	PDI [M_w/M_n]
pe1k	1 230	1 110	1 180	1.11
pe2k	2 010	1 790	2 030	1.12
pe16k	16 500	12 080	22 000	1.37
pe36k	36 500	28 000	33 500	1.31
pe60k	60 000	40 500	55 000	1.47
pe84k	84 500	66 000	73 000	1.28
pe115k	115 500	83 000	99 000	1.40
pe181k	181 000	114 000	126 000	1.59

6.2) Crystallization

Firstly, polymer solutions were cooled in a controlled manner at various rates to allow for crystallization to occur. Figure 6.1 illustrates the Scalls crystallization profiles of the PE samples at various cooling rates as obtained by the 405 nm incident laser beam. A sharp increase in crystallization peak temperature (T_c) was observed up to M_n = 12 000 g/mole; M_w = 16 000 g/mole. Changing between cooling rates from 0.2 °C/min to 0.5 °C/min had no influence on the trend, other than shifting T_c towards slightly lower temperatures. These results were in good agreement with reported literature by Nieto *et al.*[7] where Crystaf was used as fractionation method operating at a similar rate of 0.2 °C/min and temperature range from 100 °C – 30 °C. Here it was mentioned that T_c became independent of molecular weight at M_n = 18 000 g/mole and correlates well with our observations in Scalls. A further increase in cooling rate to 1 °C/min (Figure 6.1c), resulted in a somewhat different trend whereby Tc shifted slightly towards lower values when moving to the highest molecular weight sample, implying that the faster rate had a noticeable influence on the molecular weight dependency of T_c. As expected, further overall shifts in T_c towards lower temperatures were noticed. DSC analyses were also performed on the bulk materials and resulted in comparable trends as obtained with solution crystallization at higher cooling rates with T_c becoming independent after M_n = 12 000 g/mole and this can be seen by the exotherms shown in Figure 6.2. Similar to Scalls results at 1 °C/min, a gradual decrease in T_c was observed in DSC utilizing a cooling rate of 5 °C/min. Peak widths started to broaden as molecular weight decreased due to an increase in fraction of very low molecular weight chains present as the average molecular weight goes down. These low molecular weight fractions lead to a “tailing” phenomenon witnessed in crystallization profiles for M_n < 12 000 g/mole.

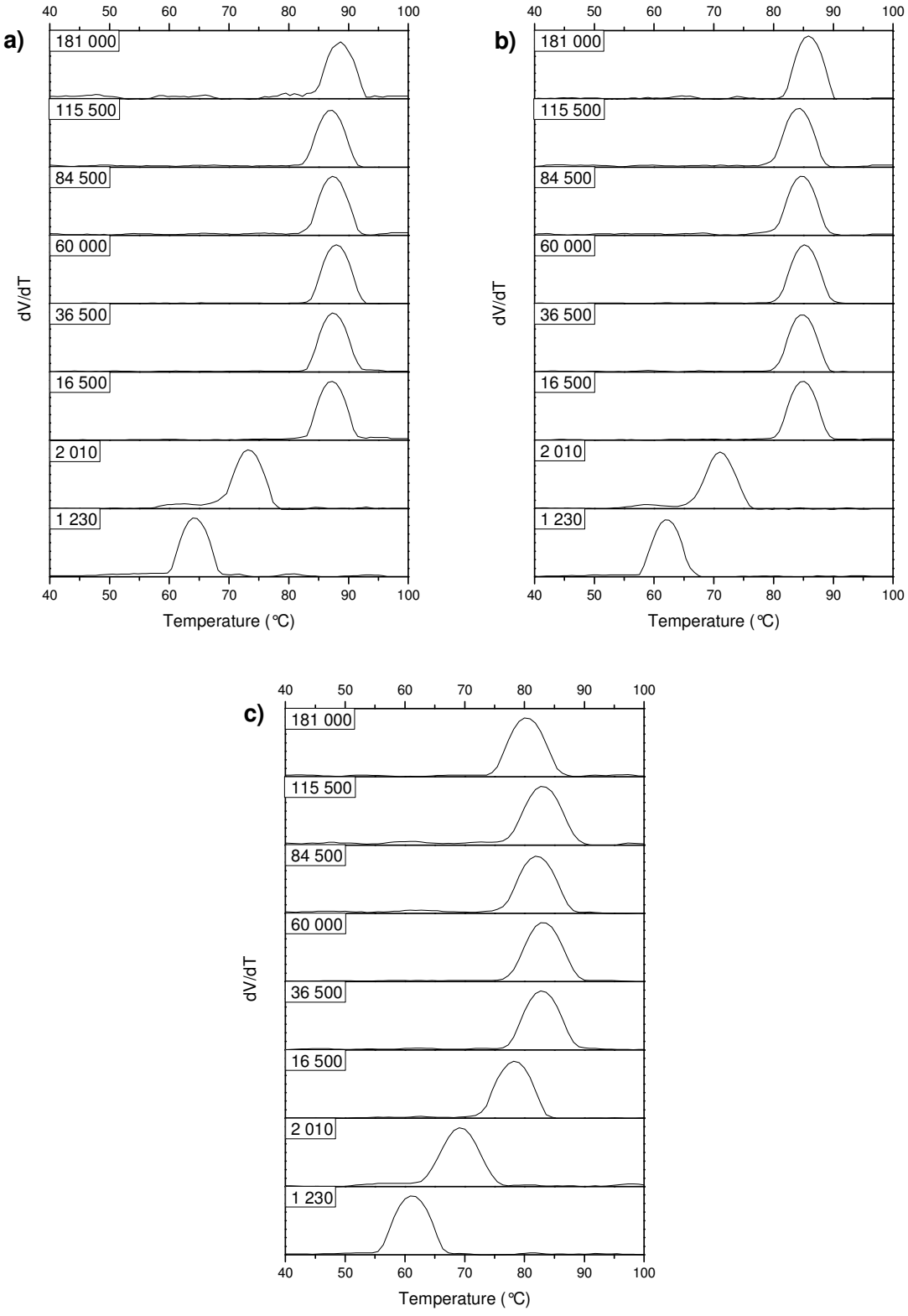

Figure 6.1: Scalls crystallization profiles of PE samples at different cooling rates: a) 0.2 °C/min, b) 0.5 °C/min, c) 1 °C/min.

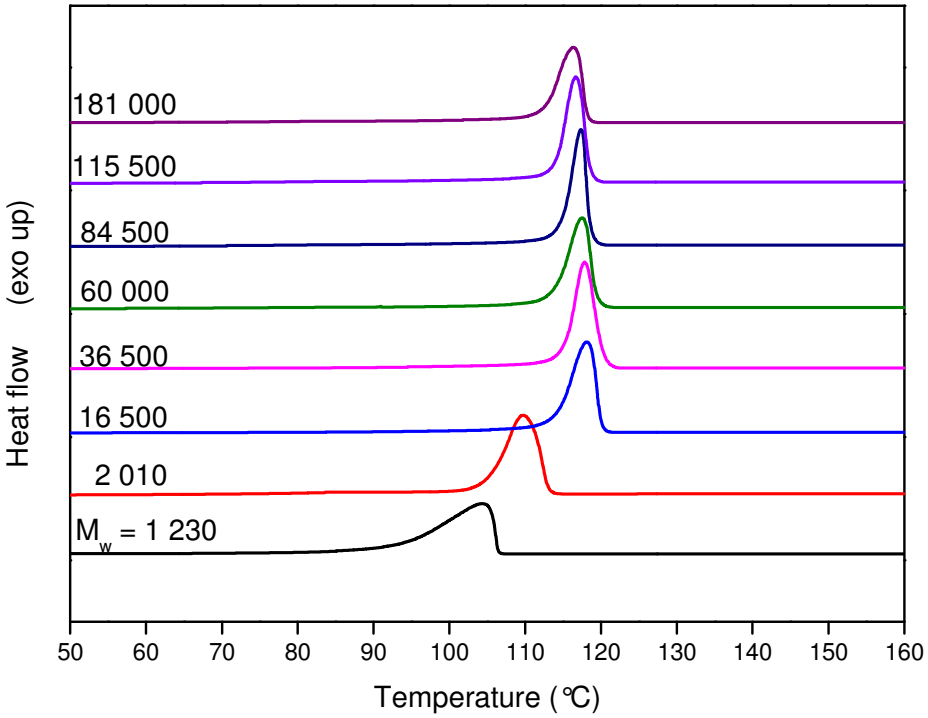

Figure 6.2: DSC crystallization exotherms for PE samples cooled at 5 °C/min.

6.3) Dissolution

One of the main advantages of Scalls is monitoring the dissolution of crystallized material back into solution to study the solution melting behavior immediately after crystallization. Figure 6.3a) and 6.3b) provide the Scalls dissolution profiles and DSC melting endotherms of the various PE's respectively. Similar to T_c, it was detected that the solution melting temperature (T_m) became independent of molecular weight at M_n > 12 000 g/mole. This trend was also clear from DSC endotherms. Once again, peak broadening occurred especially at lower molecular weights due to the larger weight fraction of lower molecular weight chains.

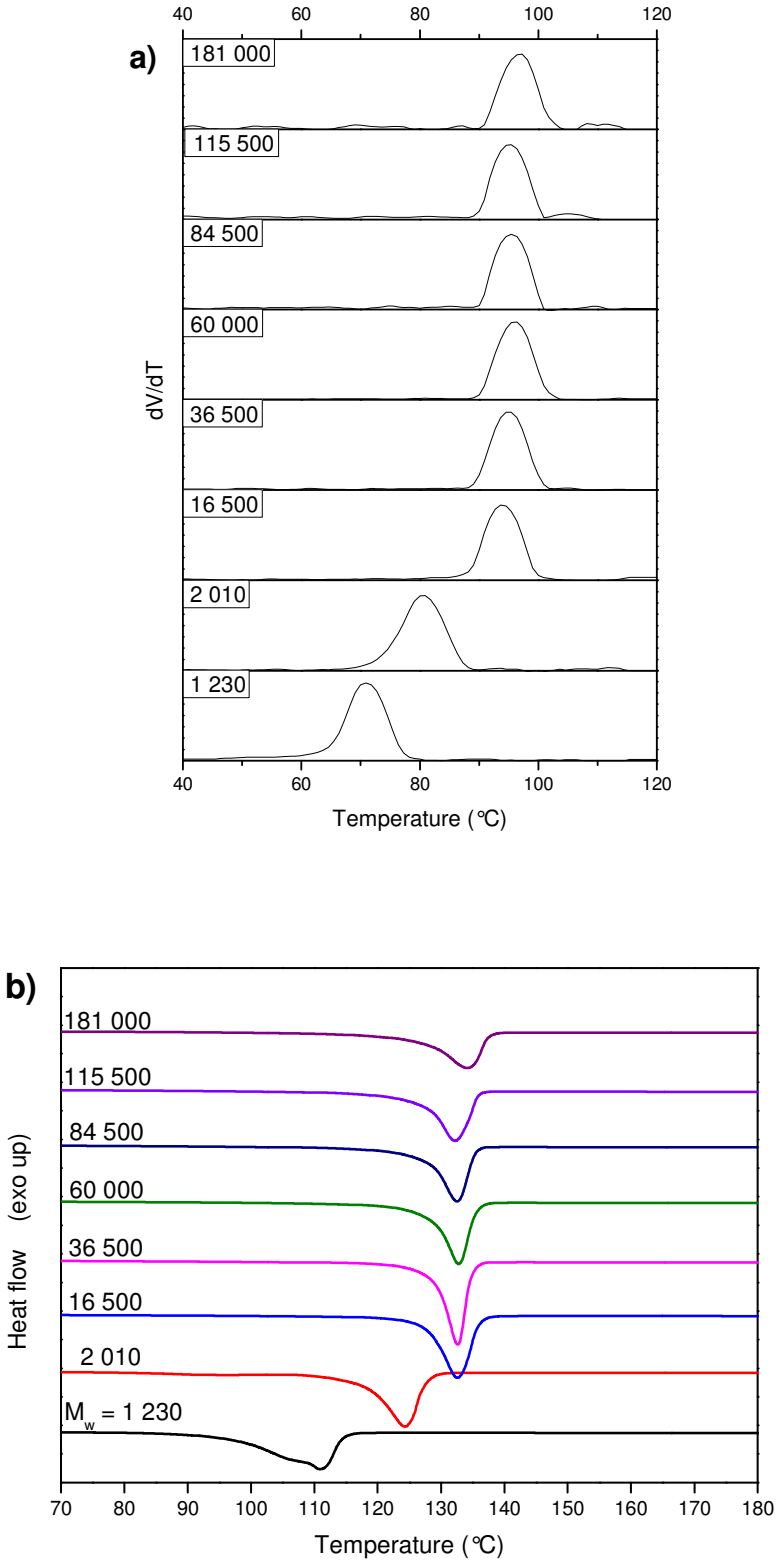

Figure 6.3: a) Scalls dissolution profiles for PE samples heated at 1 °C/min and, b) DSC melting endotherms of PE samples at heating rate of 10 °C/min.

6.4) Experimental data versus theoretical model

Figure 6.4 provides a much clearer representation of the molecular weight (M_n) versus peak temperatures for crystallization (6.4a) and dissolution (6.4b) events. All the curves showed a steep increase in peak temperature at initial stages and quickly reached a plateau after M_n = 12 000 g/mole where after the temperature became independent of M_w as discussed in earlier results. On closer investigation, a slight upwards notion in T_c was noticed at cooling rates of 0.2 °C/min and 0.5 °C/min for the highest molecular weight sample, M_w = 181 000 g/mole. This was in contrast to the faster rate. Looking at the difference in T_c at various rates, indicated to what extent the PE samples were affected by a change in cooling rate. It was found that the peak temperature were more effected when having a higher molecular weight sample as in the case of M_w = 181 000 g/mole where the difference in T_c between lowest and highest cooling rates were much larger than the rest of the samples. The mobility of chains might have been a contributing factor for this behavior because polymer chains has less time to organize themselves at higher cooling rates and longer chains will have reduced mobility in solution. It would therefore be useful to look at even higher PE molecular weights (ultra-high M_w) to conclude the solution T_c and T_m dependency when having much higher polymer chain lengths.

For further evaluation of the Scalls instrumentation performance, it was thought to compare our experimental data against theoretically established models. Through mathematical procedures and modeling by previous research groups, using Crystaf, Equation 6.1 was constructed to describe the relationship between chain length (degree of polymerization) and T_c. After obtaining Scalls crystallization peak temperatures, our data was compared to the theoretical model to see how the experimental data fitted. This was done by inserting the chain length (DP; degree of polymerization) of the PE samples used in this study into Equation 6.1 to obtain the corresponding theoretical T_c values in order to draw up the theoretical DP versus T_c curve. Afterwards, the experimental T_c values were fitted onto the same curve using the weight, number and peak average molecular weight values. Figure 6.5 illustrates the comparison of theoretical and experimental data. It is clear that a reasonable fit was acquired for our Scalls data as compared to the theoretical Crystaf results performed under similar conditions. This suggests that Equation 6.1 is suitable for modeling the dependency of T_c and M_w in Scalls when considering linear polyethylenes. Furthermore we demonstrated that Scalls provide reasonably comparable data to the traditionally used fractionation methods such as Crystaf.[7,8] Although the trends from Crystaf and Scalls

regarding molecular weight dependency were very similar, the theoretical and experimental data did not result in a perfect fit and can be attributed to a couple of factors with the major one probably being the detection method of crystallization events. Crystaf measures the decrease in solution concentration during crystallization and Scalls measures the decrease in incident laser beam intensity as a result of increased scattering during crystallization.

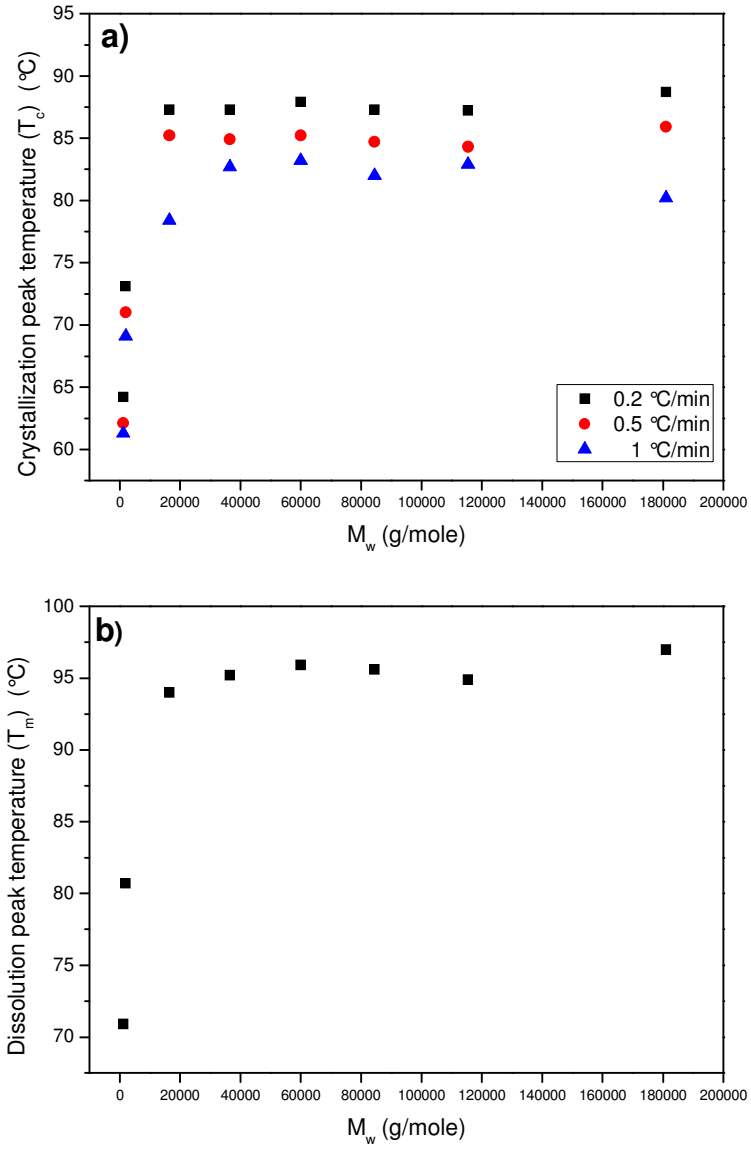

Figure 6.4: Representation of peak temperatures as function of M_w: a) overlay of T_c at various cooling rates and, b) dissolution temperatures at 1 °C/min.

$$T_c = \frac{89(r - 13.3)}{r} - 4.4$$

T_c = crystallization peak temperature; r = chain length

Equation 6.1: Theoretical relationship between crystallization peak temperature (T_c) and polymer chain length (r) as proposed by Nieto *et al.*[7] for crystallization in Crystaf.

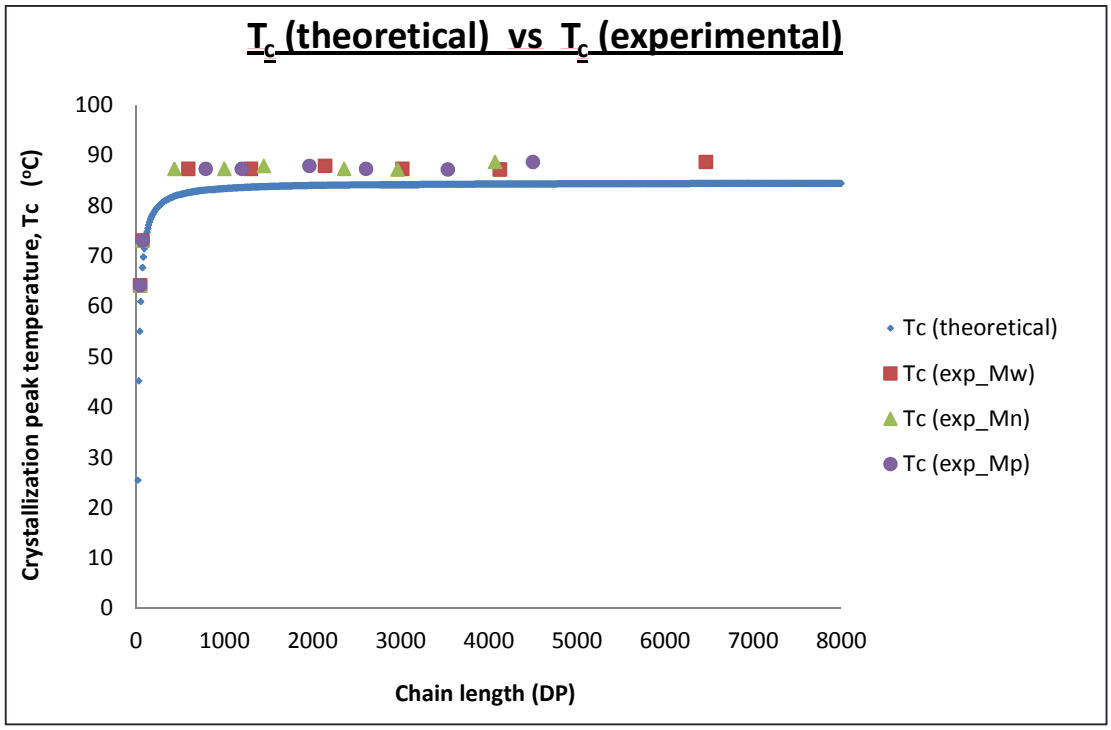

Figure 6.5: Theoretical (Crystaf) vs experimental (Scalls) data for relationship between polymer chain length and crystallization peak temperature for linear polyethylenes.

6.5) Scalls dissolution prediction model

Because Scalls also allows for the monitoring of dissolution behavior, it was thought to be very useful to come up with a model to qualitatively predict the dependency of T_m and M_w for this fractionation technique. This was done by fitting a non-linear least-square curve to the experimental data and shown in Figure 6.6(a). The theoretical fit had a R^2-value of 0.995 and gave rise to Equation 6.2. Although the R^2-value is an indication if our prediction/regression fit is adequate, it is

not totally correct to look at this value alone to establish the most perfect fit. According to statistics R^2 must be used in conjunction with a residual plot to get an idea whether the estimations or predictions are biased at certain conditions. Figure 6.6(b) illustrates the residual plot for the data set and points out the level over-estimation and under-estimation in T_c throughout the molecular weight range. No extensive deviations from the residual line, y = 0, were noticed meaning that the model predictions were in close proximity to experimental T_c values. Therefore, from results observed in Figure 6.6, in can be said that Equation 6.2 is appropriate for modelling dependency of dissolution/solution melting temperature and M_w for linear polyethylenes in Scalls. This can be very useful for using Scalls as a screening tool and complementary technique to especially preparative TREF to get an idea of fractionation temperatures.

$$T_m = e^{\left[4.57 - \frac{325.06}{(M_w - 160.64)}\right]}$$

T_m = dissolution peak temperature

M_w = weight-average molecular weight

Equation 6.2: Mathematical prediction of relationship between dissolution peak temperature (Tm) and weight-average molecular weight (M_w) for linear polyethylenes in Scalls.

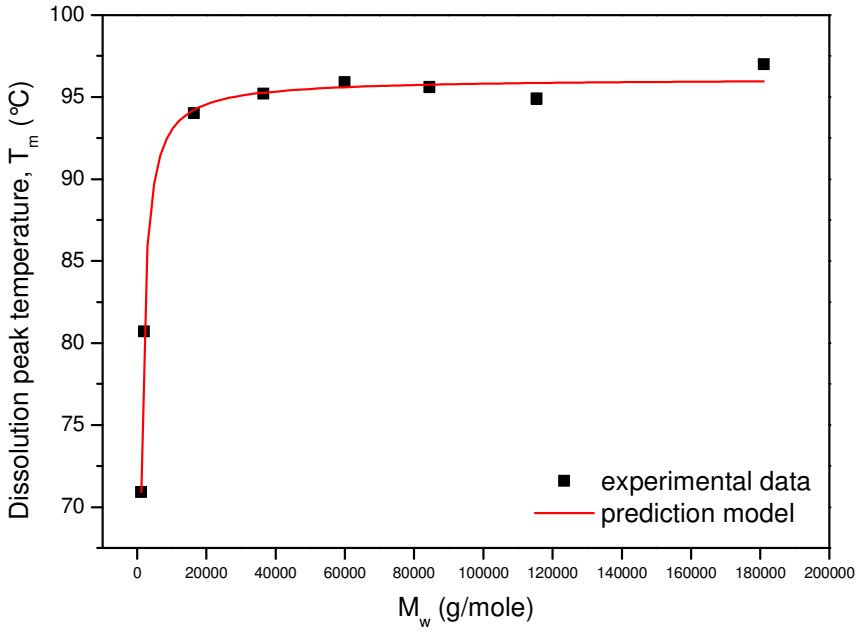

Figure 6.6: Predicted model fit versus experimental data for dissolution temperature dependency and molecular weight.

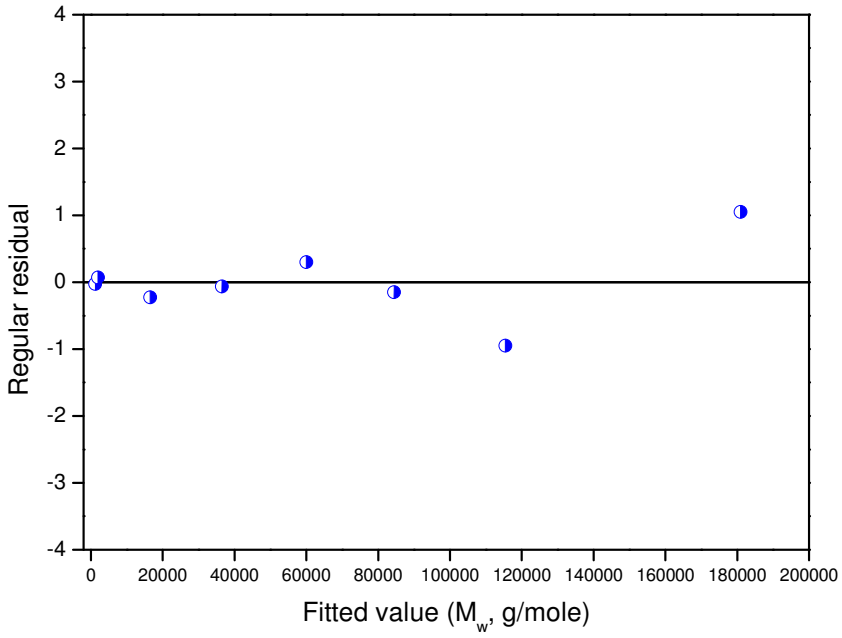

Figure 6.7: Residual curve of prediction model showing the degree of prediction accuracy in terms of over-and under estimating T_m throughout the M_w range.

The peak broadening discussed earlier has also been reported in literature for solution crystallization. It was mentioned that this phenomena can be approximated by Flory's distribution given in Equation 6.3.[7,9] It allows for a qualitative prediction of polymer chains within certain molecular weight limits. By using this equation, the plots in Figure 6.7 were constructed for ML = 2 000, 6 000, 10 000 and 20 000. A rapid decrease in fraction of polymer chains with limit below 2 000 g/mole (W_{2000}) and 6 000 g/mole (W_{6000}) were seen, meaning that the low molecular weight fraction of chains is significantly less as M_n increased and hence the sharper, narrower peaks seen in crystallization and melting profiles for both Scalls and DSC measurements. Additionally, a more gradual drop were noticed for fraction of polymer chains having a molecular weight limit below 20 000 g/mole due to higher M_n PE samples having a larger probability for some chains being below the 20 000 limit and higher than 6 000 g/mole [e.g. for M_n = 60 000 g/mole; $W_{2000} \approx 0.0005 \approx 0.05\%$ but $W_{20\,000} \approx 0.045 \approx 5\%$]. Through this example, it can qualitatively be concluded that for a linear PE sample having a M_n = 60 000 g/mole, roughly 5 wt% of polymer chains will be below 20 000 g/mole and roughly 0.05wt% of chains will have molecular weights (M_n) below 2 000 g/mole.

$$W_{ML} = \int_0^{ML} \frac{M}{M_n^2} \exp\left(-\frac{M}{M_n}\right) dM = \frac{M_n - (M_n + M_{ML}) \exp\left(-\frac{M_{ML}}{M_n}\right)}{M_n}$$

W_{ML} = weight fraction of polymer chains having a molecular weight lower than a certain limit (M_{ML})

Equation 6.3: Flory's distribution for calculating the weight fraction (W_{ML}) of polymer chains that have molecular weights lower than a certain limiting value (M_{ML})

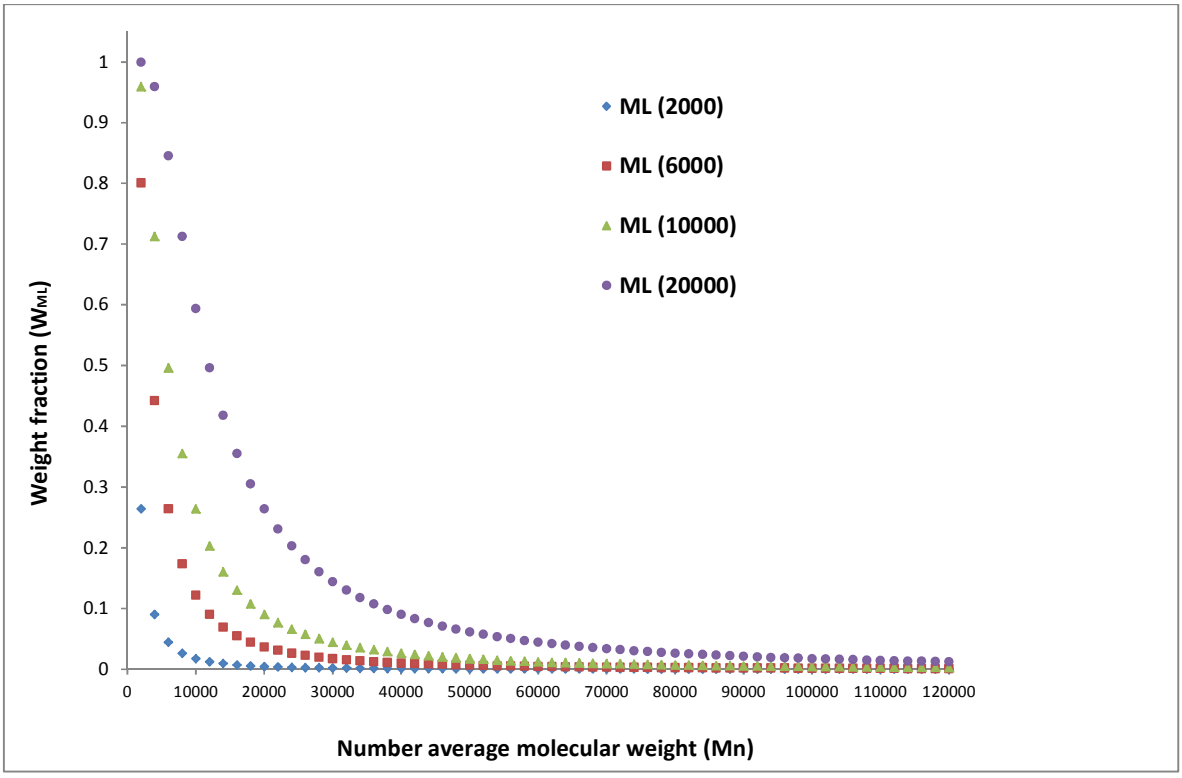

Figure 6.8: Weight fraction of chains having a molecular weight lower than a certain limit as a function of number average molecular weight (M_n)

6.6) Summary

To conclude, T_c was found to be independent of molecular weight after M_w = 16 000 g/mole. This behavior was seen during solution (Scalls) and melt (DSC) crystallization studies. Scalls results correlated well with the theoretical Crystaf model and a near perfect fit was obtained. Dissolution studies showed similar trends with Tm being independent of molecular weight at Mw = 16 000 g/mole. From these results, an equation was successfully generated to model dissolution temperatures of linear polyethylenes in Scalls.

6.7) References:

(1) Anantawaraskul, S., Soares, J.B.P. & Wood-Adams, P.M. **2005,** *Fractionation of semicrystalline polymers by crystallization analysis fractionation and temperature rising elution fractionation.*

(2) Alghyamah, A.A. & Soares, J.B. 2012, "Crystallization Elution Fractionation of LLDPEs Made with Metallocene Catalysts", *Macromolecular Symposia*Wiley Online Library, , pp. 43.

(3) Monrabal, B. **2006,** *Microstructure characterization of polyolefins. TREF and CRYSTAF*.

(4) Monrabal, B., Sancho-Tello, J., Mayo, N. & Romero, L. **2007,** "Crystallization Elution Fractionation. A New Separation Process for Polyolefin Resins", *Macromolecular Symposia,* vol. 257, no. 1, pp. 71-79.

(5) Soares, J.B.P. & Hamielec, A.E. **1995,** "Temperature rising elution fractionation of linear polyolefins", *Polymer,* vol. 36, no. 8, pp. 1639-1654.

(6) Soares, J.B.P. & Anantawaraskul, S. **2005,** "Crystallization analysis fractionation", *Journal of Polymer Science, Part B: Polymer Physics,* vol. 43, no. 13, pp. 1557-1570.

(7) Nieto, J., Oswald, T., Blanco, F., Soares, J.B. & Monrabal, B. **2001,** "Crystallizability of ethylene homopolymers by crystallization analysis fractionation", *Journal of Polymer Science Part B: Polymer Physics,* vol. 39, no. 14, pp. 1616-1628.

(8) Soares, J.B., Beigzadeh, D., Duever, T.A. & da Silva Filho, Adilson A **2000,** "Mathematical Modelling and Control of Chemical Composition Distribution of Ethylene/α-Olefin Copolymers Made with Single and Combined Metallocene Catalysts", *Polymer Reaction Engineering,* vol. 8, no. 3, pp. 241-270.

(9) Monrabal, B. 1996, "Crystaf: Crystallization analysis fractionation. A new approach to the composition analysis of semicrystalline polymers", *Macromolecular Symposia*Wiley Online Library, , pp. 81.

Chapter 7

Results and Discussion:

Effect of solvent on solution behavior of LLDPE

This chapter focuses on the results obtained for LLDPE (PE-1-octene); studying the effect of solvent on the solution crystallization and dissolution behavior

Recently Cheruthazhekatt et al.[1] reported the significance of the solvent type used during solution fractionation by crystallization of binary blends of linear polyethylene and isotactic polypropylene. It was found that both co-crystallization and co-dissolution were influenced by the type of solvent used. However, results of only one single incident laser beam (blue = 405 nm) were discussed. Because the ability of crystallites to scatter an incident beam is directly dependent on the wavelength of the beam, depending on the polymer sample, certain events might be missed when only using a single wavelength for detection. Therefore, during this study it was decided to analyze the data obtained by three different lasers with varying wavelengths namely blue (405 nm), green (532 nm) and red (635 nm) to evaluate the solution kinetics of a linear low-density polyethylene (LLDPE) (PE-1-octene) sample. The main objective was to study the influence of solvent choice on solution behavior (crystallization and dissolution) during the solution fractionation of a semi-crystalline polymer. Characterization data of the metallocene-catalyzed LLDPE sample are as follows: M_n = 76 049 g/mole, M_w = 224 462 g/mole, PDI = 2.9 and density = 0.908 g/cm^3.

7.1) Crystallization

Figure 7.1 illustrates the Scalls cooling profiles for the LLDPE sample analyzed in several solvents at a cooling rate of 0.2 °C/min. The three different colored curves represent the signals obtained by the different lasers. From the first derivative profiles it can be seen that the peak associated with the blue laser signal is always present at the highest temperature, followed by the peaks of the green and the red laser signals at lower temperatures. This phenomenon is due to the difference in laser wavelengths. At the lowest wavelength (405 nm), the blue laser will always be the first of the three beams to be scattered by the smaller sized crystallites during the initial stages of crystallization. As the crystallites grow larger, it will lead to blue laser signal obliteration and the higher wavelength laser beams (green followed by red) will start to scatter and hence the positioning of the various laser signal peaks. Thus, the positioning/shifts of the various laser peaks can provide information on crystal growth in solution during cooling.

Crystallization peak temperatures (T_c) for TCB and o-DCB (Figures 7.1a and 7.1b) were very similar at roughly 60 °C, whereas T_c for decalin and xylene were shifted slightly lower towards 45 °C and 55 °C respectively. Although decalin and xylene gave rise to lower a Tc, the onset of crystallization were similar to those of TCB and o-DCB at approximately 70 °C signifying that crystallization occurred over a much broader temperature range than in TCB. The scattering seen at

lower temperatures in Figure 7.1b) indicates that crystallization occurred over an even broader temperature range in o-DCB compared to the other solvents. A dV/dT value much higher than zero implies that crystallization was still incomplete as the temperature reached 30 °C in o-DCB and lower temperatures were needed for complete crystallization of the LLDPE sample in this particular solvent. In this case the use of higher wavelength laser beams provided valuable information on the heterogeneity of the LLDPE sample as the blue laser profiles for especially TCB and o-DCB appeared to be very similar. As mentioned earlier, the positioning of the laser profiles relative to each other, i.e. the spacing between red-green-blue peaks, can also assist in extracting useful data on the crystal growth in solution. In the case of TCB, o-DCB and decalin the signals were somewhat separated but this is in contrast with xylene analysis where all three signals were almost perfectly superimposed. It might be assumed that in solvents such as TCB, o-DCB and decalin, more uniform crystal growth occurred resulting in systematic scattering of laser beams with increasing wavelengths. On the other hand, cooling the sample in xylene led to more rapid crystal growth and simultaneous scattering, resulting in a near perfect overlay of Scalls profiles.

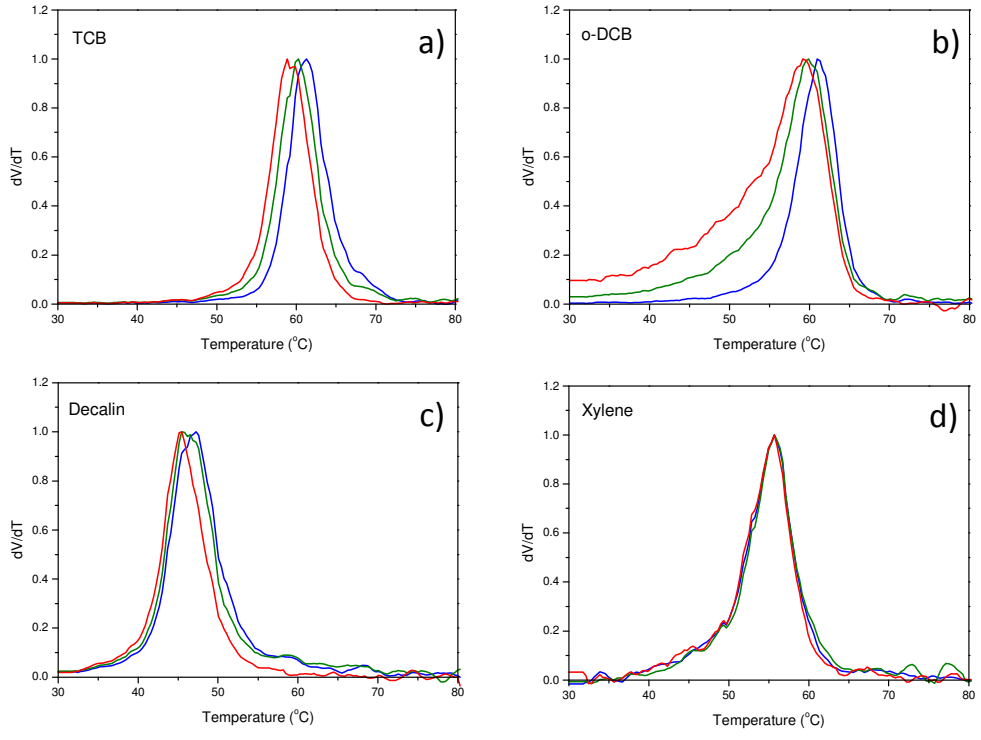

Figure 7.1: Normalized first derivative Scalls curves for crystallization at 0.2 °C/min in different solvents. The color of the curves correspond to the various lasers (blue = 405 nm, green = 532 nm and red = 635 nm).

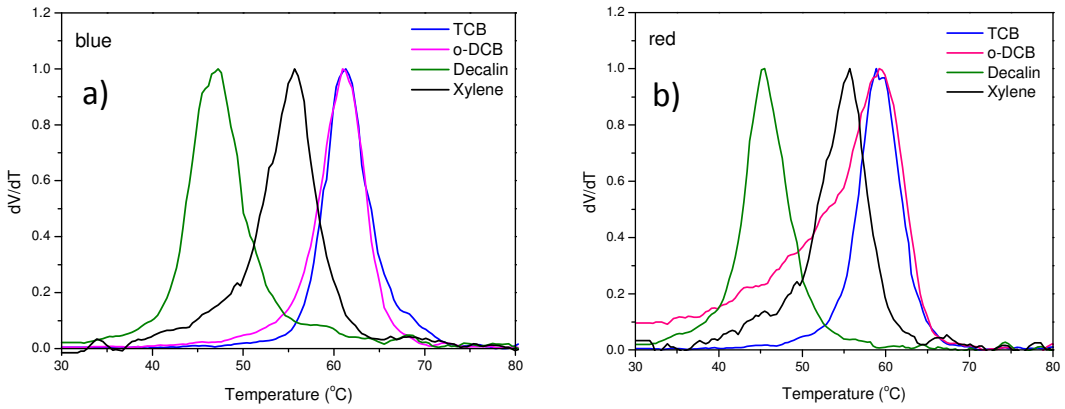

Figure 7.2: Overlay of crystallization profiles obtained with a) blue (405 nm) and b) red (635 nm) lasers in various solvents and cooled at 0.2 °C/min.

Figure 7.2a) and 7.2b) compares the data obtained by blue and red diode laser beams respectively. As mentioned previously, apart from T_c, all blue laser profiles appeared to be very similar. As seen from Figure 7.2a) it is clear that the onset of crystallization was unaffected by the type of solvent used. A close resemblance in crystallization behavior in TCB and o-DCB was observed. It can be said that the crystallization behavior at initial stages in these two solvents were very similar as indicated by the results obtained by the blue laser. It is important to note that these profiles do not present the total crystallization event as the blue laser signal is obliterated when the crystallite sizes become too large. At this stage these crystals will still increasingly scatter the higher wavelength laser beams, as long as crystal growth continues. The effect of solvent on the crystallization behavior was evident from the higher wavelength signals in depicted in Figure 7.2b). Distinct differences in crystallization curves were observed and crystallization occurred over the broadest temperature range in o-DCB. It can therefore be said that the solvent type chosen for solution crystallization analysis will influence the interpretation and discussion of the final results. This is indeed fundamental, especially for comparison purposes when looking at different techniques, using different solvent systems.

An increase in cooling rate to 1 °C/min shifted T_c to lower values and narrowed the crystallization temperature range. Peak shapes for analysis in TCB, decalin and xylene remained similar to those observed at 0.2 °C/min and are presented in Figure 7.3. Even at 1 °C/min, crystallization events could be observed in the lower temperature range when using o-DCB as solvent. The effect of cooling rate on T_c for the different solvents can be seen in Figure 7.4. As expected, a decrease in T_c was observed with an increase in cooling rate. Near perfect linear fits were applied to all curves and are indicated by the R^2-values being very close to unity ($R^2 \approx 1$). These trends were observed for all laser beams. Due to the fact that only marginal differences were found for the different slopes, implies that an increase in cooling rate, decreased T_c to a similar extent regardless of the solvent type even though crystallization behavior, as discussed earlier, were greatly influenced.

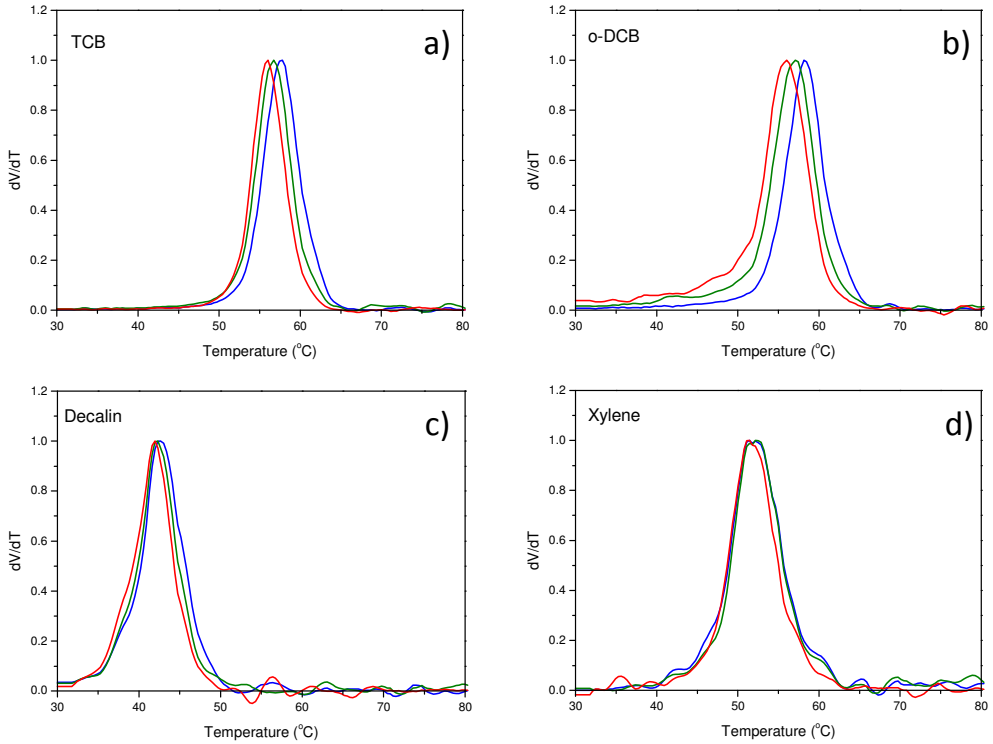

Figure 7.3: Normalized first derivative Scalls curves for crystallization at 1 °C/min in different solvents.

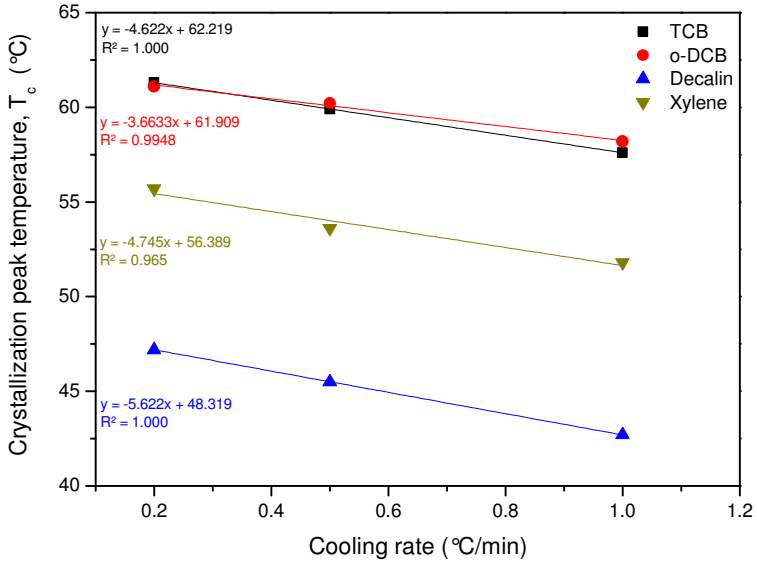

Figure 7.4: Crystallization peak temperature (T_c) as a function of cooling rate. (blue laser)

7.2) Dissolution

Following crystallization, the turbid solutions was heated at a controlled rate of 1 °C/min to allow for dissolution of the crystallized polymer. These events were studied by monitoring the increase in laser intensity as polymer crystallites melted in solution. Dissolution results obtained after 1 °C/min cooling (presented in Figure 7.3) are shown in Figure 7.5. Looking at the dissolution temperatures (T_m), similar to the crystallization profiles, TCB resulted in the sharpest dissolution peak, and dissolution of polymer occurred over the broadest temperature range when o-DCB was used as solvent. Analyses in decalin and xylene resulted in curves slightly broader than that observed for TCB. Although T_m for analysis in xylene was ± 10 °C lower than that for TCB and o-DCB, complete dissolution occurred at similar temperatures. This further confirms that solvent type influences, not only crystallization behavior, but also solution melting kinetics. Related results were reported by Cheruthazhekatt et al.[1] when studying a polyethylene (PE) and isotactic polypropylene (iPP) blend. Minimal co-crystallization effects were observed when using TCB as solvent and analysis in xylene resulted in the least co-dissolution effects. It was then proposed to use solvent combinations when fractionating according to crystallizability.

Once more, the significance of using lasers with different wavelengths can be seen in Figure 7.6 where the dissolution data for blue and red laser beams are presented in Figure 7.6a) and 7.6b) respectively. In Figure 7.6b) distinct differences could be observed for TCB and o-DCB in the lower temperature range (below 65 °C), whereas these profiles were largely identical as detected by the 405 nm blue laser. Polymer crystallites started melting at much lower temperatures in o-DCB. These observations confirm that the solvent type used, plays an essential role on the solution behavior (crystallization and melting) of polymers.

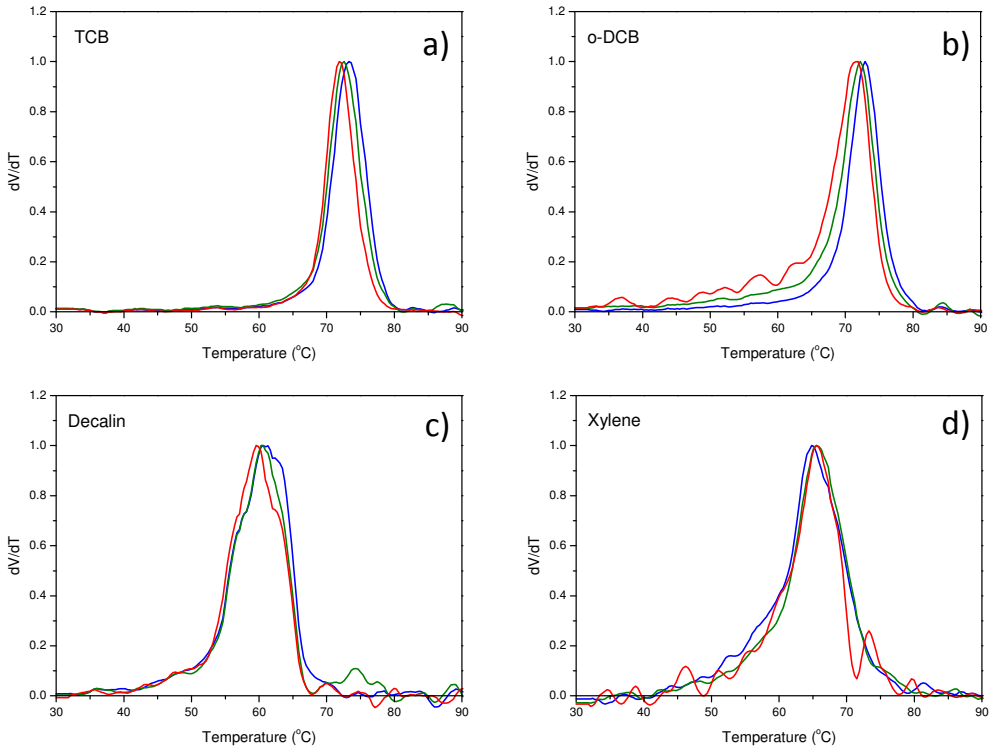

Figure 7.5: Normalized first derivative Scalls curves for dissolution at 1 °C/min. (after 1 °C/min cooling)

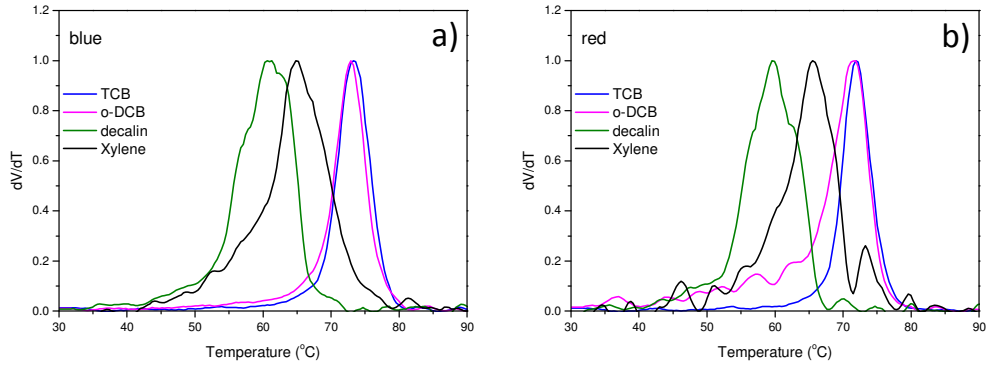

Figure 7.6: Overlay of dissolution profiles obtained with a) blue (405 nm) and b) red (635 nm) lasers in various solvents, heated at 1 °C/min. (after 1 °C/min cooling)

Results indicate that solvent choice will directly influence fractionation processes such as in the commonly used preparative temperature rising elution fractionation (p-Tref) method where polymer chains are fractionated according to crystallizability. Tref analysis done in different solvents will affect the crystallization on the inert substrate during the cooling step and ultimately result in differences of the various temperature fractions during elution due to distinct differences in crystallization and dissolution rates observed from Scalls data. According to the solvents used during this study and the low cooling rates applied during TREF fractionation, analysis in o-DCB will result in the highest soluble fraction.

7.3) Summary

A PE-1-octene LLDPE copolymer was analyzed in a range of different solvents. Not only were T_c and T_m greatly influenced by the solvent type, but crystallization and dissolution temperature ranges over which these solution events occurred were also greatly affected. Crystallization onsets were essentially unaffected by the variation in solvent. Solution kinetics was studied from laser scattering data of three lasers with varying wavelengths and allowed for improved detection of certain events over a broader temperature range. Results indicated that interpretation of data can be influenced by the solvent selected for solution analyses.

7.4) References:

(1) Cheruthazhekatt, S., Robertson, D.D., Brand, M., van Reenen, A. & Pasch, H. **2013,** "Solution Crystallization and Dissolution of Polyolefins as Monitored by a Unique Analytical Tool: Solution Crystallization Analysis by Laser Light Scattering", *Analytical Chemistry,* vol. 85, no. 15, pp. 7019-7023.

Chapter 8

Conclusions and recommendations

An overall conclusion on the various sections discussed in this manuscript is given in this chapter together with some future recommendations.

8.1) Conclusions

8.1.1) PLLA/PDLA binary blends

For the first time, non-isothermal solution crystallization and dissolution behavior of poly(L-lactic acid), poly(D-lactic acid) and their binary blends were studied. It was demonstrated that Scalls is very convenient for analyzing these phenomena in a polymer system known for its very poor crystallization rates. Distinct uni-modal crystallization profiles were seen for all samples together with a broadening in peak widths and shifting of T_c towards lower temperatures as the cooling rate was increased. Solution crystallization behavior of PLLA and PDLA homopolymers were identical throughout the cooling rate range. Furthermore, the addition of PDLA to PLLA resulted in SC crystallite formation in solution. The SC network had a nucleating effect on PLLA homocrystallite behavior throughout the entire blend composition. Crystallization peak area and onset of crystallization increased with an increase in PDLA concentration. Higher PDLA additions (30 wt% and 50 wt%) resulted in the SC network having a confining effect on homopolymer crystallization whereby SC crystallites hinders the diffusion ability of the PLLA polymer chains and shifting T_c to slightly lower temperatures. Consecutive Scalls cooling cycles showed that unmelted SC crystallites resulted in improved nucleation of homocrystallites. DSC results confirmed stereocomplex formation by the presence of characteristic SC endotherms. Enthalpies of these endotherms increased with increasing amounts of PDLA.

Solution melting by Scalls allowed for the detection of dissolution transitions upon heating. Multiple melting events were observed, which were in good agreement with calorimetric results. Re-crystallization events were more subtle for the blends, possibly due to improved crystallization kinetics during cooling. Overall, this study highlights the effectiveness of introducing PDLA for enhancing the crystallization rate of PLLA.

Particle size measurements were successfully done on the crystallized polymer. DLS data showed that addition of PDLA resulted in smaller sized particles and correlated well with reported literature from melt-crystallization studies and was reasoned to be due to higher nucleation efficiency in the presence of SC. The reason for particle sizes of DL10/90 after the second cooling being so much higher than the other blends was not very clear at the time of study but was thought to be related to the crystallization rate of the specific blend ratio because of the Scalls profiles also being different to the rest. Further crystallization occurred during the isothermal storage of the polymer solutions and was indicated by a bimodal average size distribution, pointing out the low crystallization kinetics of poly(lactic acid) and the importance of studying suitable methods to increase the

crystallization rates of this biopolymer which is quickly becoming a suitable substitute of commercial petroleum-based plastics. SEM results indicated that the surface morphology was also influenced with addition of PDLA, resulting in a smoother surface as compared to the PLLA homopolymer casted film.

8.1.2) Addition of SC to PLLA

The influence on PLLA crystallization by small additions of stereocomplex crystals was studied. SC had no effect on T_c even up to 10 wt%. However, crystallization peak area increased with an increase in SC content and was 39% more than PLLA at the highest SC content (10 wt%). Fascinatingly at a very low SC incorporation of 2 wt%, the crystallization peak area increased by roughly 14% which was found to be equivalent to the addition of 10 wt% PDLA. These results indicate that the addition of small amounts of SC can have an enhanced nucleating effect and can be useful for increasing the crystallinity of PLLA.

8.1.3) PLLA/PBS binary blends

For the first time, crystallization and dissolution events of poly(L-lactic acid) (PLLA), poly(butylene succinate) (PBS) and their binary blends were analyzed from dilute solutions. Homopolymer crystallization resulted in defined peaks with PLLA crystallizing at roughly 25 °C higher than PBS for all cooling rates. It was observed, from dissolution studies, that both polymers displayed multiple solution melting behavior due to re-crystallization of crystals with lower thermal stability, which melted at lower temperatures. These re-crystallization events were larger in the case of PLLA and were identified by a negative scattering peak amidst the two melting endotherms and also highlighted the low PLLA crystallization kinetics.

Furthermore, the effect of addition of various amounts of PBS on the thermal solution behavior of PLLA was studied. During consecutive cooling cycles, no specific trend was visible during the first cooling. From the second and third crystallization cycles it was clear that T_c for PLLA shifted to lower temperatures with an increase in PBS content above 30 wt%, indicating that PLLA crystallization was hindered at these PBS loadings. However, the crystallization rate of PLLA was increased with PBS content up to 30 wt% and this was identified by the presence of PLLA crystallization peaks at higher temperatures as compared to neat PLLA.

Dissolution studies showed that addition of PBS lead to a decrease in re-crystallization event in PLLA, indicating that more sufficient crystallization occurred during cooling in the presence of PBS. It might suggest that PBS had a nucleating effect on PLLA during crystallization although PBS were in a molten state at the time of PLLA crystallization, meaning that possible molten PBS droplets acted as nucleation sites for the formation of PLLA crystallites. A composition of 10 wt% PBS had the highest enhancing effect, showing the highest $T_{c\ (PLLA)}$ during cooling and smallest re-crystallization peak upon heating.

The presence of both polymer components was confirmed by FTIR and the characteristic carbonyl peaks for both pristine polymers were visible throughout the blend compositions. DSC analysis further confirmed that PLLA crystallization rates can indeed be increased by small additions of PBS and this was noticed by an increase in crystallization exotherm at PBS loadings below 50 wt%. In addition, it was demonstrated that Scalls is a useful analytical tool for studying solution behavior in biopolymer binary blends and is not restricted to polyolefin analysis.

8.1.4) Effect of molecular weight on solution T_c and T_m in linear PE

The solution behavior in a range of linear polyethylene samples with varying molecular weights and narrow molecular weight distributions were studied by Scalls. T_c was found to be independent of molecular weight after M_w reached a value of 16 000 g/mole and a distinct plateau was visible in T_c versus M_w curves. It was however witnessed that a faster cooling rate (1 °C/min) had a slight effect on the solution behavior whereby the crystallization plateau was reached at a higher molecular weight value (M_w = 36 000 g/mole). DSC exotherms confirmed this trend. Differences in T_c-shifts indicated that higher M_w samples were more affected by the change in cooling rate as compared to the lower molecular weight types which might be due to the lower molecular mobility of longer chains to reorganize in solution during a faster cooling scan. Experimental data were fitted to a theoretical mathematical Crystaf model and a near perfect fit was obtained. It was concluded that the theoretical estimation equation was suitable for modeling the dependency of T_c and M_w in Scalls.

Additionally, dissolution studies were done to study the dependency of T_m and M_w. Similar to crystallization analyses, T_m became independent of M_w after M_w = 16000 g/mole. DSC endotherms and Scalls profiles showed similar tendencies. A minimum least-square fit was applied to the experimental data with a resultant R^2-value of 0.995. In addition to R^2, the fitted model resulted in a

rational residual curve meaning that over- and under estimation of T_m throughout the molecular weight series will be kept to a minimum. Finally, an equation was generated to model solution melting temperatures of linear polyethylenes in Scalls. Comparison of theoretical models established through the use of conventional techniques, proved that Scalls is a useful method for the analyses of semi-crystalline polymers.

8.1.5) Effect of solvent on LLDPE solution behavior

Solution crystallization and dissolution studies of a PE-1-octene LLDPE copolymer were successfully conducted in a variety of solvents. It was found that peak temperatures (T_c, T_m) and peak distributions were greatly influenced by the type of solvent used. This knowledge is crucial especially when comparing results obtained by means of different solution fractionation methods, due to various techniques (CEF, Crystaf, Tref) using a wide range of solvents. Crystallization onsets were almost unaffected despite the variation in solvents. The use of higher wavelength lasers allowed for detection of solution events over a broader temperature range (otherwise missed when only using a single laser beam) and deeper insight into crystallization rates and kinetics. Despite the similarity in chemical nature of TCB and o-DCB, remarkable differences in crystallization and dissolution behavior in these solvents could also be pointed out.

8.2) Recommendations

On-going development of a second, more advanced Scalls instrument is in progress. This will allow for more quantitative analysis of crystallization kinetics and crystal growth rates. An increase in operating temperature range will allow for the measurement of solution behavior in a widespread selection of polymer systems. Due to the increased demand for biopolymer usage, further detailed investigations should be done on these systems, especially poly(lactic acid), due to the complexity of the crystallization and melting behavior. However, future investigations on these polymers will include the following: further detailed study on poly(lactic acid) dissolution behavior and blends of PLA with other polymers. It might also be beneficial to look at results obtained by the other two higher wavelength lasers (green = 532 nm, red = 635 nm) to see what extra information can be extracted from these polymer systems with regards to crystallization kinetics, as the ability of

crystallized particles to scatter light is dependent on the wavelength of the incident laser beam. The simple and unique Scalls technique seems to be very convenient for solution studies with the major advantages being the analysis of solution crystallization and melting in a single experiment, short analysis times and small solvent volume required.

Appendix A: Scalls data

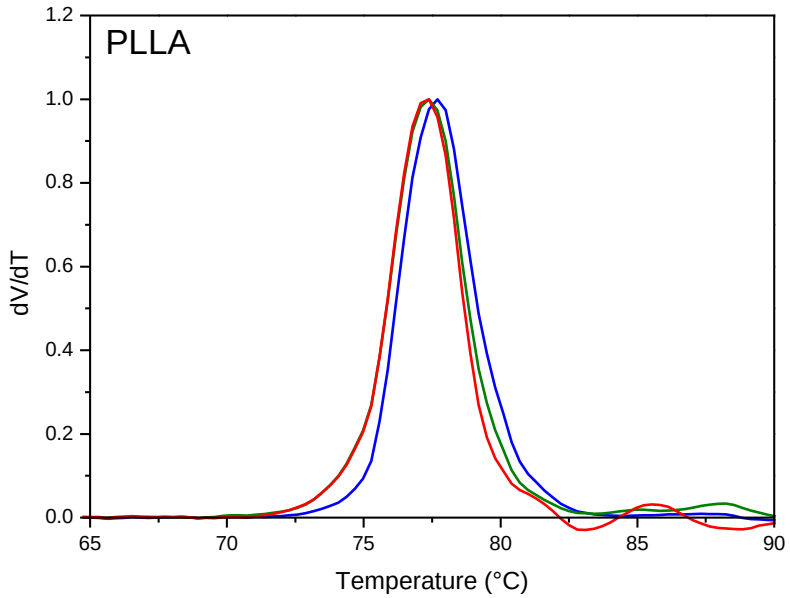

Figure A-1: Overlay of Scalls crystallization profiles for PLLA cooled at 1 °C/min, as detected by different lasers.

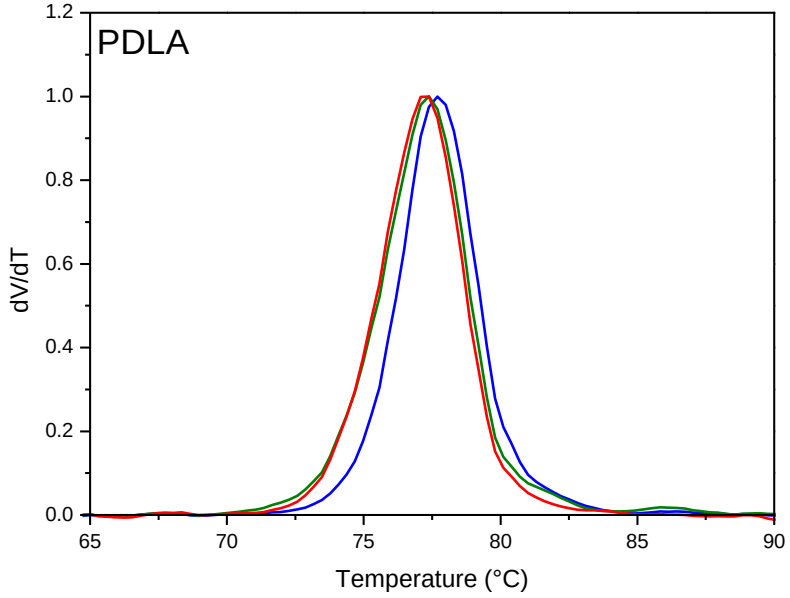

Figure A-2: Overlay of Scalls crystallization profiles for PDLA cooled at 1 °C/min, as detected by different lasers.

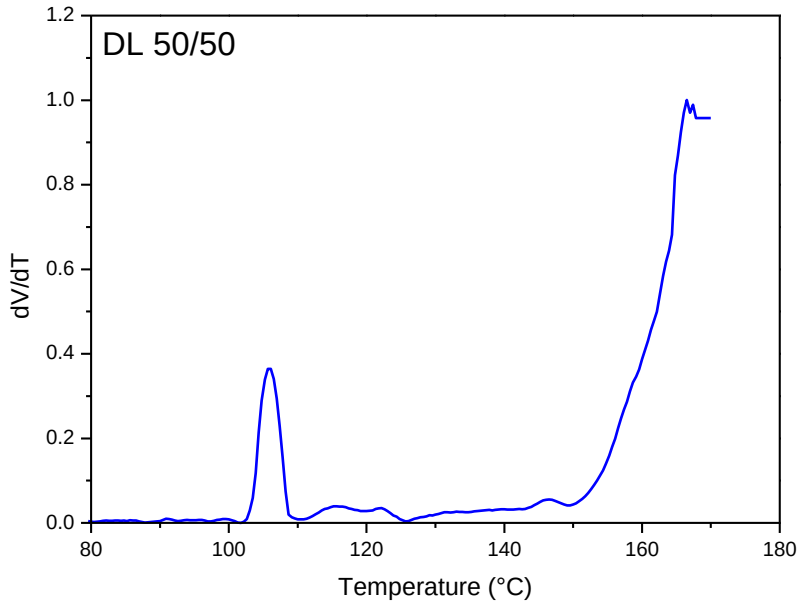

Figure A-3: Scalls dissolution profile for PLLA50/PDLA50 blend heated at 1 °C/min after crystallization at 1 °C/min. (blue laser).

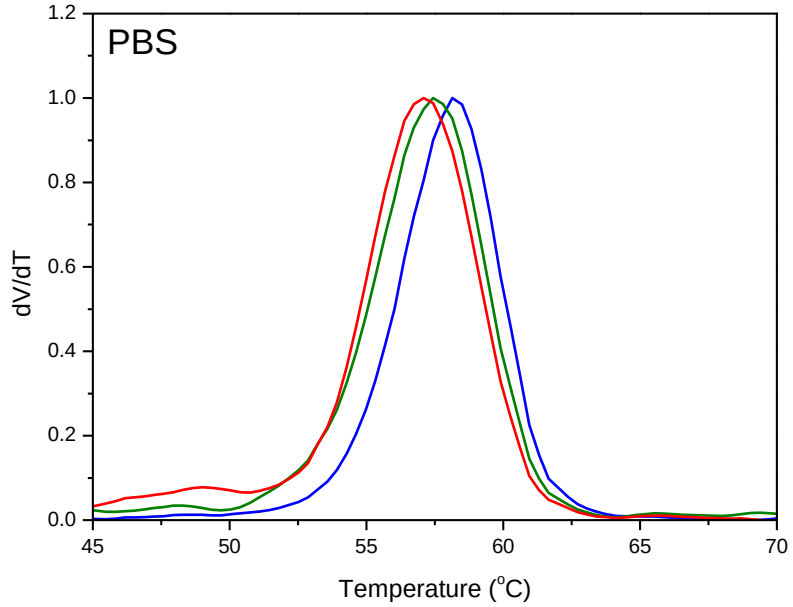

Figure A-4: Overlay of Scalls crystallization profiles for PBS cooled at 1 °C/min, as detected by different lasers.

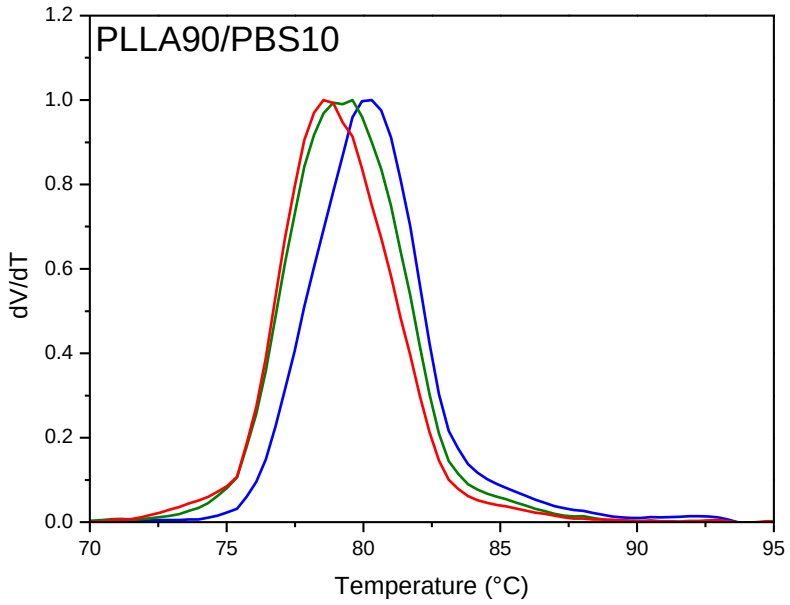

Figure A-5: Overlay of Scalls second cooling profiles for PLLA90/PBS10 blend cooled at 1 °C/min, as detected by different lasers.

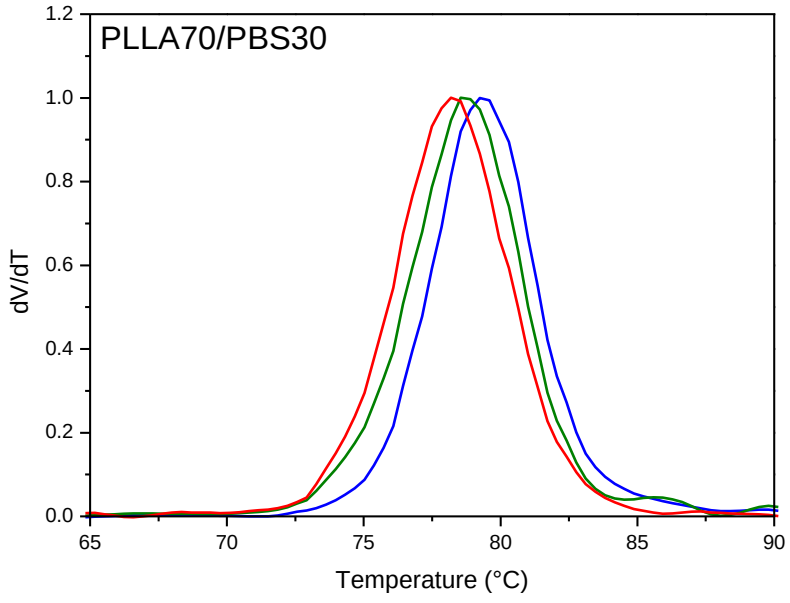

Figure A-6: Overlay of Scalls second cooling profiles for PLLA70/PBS30 blend cooled at 1 °C/min, as detected by different lasers.

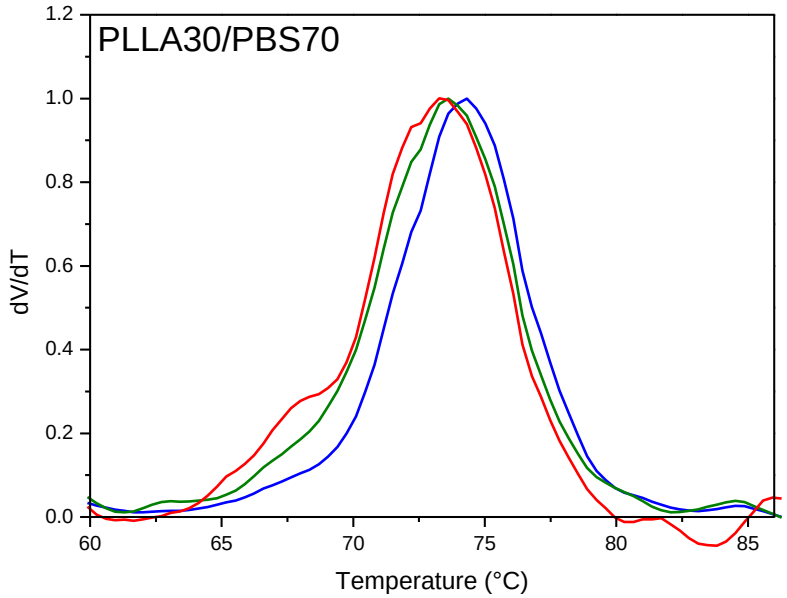

Figure A-7: Overlay of Scalls second cooling profiles for PLLA30/PBS70 blend cooled at 1 °C/min, as detected by different lasers.

Appendix B: Solid-state NMR data

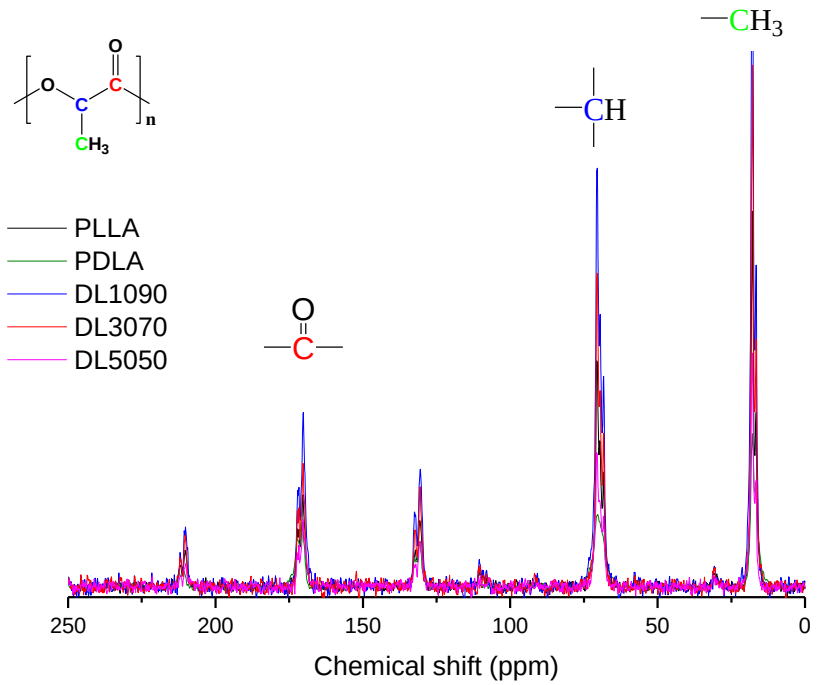

Figure B-1: Full ^{13}C solid-state NMR spectra for PLA homopolymers and PLLA/PDLA binary blends.

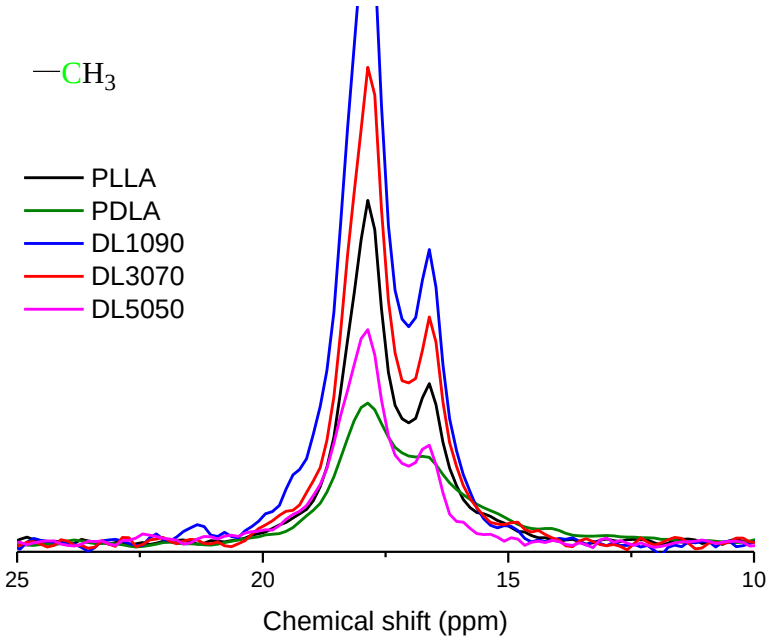

Figure B-2: ^{13}C solid-state NMR spectra of methyl region for PLA homopolymers and PLLA/PDLA binary blends.

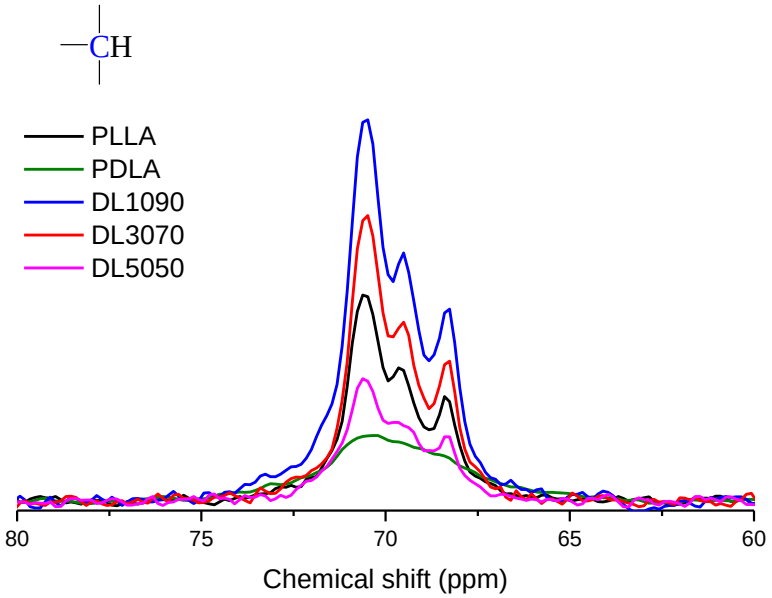

Figure B-3: ^{13}C solid-state NMR spectra of methine region for PLA homopolymers and PLLA/PDLA binary blends.

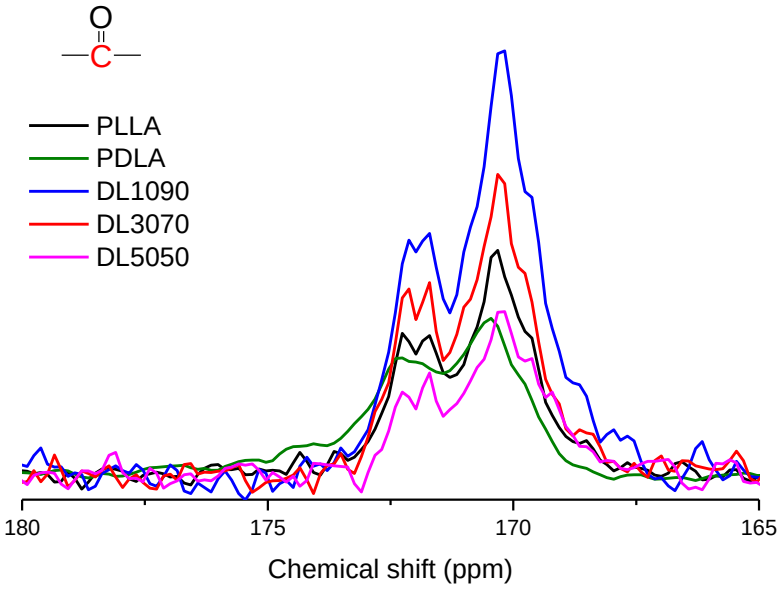

Figure B-4: ^{13}C solid-state NMR spectra of carbonyl region for PLA homopolymers and PLLA/PDLA binary blends.

Appendix C: DSC data

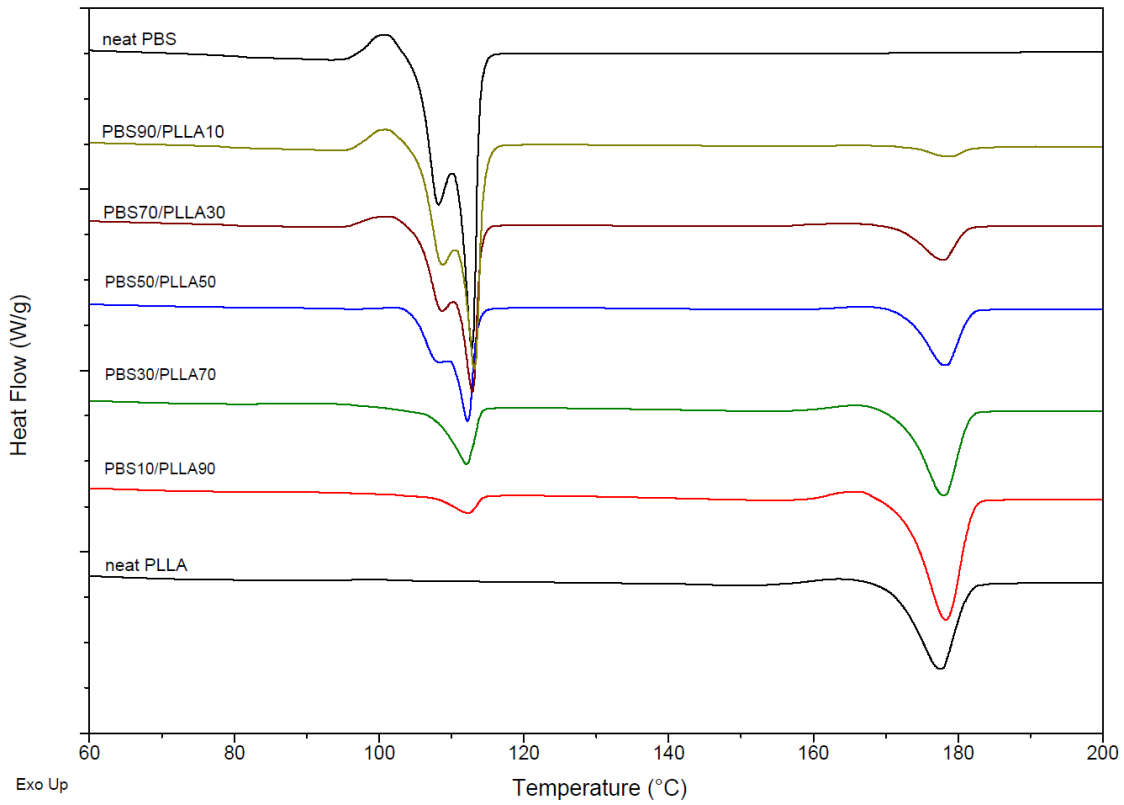

Figure C-1: DSC melting endotherms for neat PLLA, neat PBS and PLLA/PBS binary blends heated at 10 °C/min.

Appendix D: SEM data

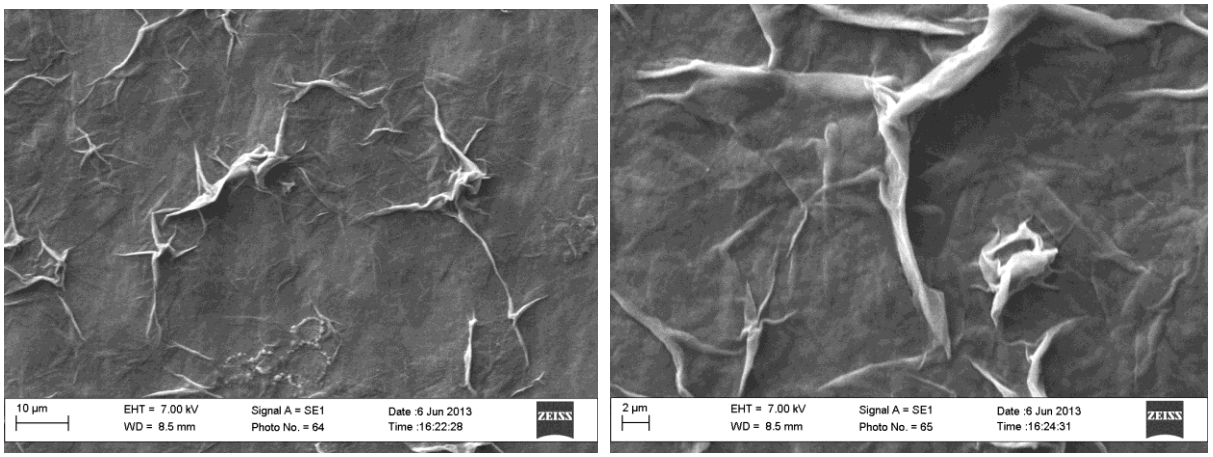

Figure D-1: SEM images of PDLA film prepared by solvent evaporation after 0.5 °C/min Scalls cooling.

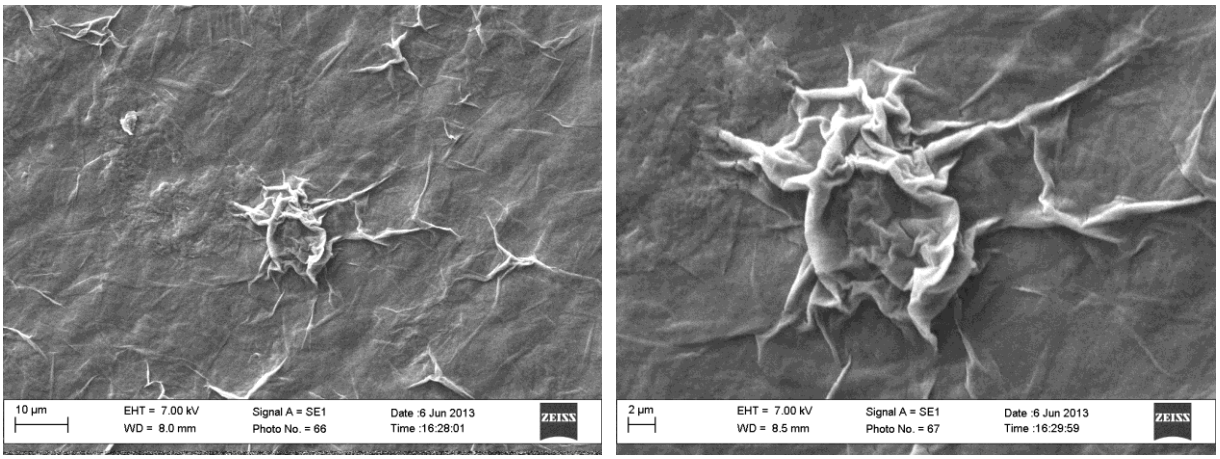

Figure D-2: SEM images of PLLA film prepared by solvent evaporation after 0.5 °C/min Scalls cooling.

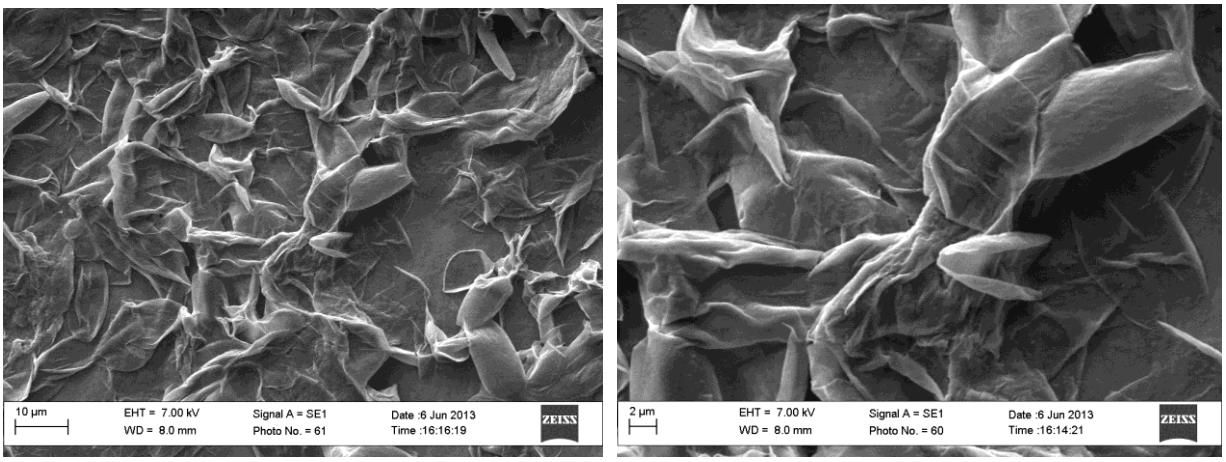

Figure D-3: SEM images of PDLA film prepared by solvent evaporation after 2 °C/min Scalls cooling.

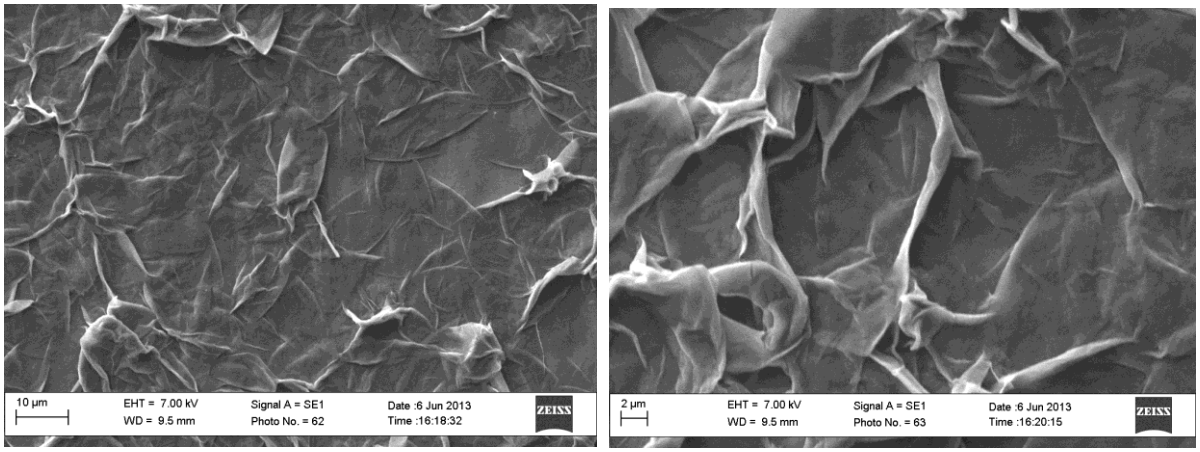

Figure D-4: SEM images of PLLA film prepared by solvent evaporation after 2 °C/min Scalls cooling

Polymer Testing 40 (2014) 79–87

Contents lists available at ScienceDirect

Polymer Testing

journal homepage: www.elsevier.com/locate/polytest

Analysis method

Solution crystallization analysis of poly(lactic acid) by Scalls: A facile approach for thermal analysis of polymers in solution

Divann D. Robertson [a], Ramesh Neppalli [b], Albert J. van Reenen [a, *]

[a] Department of Chemistry and Polymer Science, University of Stellenbosch, Private Bag X1, 7602 Matieland, South Africa
[b] Institute Physical Chemistry and Polymer Physics, Leibniz Institute of Polymer Research Dresden e.V., Hohe Strasse 6, 01069 Dresden, Germany

ARTICLE INFO

Article history:
Received 1 July 2014
Accepted 13 August 2014
Available online 4 September 2014

Keywords:
Poly(lactic acid)
Solution crystallization
Dissolution
Solution crystallization analysis by laser light scattering
Scalls

ABSTRACT

Non-isothermal solution crystallization and dissolution behaviour of both enantiomers (D and L) of poly(lactic acid) (PLA) and their blends were studied by the unique Solution Crystallization Analysis by Laser Light Scattering (Scalls) method. For the first time, we have investigated the crystallization of this biopolymer in solution, as well as the subsequent dissolution or "solution melting". It was found that addition of the D-enantiomer (PDLA) to the L-enantiomer (PLLA) in solution resulted in the formation of stereocomplex crystals (SC), and the nucleation-effect of the crystals was intensified with increase in PDLA content, leading to an earlier onset of crystallization and increased crystallization peak area. Differential Scanning Calorimetry (DSC) analysis confirmed the formation of SC during solution crystallization. Large re-crystallization events were seen for the pristine polymers, indicative of their low crystallization rates. Overall, results obtained by Scalls provided promising information regarding PLA crystallization kinetics, which significantly influences practical applications of this biopolymer.

1. Introduction

Solution crystallization techniques can provide promising results to understand microstructural behaviour in polymers and to construct much needed structure-property relationships in polymer systems. The most common, conventional techniques used for these studies thus far, are crystallization analysis fractionation (CRYSTAF), temperature rising elution fractionation (TREF) and crystallization elution fractionation ((CEF) [1,2]). Both these techniques require complex instrumentation and long analysis times. A turbidity fractionation analyser, also known as Solution Crystallization by Laser Light Scattering (Scalls), was developed in our group at University of Stellenbosch [3] following the original paper by Shan et al. [4] The Scalls system has advantages over the conventional TREF and CRYSTAF techniques when analysing the crystallization behaviour of polymers. Advantages include short analysis times, fairly inexpensive instrumentation, the ability to observe both the solution crystallization and solution melting of polymers, the small amounts of solvent required, and that the setup allows for a wide selection of solvents to be used. The use of Scalls for crystallization and dissolution studies of polyolefins has previously been reported by van Reenen et al. [3,5]. To date, only polyolefins have been studied by Scalls [6]. In recent years, biopolymers have attracted great attention in both academia and industry. Among the biopolymers, poly(lactic acid) (PLA) has been used most extensively, not only because it is biocompatible and biodegradable but also because it can be obtained from renewable resources. PLA is a linear aliphatic thermoplastic polyester, generally produced by the ring-

* Corresponding author. Tel.: +27 21 808 3168.
E-mail address: ajvr@sun.ac.za (A.J. van Reenen).

http://dx.doi.org/10.1016/j.polymertesting.2014.08.015
0142-9418/

opening polymerization of the lactide monomer. Lactide is a cyclic dimer prepared by the controlled polymerization of lactic acid, which in turn is obtained by the fermentation of corn, sugar cane, sugar beet, etc. [7] It has three isomeric systems namely poly(L-lactic acid) (PLLA), poly(D-lactic acid) (PDLA) and poly(DL-lactic acid) (PDLLA), which is a racemic mixture of L-and D-lactic acid. PLA can exhibit a variety of different properties depending on the isomeric forms present. Its ease of processing, stiffness and good strength makes this polymer a promising material and suitable to replace non-degradable commodity plastics. The major drawback is the polymer's low crystallization rate and crystallinity compared to other commonly used thermoplastics [8]. Ikada et al. [9] was the first to report formation of a stereocomplex when blending PLLA and PDLA in a 1:1 ratio. The stereocomplex displayed a different crystal structure to those of the homopolymers. Since Ikada's findings, extensive work has been done to increase the crystallization rate and to enhance the crystallization, especially of PLLA, and to study the crystal structure of these systems. These include the investigation of asymmetric blends of PLLA and PDLA [8], effect of blend ratios [10,11], the nucleation effect of stereocomplex crystals [12,13], cold-crystallization studies and blending of PLLA with inorganic nucleating agents [7,14,15] These studies were all done by calorimetric measurements from the melt using DSC. To the best of our knowledge, the crystallization and melting of PLLA and PDLA homopolymers and PLLA/PDLA blends from dilute solutions have not been reported. No research has been carried out on solution crystallization and solution melting behaviour of PLA, not even with conventional solution crystallization techniques. The Scalls method was found to be an effective tool to investigate this unexplored area of PLA research. In this study, PLLA and PDLA homopolymers and PLLA/PDLA blends with varying blend ratios were examined by Scalls, using 1,2,4-trichlorobenzene (TCB) as solvent. Promising results were obtained and compared to those reported in literature when analysed from the melt.

2. Experimental

2.1. Materials

PLLA (Purasorb® PL) and PDLA (Purasorb® PD) were supplied by Purac Co. (Netherlands). The polymers were used as obtained from the supplier. 1,2,4-Trichlorobenzene (TCB, spectrophotometric grade, (Sigma-Aldrich, > 99% purity)) was used as purchased.

2.2. Sample preparation

Sample concentrations were kept constant at 1 mg/ml. The solutions were made up by dissolving 20 mg of polymer in 20 ml TCB. For PDLA/PLLA specimens, homopolymers were transferred to a quartz tube containing the TCB. Samples were thus solution mixed within the tube during the dissolution process before crystallization studies started. The labelling was as follows: DL10/90 refers to a blend containing 10 wt% PDLA and 90 wt% PLLA.

2.3. Solution crystallization analysis by laser light scattering (Scalls)

A general schematic representation of the Scalls setup is shown in Fig. 1. The development, along with detailed information regarding the layout, has been discussed in previous literature [3,5,6]. The technique is based on the measurement of laser light intensity. A quartz tube containing the polymer solution is placed in a special opening within an aluminium block, mounted on a magnetic heater stirrer. Openings in the block allow the laser beam to pass through the solution and the changes in intensity are picked up by photodiode detectors. On cooling, polymer crystals are formed which scatters the laser beam and results in a decrease in laser intensity. Likewise, during heating, the increase in laser intensity is measured due to dissolution of the polymer. The first derivative of the raw voltage data allows for the analysis of peaks associated with crystallization and dissolution events. Three lasers with wavelengths of 405 nm (denoted blue), 532 nm (green) and 635 nm (red) were used. Crystallization studies were done by cooling polymer solutions in a controlled manner from 100 °C to 30 °C at various rates between 0.2 °C/min and 3 °C/min. Heating rates were kept constant at 1 °C/min and solutions were heated from 30 °C to 130 °C during dissolution analyses. Stirring speed was set to 500 rpm. Each experiment was repeated a minimum of three times to check the reproducibility of the results obtained.

2.4. Differential scanning calorimetry (DSC)

Thermal analysis studies were done by DSC under N_2 atmosphere. The instrument used was a TA Instruments Q100 calorimeter calibrated with an indium standard according to standard procedures. Cooling and heating rates were fixed at 10 °C/min.

3. Results and discussion

We will first discuss the results obtained for PLLA and PDLA individually, and then the PLLA and PDLA blends. It has to be mentioned that only results for the blue laser (405 nm) are shown in this paper, and curves were normalized for improved comparison of data.

3.1. PLLA and PDLA homopolymers

The crystallization profiles, as obtained from Scalls for PLLA and PDLA polymers are shown in Fig. 2 where Fig. 2a and 2b represents the raw voltage data for the blue laser signal response during cooling at different controlled rates (0.2 to 3.0 °C/min). The decrease in voltage correlates to a decrease in laser intensity so, as soon as crystals are formed in solution, the laser beam is scattered and a decrease in laser intensity was detected. From the first derivative plots (Fig. 2c and 2d), it is clear that both PLLA and PDLA crystallization phenomena can be tracked in solution due to the presence of well-defined and distinct peaks. This is advantageous due to the fact that biocompatible and biodegradable polymers such as PLA will, in the near future, become suitable alternatives to traditional petroleum-

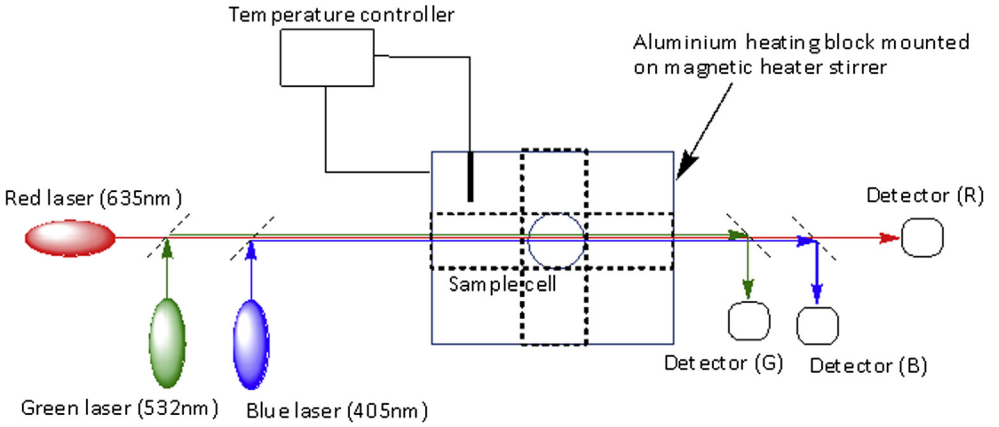

Fig. 1. Schematic diagram of the Scalls setup (viewed from top).

based polymers. It is, therefore, very important to study the solution crystallization and dissolution of these complex systems, simply due to the fact that solution fractionation techniques are mainly used to study this behaviour in commercial petroleum-based polymers and blends with PLA might be appropriate options. First, it is necessary to understand the behaviour of neat PLA in solution, hence the motivation for this study.

For both enantiomeric forms, solution peak temperatures (T_c) shifted towards lower values with an increase in cooling rate. Fig. 3 illustrates the decrease in peak temperatures. A broadening in peak width was also directly related to an increase in the cooling rate. Information on crystallization kinetics such as crystallization time can be acquired when looking at peak widths and slopes of the laser response. A steeper slope for the laser response correlates to a narrower peak, which indicates that crystallization occurred over a wide temperature range when moving to higher rates. Because Scalls is a direct intensity measuring method, it provides real-time information on

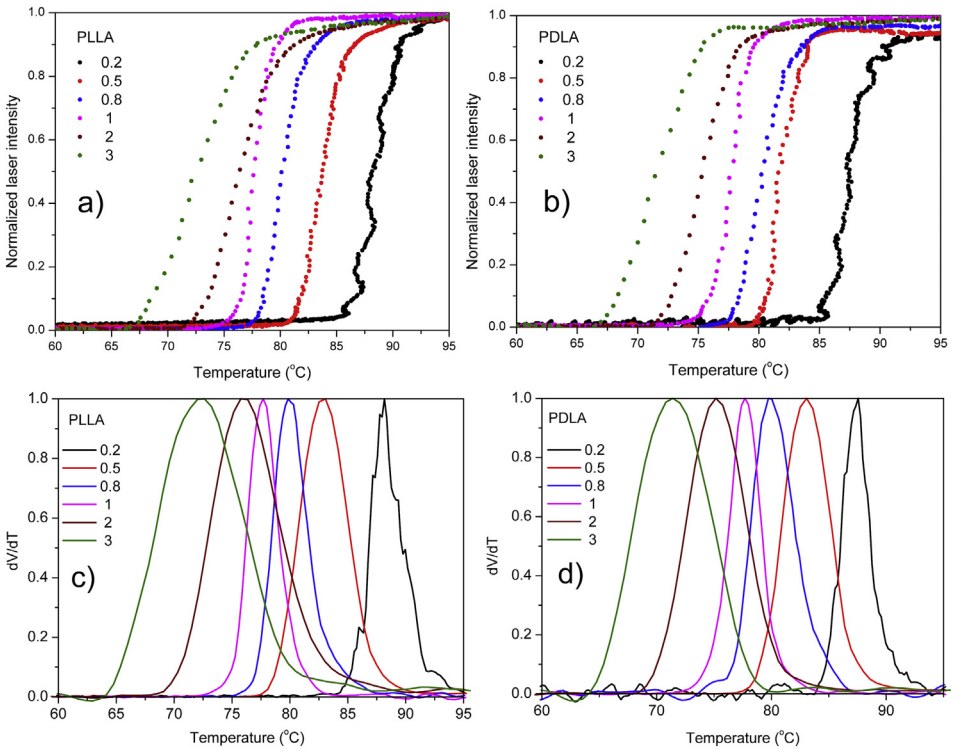

Fig. 2. Overlays of normalized Scalls cooling profiles for PLLA and PDLA pristine polymers. (a) and (b) represents the raw data laser response for PLLA and PDLA respectively. (c) PLLA and (d) PDLA are the resultant first derivative curves.

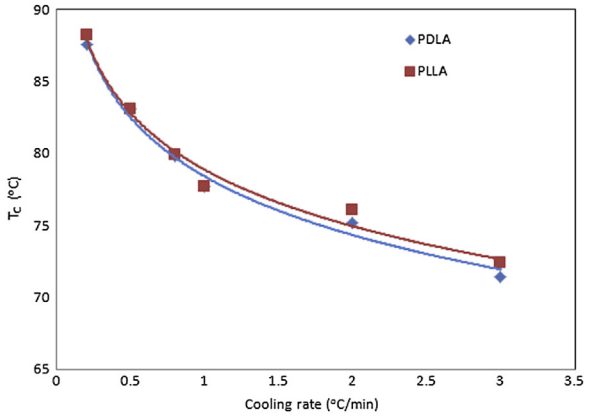

Fig. 3. Plots of cooling rate *versus* crystallization peak temperature (T_c) for PDLA and PLLA.

solution phenomena, unlike CRYSTAF where solution concentration is measured in a "delayed" fashion.

Fig. 4 shows the crystallization profiles of PLLA and PDLA at different cooling rates. With the lowest cooling rate, i.e. 0.2 °C/min, some shoulders on the main peak were observed, which can be attributed to the structural changes at molecular level in solution during the crystallization process. All other conditions resulted in smooth uni-modal profiles, indicating slightly more uniform crystallization at these rates. As expected, no major difference in T_c were observed throughout the cooling rate range for the two enantiomers. The main difference was the earlier onset of crystallization for PLLA at higher cooling rates, indicating definite differences in crystallization behaviour and kinetics for the two optical isomers under these conditions, when subjected to higher cooling rates.

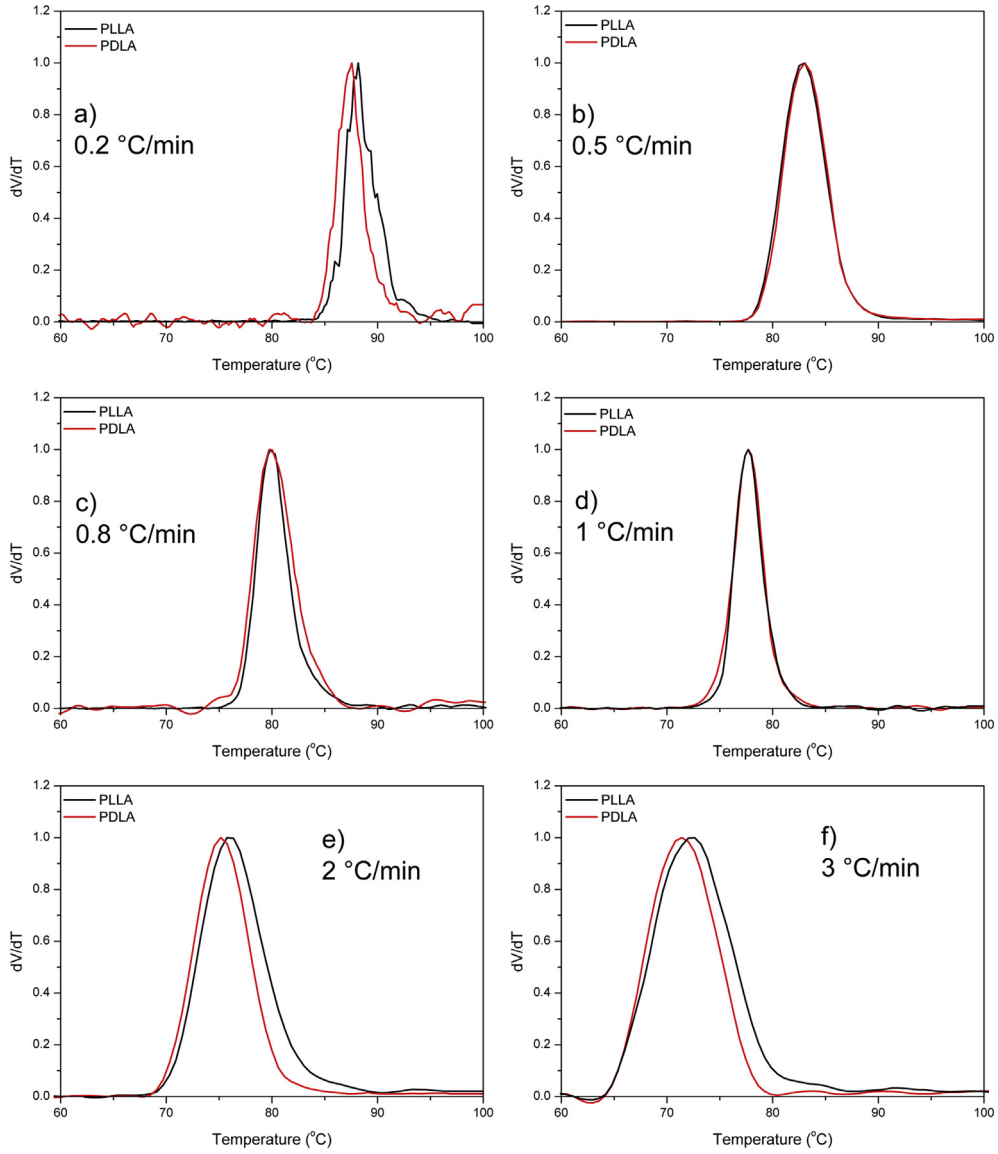

Fig. 4. Overlay of PDLA and PLLA at different cooling rates. (a) 0.2 °C/min, (b) 0.5 °C/min, (c) 0.8 °C/min, (d) 1 °C/min, (e) 2 °C/min, (f) 3 °C/min.

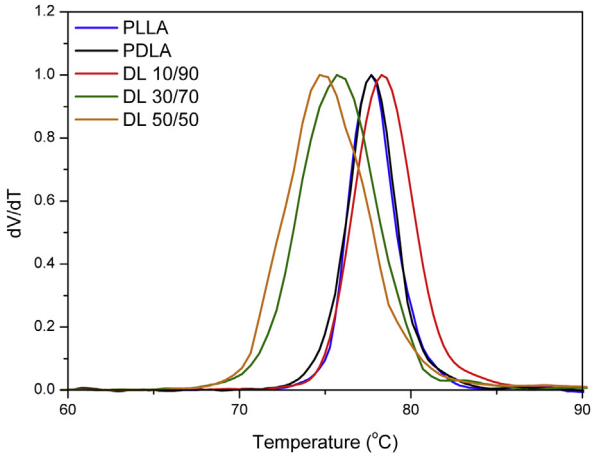

Fig. 5. Comparison of Scalls first cooling profiles for PLA homopolymers and blends with various D/L blend ratios with cooling of 1 °C/min.

3.2. PLLA/PDLA blends

The effect of the addition of PDLA on the thermal behaviour of PLLA from the melt has extensively been studied by several groups [1116–19]. Tsuji et al. [20] studied the effect of stereocomplex crystals (SC) as nucleating agent during melt crystallization and reported that the crystallization peak temperature shifts towards slightly higher temperatures as PDLA content was increased. The molecular weight of the PDLA used also greatly affects the behaviour and formation of stereocomplex crystals [19]. In Fig. 5, a comparison of crystallization peaks during first non-isothermal cooling of pristine polymers and their blends are shown. The first noticeable difference was the shift in T_c towards the lower temperature region when PDLA-content was increased from 10wt% to 50wt%. This phenomenon is entirely contradictory to the melt crystallization [20]. The main reason would probably be the difference in polymer chain mobility in the melt and solution. Stereocomplex nucleation sites could have disturbed the PLLA chain mobility because stereocomplex crystals will preferentially form. There will also be homocrystallites forming during cooling as there are only a limited number of PDLA crystallites that will be able to associate with PLLA to form SC. In this manner, an increase in SC thereby hinders homocrystallite association, resulting in a lower T_c for the blends with higher PDLA concentrations as compared to the neat polymers. It might, therefore, be assumed that solvent effects play an important role during poly(lactic acid) solution crystallization, especially for PLLA/PDLA blends.

3.2.1. Stereocomplex formation

As mentioned earlier, blending of enantiomeric poly(-lactides) results in the formation of stereocomplex crystals on crystallization from the melt. To study the possible formation of SC during solution crystallization, it was decided to heat up the turbid solutions obtained from the first cooling cycle to 130 °C to allow for the dissolution of homopolymer crystallites. During this period, the laser intensities increased sharply as the solution became less turbid due to dissolution of polymer crystals. If any SC was formed during the first cooling it would stay unmelted at this point. The polymer solutions were then subjected to a second cooling cycle to study if any noticeable variations could be identified between the two cooling profiles. Fig. 6a and 6b illustrate the peak overlays for PLLA and PDLA, respectively. It is clear to see that near perfect fits were obtained and data was nearly identical for two sequential crystallization events when looking at features such as peak shapes, crystallization onset and crystallization peak temperatures. Solutions of PLLA/PDLA blends with varying PDLA-content were also subjected to similar sequential cooling cycles as the pristine polymers. Remarkably, the profiles for the blends differed when comparing the first and second cooling results. Noticeable changes were seen in the T_c values as well as the onset of crystallization. T_c values shifted marginally towards higher temperature during the second cooling, although the changes were not significant. The major difference was certainly the onset of crystallization, which increased and shifted towards the higher temperature range. This behaviour was observed for all blend compositions and is shown in Fig. 7. As this behaviour was not observed for pristine polymers, but only in the blends, it can be attributed to the nucleating effect of PDLA on PLLA crystallization due to the unmelted SC

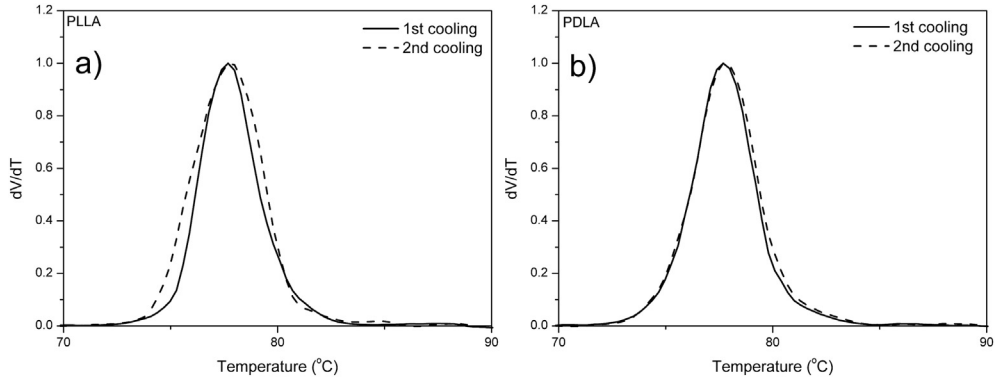

Fig. 6. Overlays of first and second cooling of PLA enantiomers: (a) PLLA, (b) PDLA.

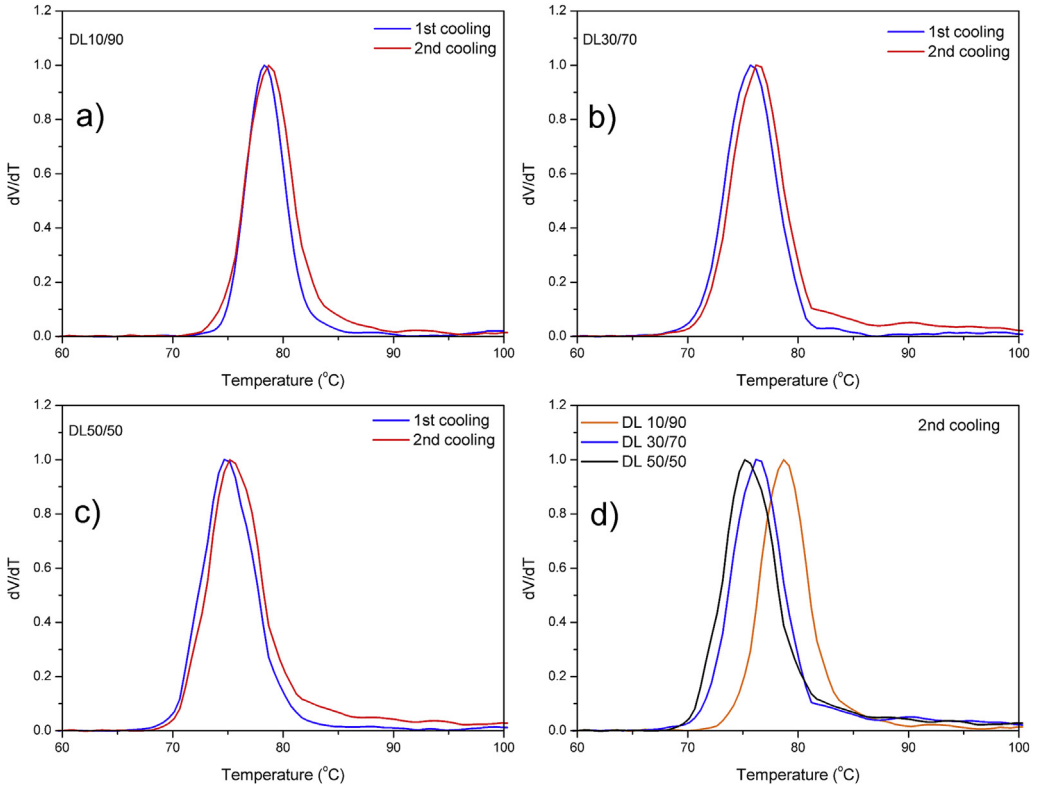

Fig. 7. First and second cooling overlays are illustrated for the respective blends in (a) DL10/90, (b) DL30/70 and (c) DL50/50. (d) Represents the second cooling for the neat polymers and blends. (Cooling rate of 1 °C/min).

present at the start of the second cooling. The unmelted SC resulted in an earlier onset of crystallization, by creating nucleation sites for the formation of homocrystallites, when compared to the first cooling. However, as the PDLA content (and amount of stereocomplex crystallites) increased, it became more difficult for homocrystals to associate, hence the lowering of T_c during both coolings when compared to pristine polymers. Increasing PDLA content to 30wt% and higher, had a confining effect on PLLA crystallization As there is no literature to fall back on, this was the first indication of possible SC formation during solution crystallization of blends of enantiomeric poly(lactide).

Crystallization peak areas, which are directly related to the amount of crystallized material as well as the crystallinity of samples, were calculated and represented in Fig. 8a. The results from the crystallization onset (Fig. 8b) and peak areas complement each other very well, both increasing with an increase in PDLA content. Table 1 illustrates the increase in crystallization peak areas, and hence an increase in the amount of crystallized material for the binary blends as compared to neat PLLA. An evident

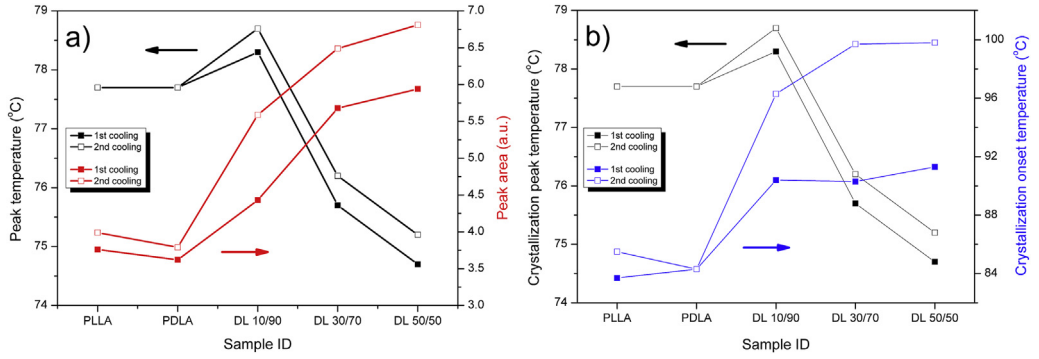

Fig. 8. Scalls data for 1st and 2nd cooling of homopolymers and blends, a) crystallization peak temperature and crystallization area, b) crystallization peak temperature and crystallization onset temperature.

Table 1
Amount of material crystallized in D/L blends relative to neat PLLA.

Sample	Percentage increase in amount of material crystallized w.r.t. neat PLLA (%)	
	1st Cooling	2nd Cooling
DL10/90	17.8	40.1
DL30/70	51.1	62.7
DL50/50	58.0	70.7

increase was seen, suggesting that PLLA crystallization kinetics was increased in the presence of PDLA in dilute solution.

Although the multiple dissolution peaks for PLA homocrystallites (around 105 °C and 120 °C) and onset of SC dissolution transitions (around 155 °C) could be observed with Scalls, it was not possible to obtain fully resolved dissolution peaks for SC in the higher temperature range as the setup at the time of this study did not allow for dissolution analyses much higher than 160 °C. It is well-known that poly(lactide) stereocomplex crystals formed during melt crystallization of PLLA/PDLA blends melt at temperatures above 200 °C, much higher than the homocrystallites [6,8,10,18]. To acquire further evidence of SC formation, the crystallized material from Scalls was analysed by DSC. Melting endotherms of SC crystallites were visible at roughly 225 °C for the binary blends (peaks absent for homopolymers), and can be observed in Fig. 9. The melting enthalpies for these peaks increased with an increase in PDLA content and are represented in Table 2. Besides the SC endotherms, three other events namely melting (T_{m1}), re-crystallization and re-melting (T_{m2}) due to PLA homocrystallites were visible at around 157 °C, 160 °C and 178 °C, respectively. Peak temperatures of these transitions were unaffected by PDLA addition. However, enthalpies of these homocrystallite endotherms decreased (see Table 3) with increasing concentration of PDLA, confirming that less homocrystallites and more SC crystallites formed in the presence of PDLA during non-isothermal solution crystallization of the PLLA/PDLA blends.

Table 2
DSC data of stereocomplex endotherm for PLLA/PDLA blends after Scalls.

Sample	SC T_p (°C)	SC ΔH_f (J/g)
DL10/90	225.2	7.2
DL30/70	224.7	13.1
DL50/50	224.0	18.2

Table 3
DSC data of homocrystallite endotherms after Scalls.

Sample	T_{m1} (°C)	ΔH_{m1} (J/g)	T_{m2} (°C)	ΔH_{m2} (J/g)
PLLA	155.0	2.6	177.9	49.8
PDLA	157.7	17.5	178.1	53.2
DL10/90	158.3	17.4	178.8	42.8
DL30/70	157.4	15.2	178.2	37.2
DL50/50	157.1	13.8	177.9	36.2

However, some valuable information could be obtained from the Scalls solution melting results for the homocrystallites. Fig. 10 shows an overlay of heating profiles for homopolymers and blends after cooling at 1 °C/min, and represents the laser intensity response as a function of temperature. An increase or decrease in laser intensity refers to dissolution or crystallization events, respectively.

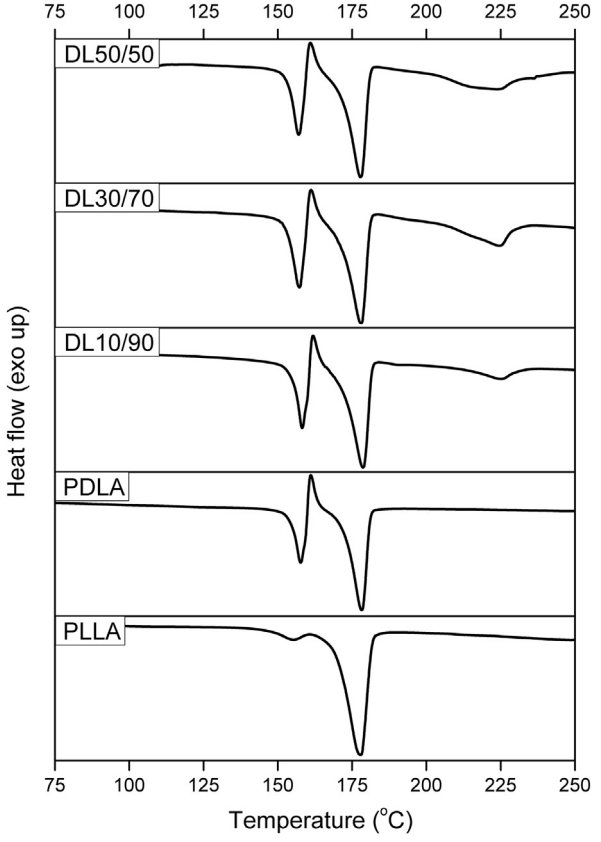

Fig. 9. DSC heating thermographs (first heating) for PLA samples after Scalls analyses.

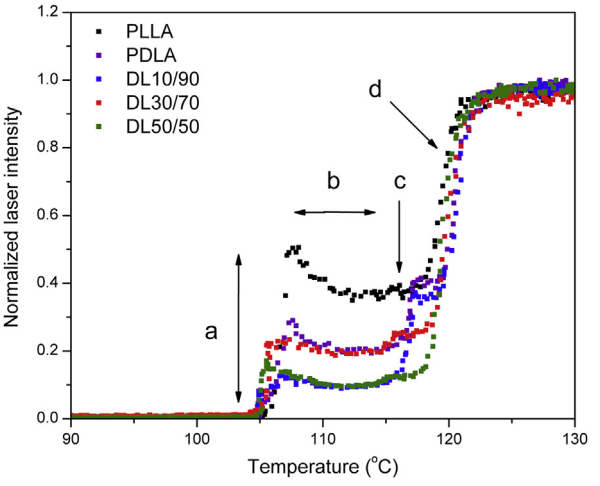

Fig. 10. Detector responses for solution melting of PLLA, PDLA and their blends heated at 1 °C/min. (After cooling at 1 °C/min).

Four distinct events were detected and marked as regions (a) to (d). Regions (a), (c) and (d) represent the multiple melting behaviour of PLA, similar to the DSC endotherms shown previously, and can be seen by the strong increase in laser intensity due to the dissolution of homocrystallites back into solution. A slight decrease in laser intensity was seen in region (b) relating to recrystallization events. These recrystallization events emphasize the low crystallization kinetics of PLA on cooling. Interestingly, the decrease in laser intensity observed in this region was much more subtle for the blends than for the pristine polymers, and suggest that the addition of PDLA leads to an increase in solution crystallization kinetics, resulting in less re-organization of polymer chains during dissolution. This provides critical information with regards to applications of PLA, as thermal properties are directly related to certain applications of these biopolymer materials [21].

4. Conclusions

For the first time, non-isothermal crystallization and dissolution behaviour of poly(L-lactic acid), poly(D-lactic acid) and their binary blends were studied in solution. It was demonstrated that Scalls is very convenient for analysing these phenomena in a polymer system known for its very poor crystallization rates. Distinct uni-modal crystallization profiles were seen for all samples together with a broadening in peak widths and shifting of T_c towards lower temperatures as the cooling rate was increased. Solution crystallization behaviour of PLLA and PDLA homopolymers was identical throughout the cooling rate range. Furthermore, the addition of PDLA to PLLA resulted in SC crystallite formation in solution. The SC network had a nucleating effect on PLLA homocrystallite behaviour throughout the entire blend composition. Crystallization peak area and onset of crystallization increased with an increase in PDLA concentration. Higher PDLA additions (30 wt% and 50 wt%) resulted in the SC network having a confining effect on homopolymer crystallization whereby SC crystallites hinders the diffusion ability of the PLLA polymer chains and shifts T_c to slightly lower temperatures. DSC results confirmed stereocomplex formation by the presence of characteristic SC endotherms. Enthalpies of these endotherms increased with increasing amount of PDLA. Consecutive Scalls cooling cycles showed that unmelted SC crystallites resulted in improved nucleation of homocrystallites.

Solution melting by Scalls allowed for the detection of dissolution transitions on heating of crystallized material. Multiple melting events were observed, which was in good agreement with calorimetric results. Re-crystallization events were more subtle for the blends, possibly due to improved crystallization kinetics. Overall, this study highlights the effectiveness of introducing PDLA for preparation of PLLA/PDLA enantiomeric blends for enhancing the crystallization rate of PLLA.

Furthermore, the simple and unique Scalls technique seems to be very convenient for this study with the major advantages being the analysis of solution crystallization and melting in a single experiment, short analysis times and small volumes of solvent required. However, future investigations on these polymers will include the following: further detailed study on poly(lactic acid) dissolution behaviour and blends of PLA with other polymers. It might also be beneficial to look at results obtained by the other two higher wavelength lasers (green = 532 nm, red = 635 nm) to see what extra information can be extracted with regards to crystallization kinetics, as the ability of crystallized particles to scatter light is dependent on the wavelength of the incident laser beam.

Author contributions

This manuscript was written through contribution of all authors. All authors have given approval to the final version of the manuscript.

Notes

The authors declare no competing financial interest.

Acknowledgments

The authors would like to thank the Laser Research Institute at Stellenbosch University for support throughout the study and assistance with the SCALLS instrumentation as well as the National Research Foundation (NRF) (grant number CPRR14080485804) for financial support.

References

[1] B. Monrabal, J. Sancho-Tello, N. Mayo, L. Romero, Crystallization elution fractionation. A new separation process for polyolefin resins, Macromolecular Symposia 257 (1) (2007) 71–79.
[2] B. Monrabal, L. Romero, N. Mayo, J. Sancho-Tello, Advances in crystallization elution fractionation, Macromolecular Symposia 282 (1) (2009) 14–24.
[3] A.J. Van Reenen, E.G. Rohwer, P. Walters, M. Lutz, M. Brand, Development and use of a turbidity analyzer for studying the solution crystallization of polyolefins, Journal of Applied Polymer Science 109 (5) (2008) 3238–3243.
[4] C.L.P. Shan, W.A. Degroot, L.G. Hazlitt, D. Gillespie, A new turbidimetric approach to measuring polyethylene short chain branching distributions, Polymer 46 (25) (2005) 11755–11767.
[5] A. Van Reenen, M. Brand, E. Rohwer, P. Walters, Solution crystallization analysis by laser light scattering (SCALLS), Macromolecular Symposia 282 (1) (2009) 25–32.
[6] S. Cheruthazhekatt, D.D. Robertson, M. Brand, A. van Reenen, H. Pasch, Solution crystallization and dissolution of polyolefins as monitored by a unique analytical tool: solution crystallization analysis by laser light scattering, Analytical Chemistry 85 (15) (2013) 7019–7023.
[7] S.S. Ray, M. Okamoto, Biodegradable polylactide and its nanocomposites: opening a new dimension for plastics and composites, Macromolecular Rapid Communications 24 (14) (2003) 815–840.
[8] J. Sun, H. Yu, X. Zhuang, X. Chen, X. Jing, Crystallization behavior of asymmetric PLLA/PDLA blends, Journal of Physical Chemistry B 115 (12) (2011) 2864–2869.
[9] Y. Ikada, K. Jamshidi, H. Tsuji, S.H. Hyon, Stereocomplex formation between enantiomeric poly(lactides), Macromolecules 20 (4) (1987) 904–906.
[10] E.M. Woo, L. Chang, Crystallization and morphology of stereocomplexes in nonequimolar mixtures of poly(l-lactic acid) with excess poly(d-lactic acid), Polymer 52 (26) (2011) 6080–6089.
[11] H. Yamane, K. Sasai, Effect of the addition of poly(d-lactic acid) on the thermal property of poly(l-lactic acid), Polymer 44 (8) (2003) 2569–2575.
[12] J. Narita, M. Katagiri, H. Tsuji, Highly enhanced nucleating effect of melt-recrystallized stereocomplex crystallites on poly(L-lactic acid) crystallization, Macromolecular Materials and Engineering 296 (10) (2011) 887–893.

[13] H. Xu, S. Tang, J. Chen, Unique crystallization behavior of poly(L-lactic acid) nucleated by stereocomplex with different Fine structure, Polymer – Plastics Technology and Engineering 52 (7) (2013) 690–698.
[14] L. As'habi, S.H. Jafari, H.A. Khonakdar, L. Häussler, U. Wagenknecht, G. Heinrich, Non-isothermal crystallization behavior of PLA/LLDPE/nanoclay hybrid: synergistic role of LLDPE and clay, Thermochimica Acta 565 (2013) 102–113.
[15] L. As'habi, S.H. Jafari, H.A. Khonakdar, B. Kretzschmar, U. Wagenknecht, G. Heinrich, Effect of clay type and polymer matrix on microstructure and tensile properties of PLA/LLDPE/clay nanocomposites, Journal of Applied Polymer Science 130 (2) (2013).
[16] D. Brizzolara, H. Cantow, K. Diederichs, E. Keller, A.J. Domb, Mechanism of the stereocomplex formation between enantiomeric poly (lactide)s, Macromolecules 29 (1) (1996) 191–197.
[17] Y. Li, C. Han, Isothermal and nonisothermal cold crystallization behaviors of asymmetric poly(L-lactide)/poly(D-lactide) blends, Industrial Engineering and Chemistry Research 51 (49) (2012) 15927–15935.
[18] J. Narita, M. Katagiri, H. Tsuji, Highly enhanced accelerating effect of melt-recrystallized stereocomplex crystallites on poly(L-lactic acid) crystallization, 2-Effects of Poly(D-lactic acid) concentration, Macromolecular Materials and Engineering 298 (3) (2013) 270–282.
[19] J. Narita, M. Katagiri, H. Tsuji, Highly enhanced accelerating effect of melt-recrystallized stereocomplex crystallites on poly(L-lactic acid) crystallization: effects of molecular weight of poly(D-lactic acid), Polymer International 62 (6) (2013) 936–948.
[20] H. Tsuji, H. Takai, S.K. Saha, Isothermal and non-isothermal crystallization behavior of poly(l-lactic acid): effects of stereocomplex as nucleating agent, Polymer 47 (11) (2006) 3826–3837.
[21] I. Engelberg, J. Kohn, Physico-mechanical properties of degradable polymers used in medical applications: a comparative study, Biomaterials 12 (3) (1991) 292–304.